

https://dspace.org/

Automated intelligent electric engine design (AIEED) application

Minucci, Giuliano Antonio Vincenzo

2018

https://hdl.handle.net/10539/26650

Minucci, Giuliano Antonio Vincenzo (2018) Automated intelligent electric engine design (AIEED) application, University of the Witwatersrand, Johannesburg, <http://hdl.handle.net/10539/26650>

Downloaded from a DSpace repository. https://dspace.org/



Automated Intelligent Electric Engine Design (AIEED) Application

Giuliano Antonio Vincenzo Minucci

(Student number: 346871)

School of Mechanical, Industrial & Aeronautical Engineering.

University of the Witwatersrand

Johannesburg, South Africa.

Supervisor: Prof. D Cipolat

A Research Report submitted to the Faculty of Engineering and the Built Environment, University of the Witwatersrand, in fulfilment of the requirements for the degree of Master's in Engineering.

14 August 2018

Faculty of Engineering and the Built Environment

Private Bag 3, Wits 2050, South Africa * Telephone (011) 717 – 7007 * Fax: (011) 717 7009 * Email: febe.pg@wits.ac.za

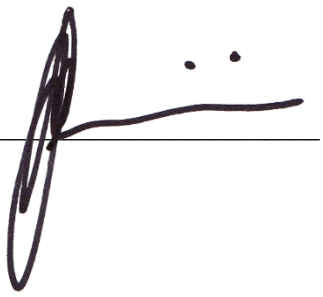
PLAGIARISM DECLARATION TO BE SIGNED BY ALL HIGHER DEGREE STUDENTS

SENATE PLAGIARISM POLICY: APPENDIX ONE

I **Giuliano Antonio Vincenzo Minucci** (Student number: **346871**) am a student registered for the degree of **Master of Science in Engineering (Mechanical)** in the academic year **2018**.

I hereby declare the following:

- I am aware that plagiarism (the use of someone else's work without their permission and/or without acknowledging the original source) is wrong.
- I confirm that the work submitted for assessment for the above degree is my own unaided work except where I have explicitly indicated otherwise.
- I have followed the required conventions in referencing the thoughts and ideas of others.
- I understand that the University of the Witwatersrand may take disciplinary action against me if there is a belief that this is not my own unaided work or that I have failed to acknowledge the source of the ideas or words in my writing.

Signature: 

Date: 14 August 2018

EXECUTIVE SUMMARY

The automotive industry is experiencing a major transition with regards to powertrain where the traditional internal combustion engine is being replaced by hybrid or all-electric solutions. As a result of this transition, many powertrain engineering firms, such as Integral Powertrain, are required to adapt or develop tools to improve the quality and time to respond to the rapid increase in new electric motor enquiries.

This paper details the development of the foundations of a software tool (AIEED) used to improve the time and quality of response to new motor enquiries. The foundations of the AIEED tool are built into a Microsoft Excel document which contains the necessary logic required to convert customer requirements data into geometrical design data. A series of macros are included in the tool which allow for the automated generation of a first-level computer-aided design (CAD) model of the motor, including the following components; stator, windings, rotor, magnets, housing and cover. The CAD models, which serve to improve the quality of response to new motor enquiries and provide a basis for further detailed development, are generated on the CATIA V5 design platform. In addition, the tool makes use of the CAD model to determine the estimate cost of the unit based on average material costs per unit mass defined in the materials database stored in the tool. It is estimated that the AIEED tool reduces the response time to new motor enquires by 75%.

Certain assumptions and limitations have been applied such that the foundations of the tool only include support for the following motor specifications:

- Surface Permanent Magnet Alternating Current cylindrical radial flux motors (external stator and internal rotor).
- The units are designed for 3-phase supply.
- The winding configuration is limited to concentrated double layer option.
- Parallel tooth, arc-bottom, semi-closed stator slot profiles.
- Arc-shaped radially magnetised surface magnet rotor configuration option.

A simple data verification filter is applied to minimise the potential for invalid inputs. However, a full validation and verification process is recommended for future work. In

addition, it is recommended that the tool be expanded to support additional motor types and specifications as well as package the foundations into a single, easy-to-use utility.

CONTENTS

Declaration i

Executive Summary ii

List of Figures vi

List of Tables ix

Nomenclature x

1 Introduction 1

1.1 Purpose of the Study 1

1.2 Objective of the Study 2

1.3 Research Motivation 2

1.4 Problem Statement 3

1.5 Assumptions and Restrictions 3

2 Literature Review 5

2.1 Electric Motor Theory 5

2.1.1 Surface Permanent Magnet versus Interior Permanent Magnet Motors 9

2.2 Surface Permanent Magnet Alternating Current Motor Design Principles 12

2.2.1 SPM Motor Operating Principles and Analytical Investigation (Performance) 12

2.2.2 Stator Assembly 40

2.2.3 Rotor Assembly 48

2.2.4 Permanent Magnets 50

2.2.5 Housing Components 54

2.3 CATIA V5 and 3DExperience Platform – Automation Techniques 57

3 Research Objectives 60

4 Research Methods 61

5 Criteria for Validation and Verification 62
6 AIEED Development Process 63
6.1 Development Platform Decisions 63
6.2 Design Calculator Build 65
6.3 Design Model Template Build 74
6.3.1 Stator Template Model 74
6.3.2 Windings Representation Template Model 76
6.3.3 Rotor Template Model 77
6.3.4 Permanent Magnets Representation Template Model 79
6.3.5 Housing Template Model 81
6.3.6 Cover Template Model 83
6.4 Automating the Modelling Process 85
6.5 AIEED Tool Verification and Validation 89
7 Conclusions 93
8 Recommendations for Future Work 95
References 98
Appendices 103
Appendix A: Materials Catalogue Database 104
Appendix B: CATIA V5 Automation Objects 109
Appendix C: Project Schedule 110
Appendix D: AIEED Tool 112
Appendix E: AIEED Tool – VBA Code 115

LIST OF FIGURES

Figure 1: Hybrid drive vehicle electric motor developed by Integral Powertrain [2] 1

Figure 2: Electric motor classification [5] 5

Figure 3: Typical Permanent Magnet Alternating Current (PMAC) Motor [11] 7

Figure 4: Stator and busbar assembly of an Integral Powertrain electric motor [13]. 8

Figure 5: Example of rotor assembly inserted into stator and housing assembly [14]. 9

Figure 6: Surface Permanent Magnet motors versus Interior Permanent Magnet motors [15] 10

Figure 7: Inductance path comparison - Surface Permanent Magnet versus Interior Permanent Magnet [17].....10

Figure 8: Permanent magnet with magnetic field line representation [22].....13

Figure 9: Sample magnetic hysteresis loop [23].....14

Figure 10: B-H Curves for common material groups indicating magnetic saturation points [23] 15

Figure 11: Magnetic field flux density at distance z along symmetrical axis of block magnet [27].....17

Figure 12: Infinitely thin magnetic block and magnetic block of defined thickness.....17

Figure 13: Example of magnetic field induced by current flow through conductor.....19

Figure 14: Magnetic field lines induced by current travelling through coil [26].....20

Figure 15: Coil wrapped around magnetic core material.....20

Figure 16: Force experienced by current carrying conductor in magnetic field.....22

Figure 17: Magnet free to spin in simple ring and ring with two poles.....23

Figure 18: Torque variation with angular position experienced by magnet in two-pole ring [5] 24

Figure 19: Current carrying conductor introduced to generate mutual/alignment torque component and extended multi-pole stator.....25

Figure 20: Typical SPM motor power and torque versus speed characteristics [32] 26

Figure 21: Comparison of magnetic circuit and electrical circuit schematics 31

Figure 22: Magnetic circuit schematic for permanent magnet 32

Figure 23: Radially magnetised arc-shaped permanent magnet 32

Figure 24: Airgap modelling schematics for magnetic circuit analysis 33

Figure 25: Simplified SPM motor for MCA analysis 35

Figure 26: Magnetic circuit model for simplified SPM motor 36

Figure 27: Simplified magnetic circuit for SPM motor analysis 37

Figure 28: Full motor MCA analysis diagram 39

Figure 29: Honda Accord hybrid motor stator assembly [36] 40

Figure 30: Internal and external stator configuration examples [37] [38] 41

Figure 31: Stator tooth profile dimensions 43

Figure 32: Small high-speed hobby motor stator assembly [40] 44

Figure 33: Single versus double layered windings [48] 48

Figure 34: Stator slot winding fill factor [49] 48

Figure 35: Carbon fibre composite rotor containment sleeve [51] 50

Figure 36: Sample demagnetisation curves at various temperatures for N40UH permanent magnet [24] 52

Figure 37: Example of Integral Powertrain Motor Housing Components [61] 54

Figure 38: 2-Piece and 3-Piece motor housing configurations. [62] [63] 55

Figure 39: Examples of fully encapsulated stator assemblies including sectioned views [65] [66] 56

Figure 40: Creepage and clearance measurements across insulation barrier 57

Figure 41: Examples of automation techniques within the Dassault Systemes software platforms [73] 59

Figure 42: AIEED Tool: High-level data flow and interaction diagram 65

Figure 43: Calculator inputs: Permanent magnet material selection drop-down list 69

Figure 44: Stator template model 75
Figure 45: Stator template model: Tooth profile sketch (Sample dimensions) 75
Figure 46: Windings representation template model 76
Figure 47: Windings representation template model: Windings volume profile sketch 77
Figure 48: Rotor template model 78
Figure 49: Rotor template model: Rotor profile sketch 78
Figure 50: Rotor template model: Additional rotor detail dimensions 79
Figure 51: Permanent magnets representation template model 80
Figure 52: Permanent magnets representation template model: Magnet profile sketch 80
Figure 53: Housing template model 81
Figure 54: Housing template model: Housing profile sketch 82
Figure 55: Housing template model: Additional housing detail dimensions 82
Figure 56: Cover template model 83
Figure 57: Cover template model: Cover profile sketch 84
Figure 58: Full motor assembly template model (Sample parameters) 84
Figure 59: Macro buttons available in AIEED tool 87
Figure 60: AIEED Tool: Part numbering fields 87
Figure 61: AIEED tool: Sample estimate mass and material cost message box 88
Figure 62: Data validation: Example of invalid input data entry error message 91
Figure 63: Example of parameter description diagram included in AIEED tool 92
Figure 64: Possible layout of the final AIEED tool 97

LIST OF TABLES

Table 1: High-level design parameters in electric motor design 26

Table 2: Magnetic circuit analysis analogy with electrical circuit analysis [5].....29

Table 3: Common stator slot geometries [39].....41

Table 4: Comparison between common winding layout configurations [45] [46] [47] 47

Table 5: Common rotor magnet configuration geometries (SPM) [39] 49

Table 6: Comparison of typical permanent magnet materials [57].....53

Table 7: Calculator inputs: Performance and characteristics (Sample values).....66

Table 8: Calculator outputs: Performance 67

Table 9: Calculator inputs: Materials, Magnets, Stator & Windings and Rotor (Sample values) 68

Table 10: Calculator inputs: Material properties 69

Table 11: Calculator outputs: Rotor and Magnets 70

Table 12: Calculator outputs: Stator 72

Table 13: Calculator inputs: Packaging considerations and Mass (Sample values).....73

Table 14: Calculator outputs: Mass and Cost 73

Table 15: AIEED Macros and their description 86

Table 16: Data validation criteria applied to input data.....90

NOMENCLATURE

AC	Alternating Current	
$AIEED$	Automated Intelligent Electric Engine Design	
API	Application Programming Interface	
BOM	Bill of Material	
CAD	Computer Aided Design	
CAE	Computer Aided Engineering	
$CATIA$	Computer Aided Three-Dimensional Interactive Application	
$CPSR$	Constant Power Speed Range/Ratio	
DC	Direct Current	
EM	Electromagnetic	
EMF	Electro-Motive Force	
FEA	Finite Element Analysis	
ICE	Internal Combustion Engine	
IP	Integral Powertrain Ltd.	
IPM	Interior Permanent Magnet	
MCA	Magnetic Circuit Analysis	
MMF	Magnetomotive Force	
MS	Microsoft	
PLM	Product Lifecycle Management	
PM	Permanent Magnet	
$PMAC$	Permanent Magnet Alternating Current	
$PMSM$	Permanent Magnet Synchronous Motor	
RMS	Root Mean Square	
SPM	Surface Permanent Magnet	
$SPMAC$	Surface Permanent Magnet Alternating Current	
B_g	Air Gap Flux Density	$\left[T\ OR\ {}^{Wb}/_{m^2}\right]$
L_{Airgap}	Airgap Length	$[m]$
C_x	Average Cost Per Unit Mass of Component Material x	$[£/kg]$
L_{st}	Axial Stack Length of Motor	$[m]$
V_x	CAD Volume of Component x	$[m^3]$
H_c	Coercive Force	$\left[{}^{A}/_{m}\right]$
i	Current	$[A]$

ρ_x	Density of Component Material x	$[kg/m^3]$
P_{max}	Expected Maximum Power Output	$[W]$
$C_{\emptyset}$	Flux Concentration Factor	$[-]$
SF_g	Gross Slot Fill Percentage	$[-]$
$H_{ci}\ OR\ H_{cJ}$	Intrinsic Coercivity	$[{}^{A}/_{m}]$
K_{st}	Lamination Stacking Factor	$[-]$
K_l	Leakage Factor	$[-]$
L_m	Magnet Length in Magnetised Direction	$[m]$
$B_{r20degC}$	Magnet Residual Induction at 20° C	$\left[T\ OR\ {}^{Wb}/_{m^2}\right]$
H	Magnetic Field Intensity	$[{}^{A}/_{m}]$
$\emptyset$	Magnetic Flux	$[T.m^2\ OR\ Wb]$
B	Magnetic Flux Density	$\left[T\ OR\ {}^{Wb}/_{m^2}\right]$
$\emptyset_g$	Magnetic Flux Through Airgap	$[T.m^2\ OR\ Wb]$
M_x	Mass of Component x	$[kg]$
n_{max}	Maximum Rotational Speed	$[RPM\ or\ rad/s]$
N_{ph}	Number of Electrical Phases	$[-]$
N_{PP}	Number of Magnet Pole Pairs	$[-]$
N_s	Number of Stator Slots	$[-]$
N_{spp}	Number of Stator Slots Per Pole Per Phase	$[-]$
n_{turns}	Number of Turns in Windings	$[-]$
B_{T_pk}	Peak Flux Density Through the Stator Tooth	$\left[T\ OR\ {}^{Wb}/_{m^2}\right]$
B_{SY_pk}	Peak Flux Density Through the Stator Yoke	$\left[T\ OR\ {}^{Wb}/_{m^2}\right]$
P	Permanence of the Material	$\left[{}^{Wb}/_{A}\ OR\ H\right]$
μ_0	Permeability of Free Space $(4\pi \times 10^{-7})$	$[{}^{H}/_{m}\ OR\ T.{}^{m}/_{A}]$
μ	Permeability of the Material	$[{}^{H}/_{m}\ OR\ T.{}^{m}/_{A}]$
P_c	Permeance Coefficient	$[-]$
μ_r	Relative Permeability	$[-]$
K_r	Reluctance Factor	$[-]$
R_g	Reluctance of the Airgap	$\left[{}^{A}/_{Wb}\ OR\ H^{-1}\right]$
L_{Rotor}	Rotor Length	$[m]$
D_R	Rotor Magnet Outer Diameter	$[m]$
V_R	Rotor Volume	$[m^3]$

ID	Stator Inner Diameter	$[m]$
OD	Stator Outer Diameter	$[m]$
TWS	Stator Tooth Body Width	$[m]$
SD	Stator Tooth Slot Depth	$[m]$
SO	Stator Tooth Slot Opening	$[m]$
TGD	Stator Tooth Tang Depth	$[m]$
WSY	Stator Yoke Depth	$[m]$
$rM_{PerRotorVolume}$	Torque Per Unit Rotor Volume	$[Nm/m^3]$

1 INTRODUCTION

Integral Powertrain (IP), founded in 1999, is a powertrain engineering consultancy. IP have capability and expertise in powertrain development for use in multiple industries including the automotive, motorsport, aerospace, defence and marine markets. Aligned with a notable trend in the overall industry, the primary focus of IP's business activity has progressed from internal combustion engines (ICE) to electric machines and associated controls. The current and expected future activity encompasses primarily the development and application of hybrid drive systems (See Figure 1), electric motor/generator design & development and engine downsizing and emissions reductions through novel pressure-charging systems which incorporate e-motors. [1]



Figure 1: Hybrid drive vehicle electric motor developed by Integral Powertrain [2]

During the design and development of traditional ICE components, IP implemented numerous software tools to improve time-to-market, cost efficiency and product performance. Amongst these tools, included several design template tools that allowed for efficient and simple generation of initial design data. This data was typically used to reduce the time-to-market and increase the competitiveness of the company. Now that IP is transitioning its focus from ICE design to e-motor design, template design tools are required to be developed. [3]

1.1 Purpose of the Study

The recent strategic shift to focus on delivering high-performance electric motors has resulted in the need to develop a series of software tools to assist in the design and development of new units. A key area of focus in this regard is with respect to the initial costing and primary computer-aided design (CAD) development phase of new projects. The current process is inefficient and labour intensive as most of the

functions are performed manually and much of the engineering knowledge is not easily accessible to all designers. This often leads to time wasted on tedious design tasks and searching for engineering information. Since majority of the tasks involved in the initial design and costing phase involve repetitive design and analysis functions, a large portion of this phase of development can be automated.

The purpose of this study is to investigate and develop the foundations of a tool that can assist in automating many of the repetitive tasks encountered in the initial design and costing phase of development for new electric motors.

1.2 Objective of the Study

The objective of this study is to develop the foundations of a software tool that can be used to create a first level design model and indicate a bill of material (BOM) cost for an electric motor based on the parameters defined by a potential customer. The customer would be able to input several parameters (e.g. performance output figures and packaging constraints) into the software tool which will generate a first level CAD model and provide an indication of the material costs for the electric motor. For the purposes of this document, the software tool will be referred to as the AIEED (Automated Intelligent Electric Engine Design) application.

The AIEED tool will help to bridge the gap between the design and analysis functions involved in the initial design and costing phase of a new motor project and helps to speed up the cycle time for the generation of viable concepts for new customer proposals. This will provide a great advantage as there is generally little time and resource available during the decision phase that a prospective customer endures when selecting a technology partner for its e-motor development.

The tool will consist of a series of parametric models that, in conjunction with design rules, would allow for a significant number of parameters to be linked such that the user is only required to define ‘high-level’ feature inputs. The first-level CAD models that are developed by the tool can be used to present viable solutions to the prospective customer and be used as the basis for further detailed design should the customer wish to proceed. In addition to the CAD model output, the tool will also be able to deliver a rough estimate of the material costs for the unit.

1.3 Research Motivation

The motivation behind the study is related to the cycle time associated with the proposal generation and delivery processes for interested potential customers who have submitted formal requests for quotation.

The current processes require significant amounts of labour and time. Since majority of the tasks that need to be undertaken to provide a response to these requests involve repetitive design functions, an electric motor design template and cost estimation tool has been recommended. This research study intends to investigate and develop a tool that can assist in reducing the cycle time and enable a quicker and more valuable response to potential customer enquiries.

1.4 Problem Statement

The cost of delivering a response to new electric motor enquiries is significantly large. This cost is as a result of the time and effort required to determine the characteristic geometrical specifications of the motor and estimate the material cost of the unit. The geometrical specifications and estimate material cost of a motor form part of the fundamental details required in response to new motor enquiries. It is estimated that IP spend 3-4 weeks preparing a response to new motor enquiries [3]. Improving this step in the business process can lead to improved market competitiveness and assist in maintaining IP's market position.

A potential solution to this problem is to develop a software tool (AIEED) to aid in the first-level design development and costing phase of a new electric motor project. The aim of the tool is to reduce the response time and provide an estimate materials cost for new electric motor enquiries. The tool will develop a CAD model of the electric motor which will provide a basis for further detailed development of the final 'delivered' unit.

1.5 Assumptions and Restrictions

The foundations of the AIEED tool will be developed based on the following assumptions and restrictions:

- Integral Powertrain's first business priority is to deliver high performance permanent magnet alternating current (PMAC), more specifically, Surface Permanent Magnet (SPM) motors for electric and hybrid automotive vehicle application. For this reason, the electric motor type will be limited to SPM PMAC units.
- The shape of the electric motor units will be limited to the common radial flux cylindrical type.
- The electric motor units will be limited to 3-phase supply.
- The motor configuration will be limited to external stator and internal rotor type.
- Design options for the windings of the motor will be limited to concentrated double layer windings only.

- The material cost output will be a rough estimate based on general material costs and CAD volume/mass.
- The application will be developed to produce CAD models based on the CATIA V5 or 3DExperience platform (Dassault Systèmes computer aided engineering products). This is the company standard and is recognised as one of the industry standards.
- Certain assumptions and restrictions will be applied to the electromagnetic (EM) and mechanical design specifications that will be included in the application. This is to comply with the necessary intellectual property protection that Integral Powertrain and Intrinsys possess whilst maintaining sound scientific principles.

2 LITERATURE REVIEW

A general literature review was undertaken. The focus of this research was performed on the following aspects; Electric motor theory with specific focus on Permanent Magnet Alternating Current (PMAC) units; PMAC components and their respective design principles and scripting and automated design methods using the CATIA V5 and 3DExperience computer-aided design (CAD) platforms.

2.1 Electric Motor Theory

An electric motor is an electro-mechanical device that converts electrical energy into rotational mechanical energy using the principles of electromagnetism to do so [4]. Electric motors can be classified into several different categories based on the design supply conditions (Alternating Current (AC) or Direct Current (DC)) and physical configuration [5]. A breakdown of the motor classification can be seen in Figure 2.

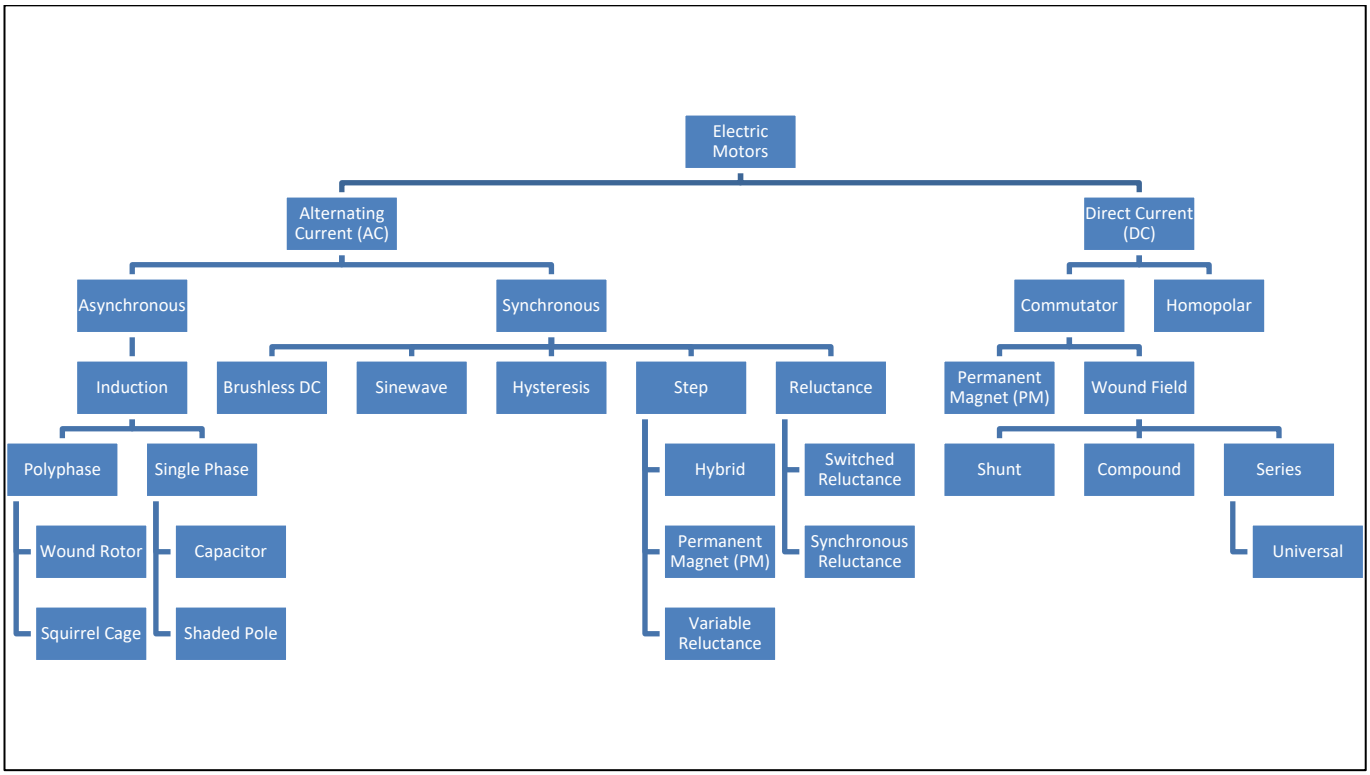


Figure 2: Electric motor classification [5]

Permanent magnet alternating current (PMAC) motors, which form part of the synchronous AC subset, take advantage of the principles of magnetic inductance to convert electrical energy into rotational mechanical energy by making use of permanent magnets to generate the fundamental interaction field [4]. The permanent magnets (PM) that produce the magnetic fields have a significant impact on the performance

of PM motors. Replacing the field windings found in asynchronous induction motors with permanent magnets results in the following benefits: Increased power density, increased efficiency and a more compact design [6].

The permanent magnets provide a low-loss magnetic field without the need for external excitation [7]. This leads to improved efficiency, since no additional power is required to develop the PM magnetic field [8]. In addition, increased efficiency is gained through the increased magnetic field density associated with permanent magnets versus externally excited windings found in induction motors [6]. The improved efficiency and absence of an excitation voltage leads to improved thermal conditions enabling a lightweight and compact motor design [7].

In addition to the low losses associated with PMAC motors, the following characteristics make them suitable to hybrid vehicle application [8] [9]:

- Overall large torque and high-power density.
- High torque at low operating speeds which is suitable for vehicle initial launch and for climbing gradients.
- High power at high operating speed.
- Maximum efficiency over both a wide speed and wide torque range.
- Short-term overload capacity[1]. This is typically around two times the rated torque over a short duration.
- Relatively low cogging torque[2] and low torque ripple[3].
- High reliability for all operating conditions.
- Minimal weight and space occupation and low acoustic noise.
- Low maintenance requirement, high reliability and high efficiency

[1] Overload capability: There are certain instances in a motors operation, typically at start-up, where the current draw is very high for a short duration. The extent and duration to which the motor can operate beyond the rated performance is defined as the overload capacity. [81]

[2] Cogging torque is defined as the parasitic torque produced due to a variation in self-inductance typically as a result of slots on stator or rotor of a motor. [4]

[3] Torque ripple is defined as the torque variations about a constant value present at stable supply conditions. [4]

However, despite these benefits, PMAC motors have inherent difficulties related to the use of permanent magnets. Permanent magnets tend to be relatively high cost and difficult to manufacture [7]. In addition, permanent magnets are susceptible to demagnetisation and sensitive to thermal and chemical factors which may influence their behaviour and magnetic strength [10]. The factors that need to be considered when selecting permanent magnets for PMAC motor design are discussed further in sections *2.2.1 Fundamental Electromagnetic Theory* and *2.2.4 Permanent Magnets*

As illustrated in Figure 3 a typical PMAC motor is made up of the following key components: Rotor and permanent magnets, stator and windings, busbars and termination rings, resolver or encoder and the housing elements [11]. The design details of the primary components are discussed further in section *2.2 Surface Permanent Magnet Alternating Current Motor Design Principles*.

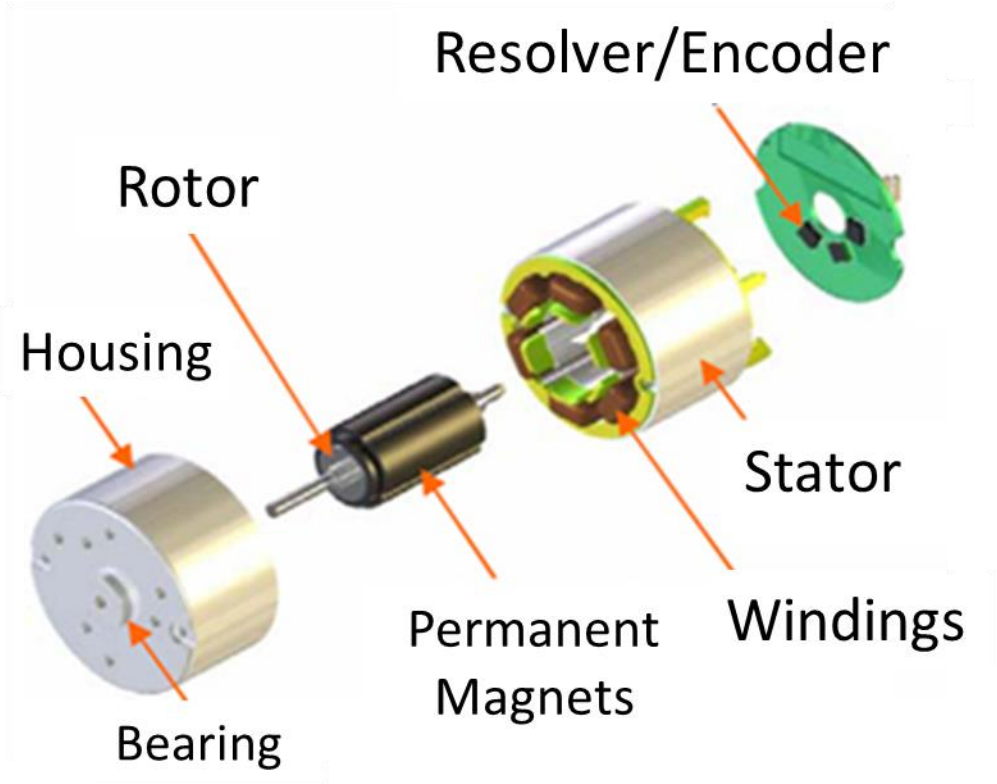


Figure 3: Typical Permanent Magnet Alternating Current (PMAC) Motor [11]

The stator assembly of a PMAC motor is the stationary component that contains the windings or coils that receive electrical charge. The flow of electrical charge through the windings induces a magnetic field [12]. The stator is typically made up of a series of stator 'teeth' which consist of an iron core wrapped by a coil of conducting wire (generally copper). The stator windings are terminated at one end to the busbar

assembly. The busbar assembly is responsible for carrying the electrical charge from each phase of the 3-phase input AC current and distributing the charge amongst the stator windings. The other ends of the windings are terminated to a common conductive ring. Figure 4 illustrates a stator ring assembly terminated to a busbar assembly. [4]

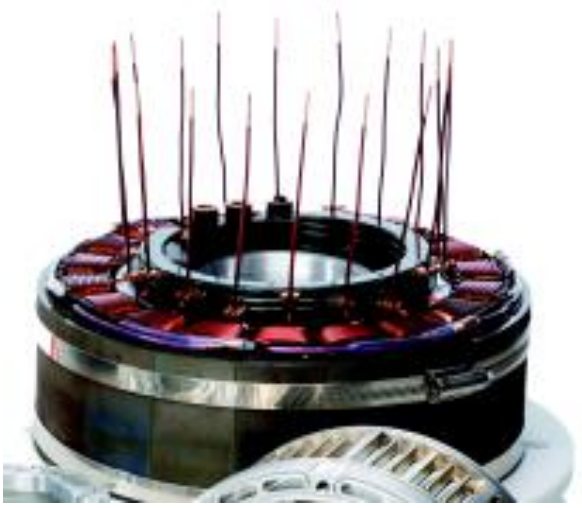


Figure 4: Stator and busbar assembly of an Integral Powertrain electric motor [13].

The full stator, complete with fully wound coils, is inserted into a housing. It is critical that the housing is fully isolated from the windings, and other charged elements, such that no high-voltage charge flows through it [4]. The housing design must take into account stator cooling, include features for mounting to the rest of the powertrain and be robust enough to cope with the stresses it experiences. [5]

The rotor assembly of a PMAC motor is the driven component that exhibits rotational mechanical energy. The rotor assembly is made up of a rotor hub, a rotor stack and the permanent magnets. The rotor assembly is inserted into the stator and housing assembly with bearings such that it can rotate freely. As can be seen in Figure 5 the air gap between the rotor and stator is generally very tight and geometrically controlled. [4] This is an important factor that contributes to the performance of the PMAC motor and is discussed further in *2.2 Surface Permanent Magnet Alternating Current Motor Design Principles*.



Figure 5: Example of rotor assembly inserted into stator and housing assembly [14].

The permanent magnets in the rotor assembly are orientated in a manner which allows the interaction between their respective magnetic fields and the induced magnetic fields present in the stator windings to develop a torque on the rotor assembly [4]. PMAC motors are externally commutated by means of an inverter which controls the electrical charge distribution amongst the groups of windings of the stator in a manner which allows for the speed and torque outputs of the motor to be controlled. [4]

There are 2 primary configurations of PMAC motors, namely: Surface Mounted Permanent Magnet (SPM) and Interior Permanent Magnet (IPM) units [4].

2.1.1 Surface Permanent Magnet versus Interior Permanent Magnet Motors

The principal difference between SPM and IPM motors is with regards to the location of the permanent magnets [15]. As can be seen in Figure 6, magnets in SPM motors are mounted to the exterior surface of the rotor stack, whereas in IPM motors the magnets are mounted within cut-outs in the rotor stack.

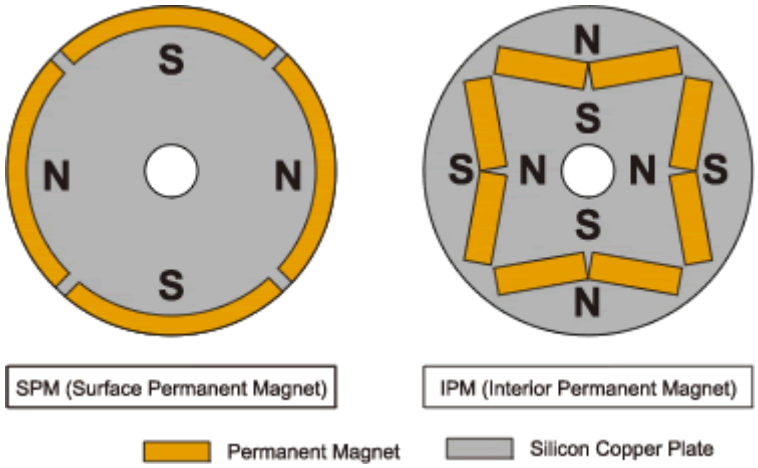


Figure 6: Surface Permanent Magnet motors versus Interior Permanent Magnet motors [15]

These architectural differences do have an impact on the electromagnetic performance characteristics of the motor. The orientation, alignment and location of the magnets in IPM motors results in saliency[4] characteristics which provides certain performance and control advantages. As illustrated in Figure 7, the inductance path, described in further detail in *2.2.1 SPM Motor Operating Principles and Analytical Investigation (Performance)*, between the rotor and stator is inconsistent. This is as a result of the discontinuities introduced by inserting the magnets within the rotor core. Typically, the permanent magnet will exhibit lower inductance characteristics in comparison with the rotor core material, hence the inductance measured in the flow path passing through the magnets (L_d) is lower than the inductance measured across the path passing through the rotor core material (L_q) only [16].

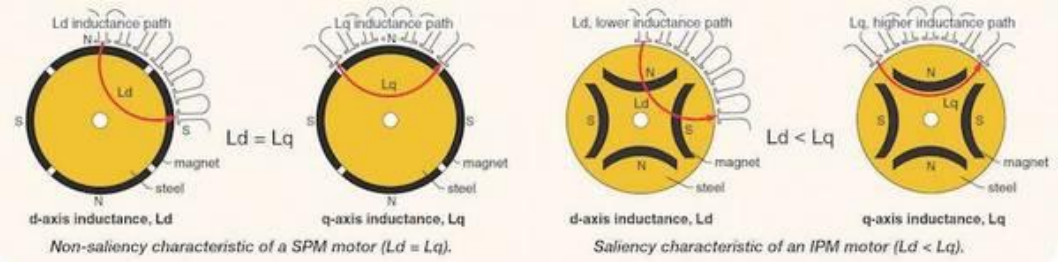


Figure 7: Inductance path comparison - Surface Permanent Magnet versus Interior Permanent Magnet [17]

[4] Saliency is a measure of a motors inconsistency with regards to magnetic properties. This inconsistency, or non-symmetry, is as a result of differences in reluctance path between the rotor and stator. This difference is either as a result of geometry or material properties. [15]

SPM motors, however, tend to exhibit fairly constant magnetic flux between the rotor and stator. As can be seen in Figure 7, since the magnets do not interfere with the rotor core material, SPM motors exhibit constant inductance regardless of the path ($L_d = L_q$) [17].

As a result of the saliency characteristics, IPM motors produce two components of torque, namely: magnetic (alignment) torque and reluctance torque [18]. The reluctance torque component provides an advantage with regards to motor control and high-speed operation. By employing flux-weakening methods IPM motors can be designed and controlled to have a greater constant power speed range (CPSR)[5] [14] [19]. In addition, flux concentration methods can be applied in the design of IPM motors to reduce the quantity of permanent magnet material required, potentially leading to a more cost-effective solution [20]. Since SPM motors are non-salient, the torque produced is purely in the form of magnetic (alignment) torque [17].

SPM motors typically have lower peak operating speed capacity because of the limited mechanical strength between the bonds securing the magnets to the rotor hub. In IPM motors, however, the mechanical strength tends to be higher since the magnets are embedded in the rotor hub. The rotor hub iron core tends to provide greater mechanical strength to overcome the centripetal loads experienced during operation. [5]

IPM motors are more suited to applications where greater operating speed range is required. This is because of their excellent field weakening capability [21]. SPM motors typically have the advantage of a simpler design but tend to offer very little overload protection. On the other hand, IPM motors provide good overload capacity but tend to be more complex to manufacture [8]. Although both SPM and IPM motors exhibit good efficiency and high-performance, SPM motors tend to suffer from extra losses at high operating speeds and IPM units suffer at low speeds. These characteristics are as a result of the configuration and associated manufacturing limitations plus harmonics loss issues [8].

Although IPM motors do have certain performance advantages over SPM motors, the simplicity in design and manufacture means that majority of Integral Powertrain's customers select this motor type for their application. For this reason, the project scope has been limited to SPM motors only, however, it will be beneficial to extend the application scope in future to incorporate IPM motors.

[5] The constant power speed range or ratio (CPSR) is defined as the operating speed range of a motor where constant maximum power can be achieved. [31]

2.2 Surface Permanent Magnet Alternating Current Motor Design Principles

An investigation of the design principles specific to SPM AC motors was completed, this includes an analytical investigation of performance and detailed investigation into each of the fundamental components that make up an SPM motor, namely: stator assembly, rotor assembly, permanent magnets and housing elements.

2.2.1 SPM Motor Operating Principles and Analytical Investigation (Performance)

The electromagnetic principles that govern the performance of SPM motors involves microscopic interactions which can be described at a macroscopic level [12]. For this reason, the analytical investigation will be limited to the macroscopic elements of electromagnetism. Although some concepts have already been introduced, a more detailed investigation, with emphasis on the analytical aspects related to SPM motor design, is presented.

PMAC motor operation relies on the conversion of electrical energy to mechanical energy by leveraging the principles of magnetism. The conversion from electrical energy to mechanical energy is completed by using magnetic energy [5]. The function of a PMAC motor is to produce rotational power and torque [5]. To determine the torque production capability of a motor, it is necessary to understand and formulate analytical methods to describe the impact of magnetic energy on the torque output. It is therefore necessary to present the relevant fundamental theory.

Fundamental Electromagnetic Theory

Magnetism is a natural phenomenon including a force field, or magnetic field, which is developed as a consequence of an electromagnetic force [12]. A magnetic field can be developed as a result of a permanent magnet, which has a particular microscopic structure, electrical charge or moving particle [12]. All magnets have 2 poles (North and South) between which the magnetic field can be drawn. Conventionally the magnetic field produced by a magnet is visualised with 3-dimensional field lines drawn perpendicular to the surface of each pole with the flow defined as positive from the north-pole to the south-pole. An example of a magnetic field can be seen in Figure 8 [22].

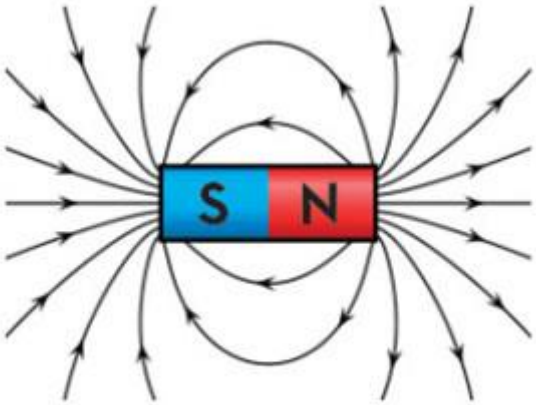


Figure 8: Permanent magnet with magnetic field line representation [22]

It is important to understand that an attractive force is experienced between opposite magnetic poles (N-S and S-N) and a repulsive force experienced between like magnetic poles (N-N and S-S) [12]. Ferrous materials are magnetic and as such, iron filings often used to visualise the magnetic field generated by a permanent magnet or electromagnet [12].

A magnetic field can be described by the two vector quantities of magnetic flux density[6] and magnetic field intensity/strength[7]. This relationship can be approximated to follow a linear relationship over typical operating conditions for many materials and can be described as follows [5]:

$$B = \mu H \tag{1}$$

$B - Magnetic\ flux\ density\ \left[T\ OR\ {}^{Wb}/_{m^2}\right]$

$H - Magnetic\ field\ intensity\ \left[{}^{A}/_{m}\right]$

$\mu - Permeability\ of\ the\ material\ \left[{}^{H}/_{m}\ OR\ T \cdot {}^{m}/_{A}\right]$ [8]

[6] Magnetic flux density can be described as the density of a magnetic field flowing through a given area of the medium. [19]

[7] Magnetic field intensity/strength can be described as the resulting change in intensity of the magnetic field due to the interaction of the magnetic flux with the material interacting in the magnetic field. [19]

[8] The permeability of a material is the measure of how well it promotes magnetic flux flow, with a greater value indicating greater flux flow capacity.

The electromagnetic interactions between ferrous materials, typically electrical steels, and permanent magnets, is important in motor design [5]. Therefore, it is necessary to understand how a material is affected by magnetisation. These ferrous materials are commonly used in motor construction [5]. However, their permeability and other electromagnetic properties are non-linear and often have multiple values [5]. The properties are a function of the historical field intensities to which the material has been exposed. For this reason, it is common to describe the behaviour and properties of a ferromagnetic material using its hysteresis loop (B-H Curve) [5]. An example of a typical hysteresis loop can be seen in Figure 9.

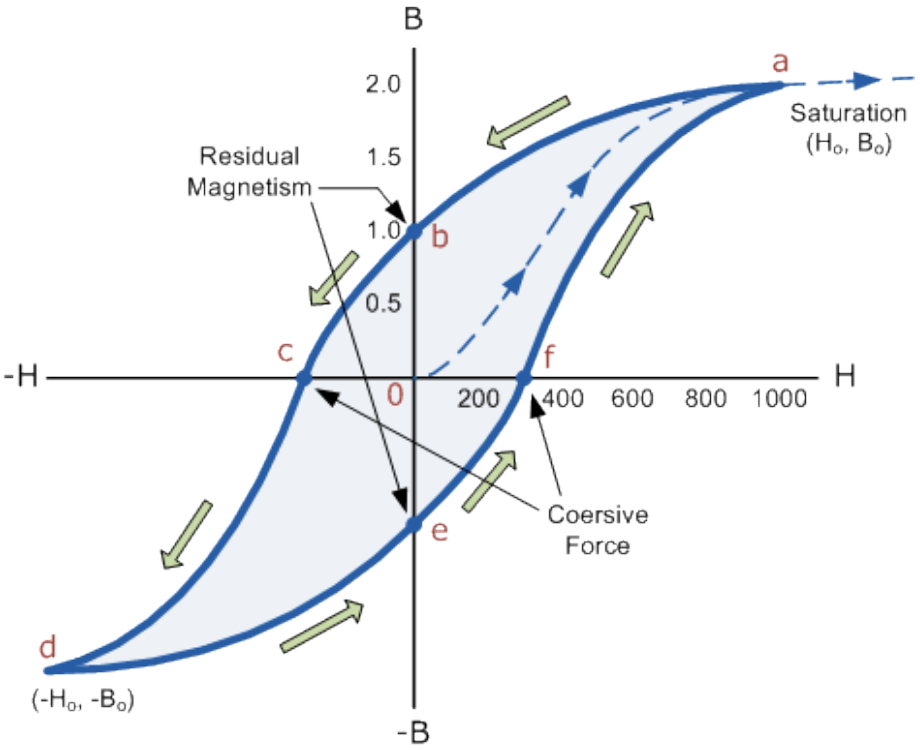


Figure 9: Sample magnetic hysteresis loop [23]

It is important to note that ‘B’ represents the measured or induced field and ‘H’ represents the applied field. The curve can be described as follows. Assume that an unmagnetised piece of ferromagnetic material (sample) is exposed to zero magnetic field. In this instance, the magnetic domains within the material counteract each other and are in equilibrium [24]. This state results in zero magnetic field and the materials magnetic state is at the origin on the B-H curve (See Figure 9). Let’s assume that an external magnetic field is applied (positive H is introduced). This energy causes some of the magnetic domains within the sample material to re-orientate, by induction, in the direction of the external field [24]. As the external field is increased, the sample begins to produce a magnetic field (B is the combination of the applied field, H, and the induced field). The magnetic field strength produced by the sample increases with increasing external

field until a saturation point is reached. This is illustrated in Figure 9 as the curve moves from the origin to point a. At the saturation point a, any additional external magnetic field strength will not increase the magnetisation of the sample [24]. The saturation point of the material is dependent on its molecular structure. An indication of the saturation points of certain common material groups can be seen in Figure 10.

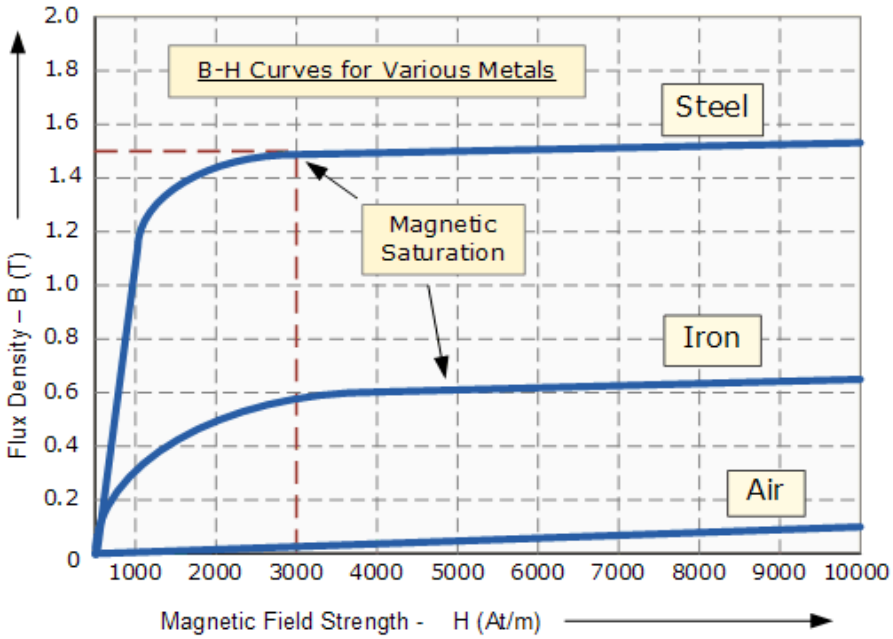


Figure 10: B-H Curves for common material groups indicating magnetic saturation points [23]

As the applied external magnetic field strength is reduced (reducing H), the sample's magnetic field reduces. However, when the external field reaches zero, the sample's field settles at point b due to residual magnetism in the material [24]. In a permanent magnet, the point b in Figure 9 is known as the residual induction or remanence of the magnet (B_r) and is defined as the magnetic induction remaining in the material after it has been magnetised [25]. This is effectively a measure of the 'magnetisation' of a magnet.

The magnetic field of the sample can be reduced to zero again, however, it is necessary to reverse the direction or polarity of the external field to do so [24]. Increasing this reverse magnetic field will take the curve from point b to c which is known as the coercive force (H_c) [24]. The coercive force is defined as the external magnetic field strength which will result in null overall magnetic field [24]. A material property often used when selecting a permanent magnet is its intrinsic coercivity $\left(H_{ci}\ OR\ H_{cJ}\right)$. This is a measure of the magnets resistance to de-magnetisation [24]. Should the external field drop below the intrinsic coercivity the sample will exhibit zero magnetic field strength [24]. The onset of demagnetisation does

occur at a stage prior to the intrinsic coercivity value and this H_k value is important when selecting a permanent magnet.

Increasing the reverse field further will induce a magnetic field in the sample in the reverse direction. Increasing this field further will eventually lead to a reverse saturation point at d [24]. The point d is symmetrical to b in that the magnitude of the field strength is the same [24]. Reducing the reverse field will move the operating point along the curve to a negative residual induction point at e [24]. Increasing the external field strength in the positive direction again will move the operating point from e to f at which zero magnetic field strength is produced [24]. The external field strength at this point is equal to the coercive force. A further increase in the external field strength will move the operating point to saturation at a. [24]

The full curve is known as the magnetic hysteresis loop and is applicable to the ferromagnetic materials often used in stator and rotor cores and for permanent magnets. [24]

The magnetic fields described thus far are theoretically infinitely big; however, the flux density and field strength diminishes significantly as one travels away from the flux source [26]. The field strength effectively becomes insignificant beyond a certain distance from the magnet. This distance is dependent on the magnets inherent magnetic field strength defined by the residual induction or remanence of the magnet [24]. The relationship between the magnetic flux density and the distance from the source is a complex relationship, however an example of this can be seen in the following simplified expression for a symmetrical rectangular magnet of defined dimension. This expression can be used to determine the magnetic flux density observed at a specific distance along the symmetry axis (See Figure 11) [27]:

$$B = \frac{B_r}{\pi}\left[\tan^{-1}\left(\frac{LW}{2z\sqrt{4z^2 + L^2 + W^2}}\right) - \tan^{-1}\left(\frac{LW}{2(D+z)\sqrt{4(D+z)^2 + L^2 + W^2}}\right)\right] \quad (2)$$

$B - Magnetic\ flux\ density\ at\ point\ where\ field\ is\ being\ determined\ \left[T\ OR\ {}^{Wb}/_{m^2}\right]$

$B_r - Residual\ induction\ or\ Remanence\ field\ of\ the\ magnet\ (Physical\ magnetic\ property)\ \left[T\ OR\ {}^{Wb}/_{m^2}\right]$

$L - Length\ of\ magnetised\ block\ \ [m]$

$W - Width\ of\ magnetised\ block\ \ [m]$

$D - Thickness\ or\ height\ of\ magnetised\ block\ \ [m]$

$z - Distance\ from\ pole\ face\ to\ point\ where\ field\ strength\ is\ being\ measured\ along\ symmetry\ axis\ \ [m]$

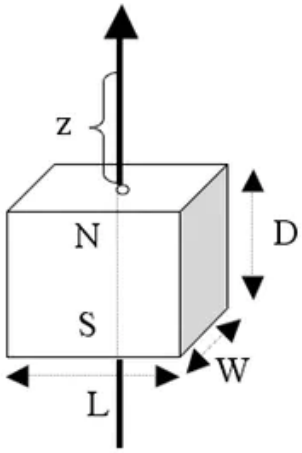


Figure 11: Magnetic field flux density at distance z along symmetrical axis of block magnet [27]

If a very thin rectangular magnetic block (or magnetic material), which produces a magnetic field, is considered and it is assumed that the flux density experienced across the block remains constant, the magnetic flux can be determined as follows [5] (See Figure 12):

$$\emptyset = BA \tag{3}$$

$\emptyset - Magnetic\ flux\ [T.m^2\ OR\ Wb]$

$A - Cross\ sectional\ area\ of\ magnetic\ block\ [m^2]$

If the block is extended such that is has a significant length in the direction of the flux flow, it is possible to determine the total change in field intensity as follows (See Figure 12) [5]:

$$MMF = Hl \tag{4}$$

$MMF - Magnetomotive\ force\ [A]$

$l - Length\ of\ block\ in\ the\ direction\ of\ magnetic\ flux\ [m]$

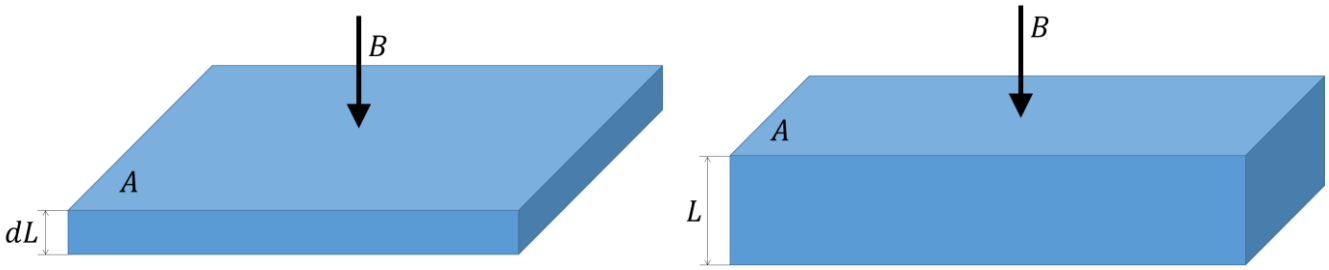


Figure 12: Infinitely thin magnetic block and magnetic block of defined thickness

The magnetomotive force (*MMF*) can be defined as the driving force for magnetic flux and is analogous to electromotive force (*EMF*) in electrical circuits [28]. Therefore using (1) (2) and (4):

$$\emptyset = \mu H A \tag{5}$$

$$\emptyset = \frac{\mu A}{l} MMF$$

Where the permeance of the material can be defined as [5]:

$$P = \frac{\mu A}{l} \tag{6}$$

$P - Permanence\ of\ the\ material\ \left[{}^{Wb}/_{A}\ OR\ H\right]$

$$\therefore \emptyset = P \times MMF \tag{7}$$

It is evident therefore that materials with greater permeability have greater permeance which indicates a greater flux flow capacity [5].

The inverse of permeance is known as reluctance. Reluctance is a measure of the material's ability to resist flux flow and is defined as [5]:

$$R \equiv \frac{1}{P} = \frac{l}{\mu A} \tag{8}$$

$$\therefore MMF = \emptyset R \tag{9}$$

SPM motors generate torque as a result of the interaction between the magnetic fields of the permanent magnets on the rotor and those induced within the stator windings [5]. The stator windings consist of copper wire wound in a coil. These windings carry electrical current which induces a magnetic field based on the principles of electromagnetism [5]. Amperes law indicates that current flowing through a conductor generates a magnetic field. The magnetic field magnitude at a point within the medium induced by current flowing through a very long and straight conductor can be described as follows (See Figure 13) [12]:

$$\left|\vec{B}\right| = \frac{\mu_0 i}{2\pi r} \tag{10}$$

$i - Current\ flow\ through\ conductor\ [A]$

$r - Distance\ from\ conductor\ to\ point\ in\ magnetic\ field\ where\ magnetic\ field\ strength\ is\ being\ measured\ [m]$

$\mu_0 - Permeability\ of\ free\ space, \mu_0 = 4\pi \times 10^{-7} [^{H}/_{m}\ OR\ T \cdot {}^{m}/_{A}]$

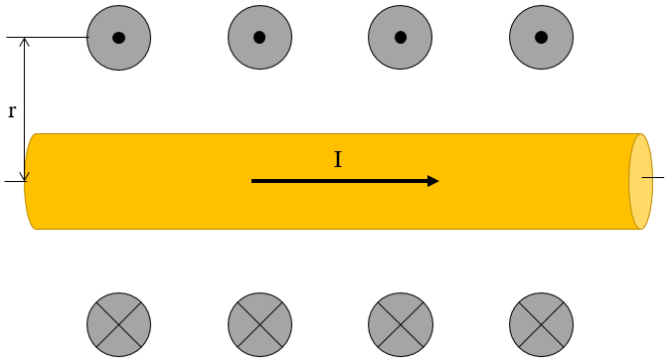


Figure 13: Example of magnetic field induced by current flow through conductor

The magnitude of the magnetic field can be determined using equation (10) however, to fully define the vector quantity, it is necessary to determine the direction of the magnetic field. As illustrated in Figure 13, Amperes law indicates that the right-hand rule be used to determine the vector direction [26]. It is possible to see that by closing the right hand with the thumb pointing outwards and orientating the thumb such that it is aligned with the direction of current flow, the other curved fingers will determine the direction of the magnetic field, which is made up of many concentric circles [26]. From (10) it is evident that the field strength magnitude reduces as the distance from the conductor increases.

An application of this principle is very important in SPM motors which make use of conductors formed into a coil (windings). When doing so, the magnetic field induced in the conductor is generated in a manner illustrated in Figure 14, which is approximately uniform in the volume contained by the coils [26]. The magnetic field generated can be derived in terms of the number of turns in the coil and if assumed ideal can be expressed as [26]:

$$B = \mu_0 \frac{N}{l} i \tag{11}$$

$N - Number\ of\ turns\ in\ coil\ [-]$

$l - Length\ of\ coil\ [m]$

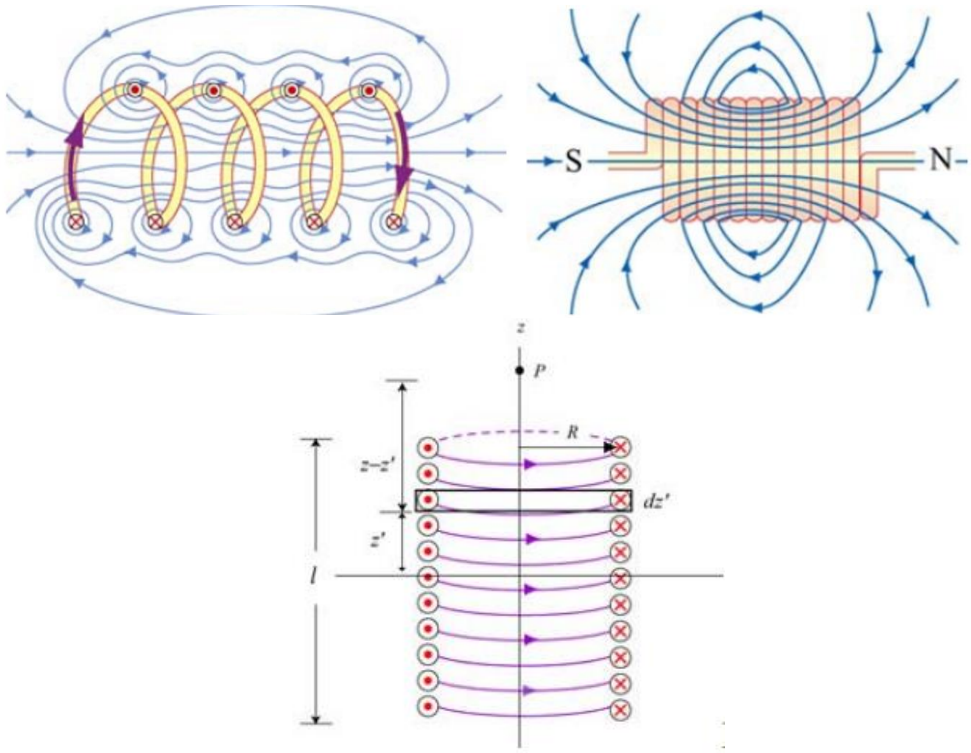


Figure 14: Magnetic field lines induced by current travelling through coil [26]

Should the coil be wrapped around a highly permeable core material (See Figure 15), it is acceptable to assume that the field is confined to travel through the material exclusively [5].

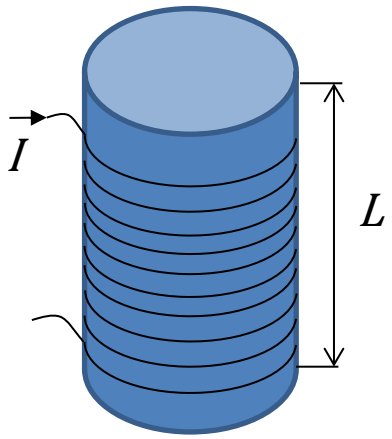


Figure 15: Coil wrapped around magnetic core material

If it is assumed that the core material be infinitely permeable, the field intensity can be determined using the following [5]:

$$H = \frac{Ni}{L} \tag{12}$$

$L - Length\ of\ coil\ wrapped\ around\ core\ material\ [m]$

Faradays law of induction indicates that the inverse of the above principles is true in that an electromotive force (or voltage) is induced by a change in magnetic field. The law is described as follows [26]:

$$\varepsilon = -\frac{d}{dt}(BA\cos\theta) \tag{13}$$

$\varepsilon - Induced\ EMF\ [V]$

$A - Area\ enclosed\ by\ conducting\ loop\ [m^2]$

$\theta - Angle\ between\ the\ magnetic\ field\ and\ the\ normal\ to\ the\ conducting\ loop\ area\ [°]$

An important factor linked to Faradays law is formalised in Lenz's law [29] which states that "the induced current in a loop is in the direction that creates a magnetic field that opposes the change in magnetic flux through the area enclosed by the loop" [12]. This phenomenon contributes to a performance inhibiting factor known as back *EMF*. As current (or *EMF*) is supplied to a motors coils, the induced magnetic field interacts with the magnetic field from the permanent magnets and generates torque. Dependent on load, the torque will generate rotational motion. This motion will result in an additional *EMF* which opposes the supplied voltage and reduces the overall current flow in the desired direction, hence limiting the available power [30].

Another interesting phenomenon that results from these principles is the formation of eddy currents. Eddy currents are circulating currents induced in pieces of conducting material as they pass through a magnetic field [12]. The changing magnetic flux experienced by the material travelling through the magnetic field causes free electrons in the material to move in a swirling motion which results in the eddy currents [12]. Lenz's law dictates that these eddy currents travel in a way such that they create magnetic fields to oppose the original change in magnetic flux inducing the current [29]. For example, if a plate of conducting material is passed through a magnetic field with significant speed, eddy currents will form. The eddy currents will be generated such that they create their own magnetic field which seeks to oppose the motion of the plate. This electromagnetic phenomenon has a significant role to play in efficient electric motor design [12].

The fundamental electromagnetic principle which links electromagnetism to a physical field is described by Lorentz force which explains that a particle experiences a physical force due to electric and magnetic

fields [31]. This can be extended to analyse current flow through a conductor, which experiences a force described as follows (See Figure 16) [31]:

$$F = Bil \sin\theta \tag{14}$$

$F - Force\ experienced\ by\ current\ carrying\ conductor\ [N]$

$l - Length\ of\ conductor\ interacting\ with\ magnetic\ field\ [m]$

$\theta - Angle\ between\ the\ magnetic\ field\ direction\ and\ direction\ of\ current\ flow\ in\ conductor\ [°]$

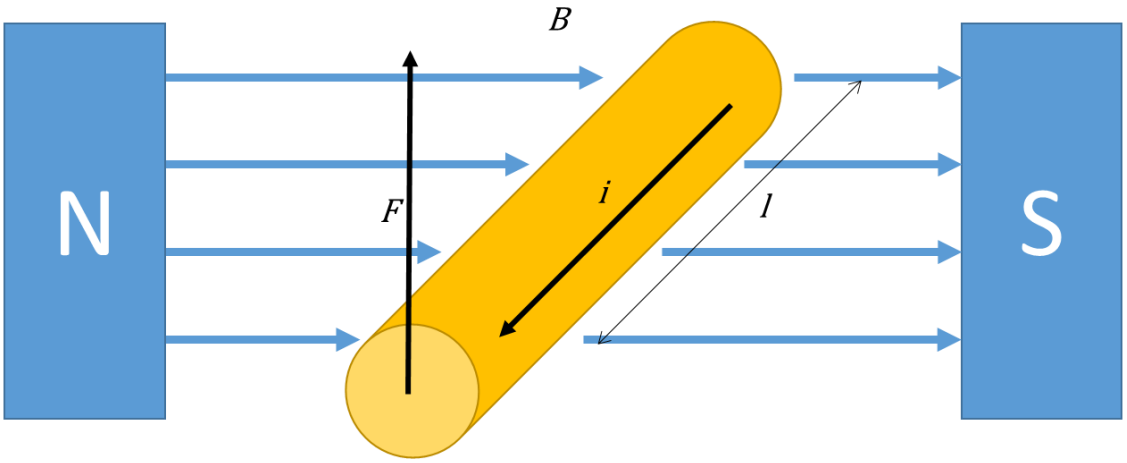


Figure 16: Force experienced by current carrying conductor in magnetic field

The magnetic field induced in the conductor interacts with the external magnetic field resulting in a region of greater magnetic flux. The conductor experiences a force which tends to 'push' the conductor into the region of less magnetic flux [31]. The direction of the force experienced by the conductor is determined using Fleming's left-hand rule [12]. The rule explains that one must align their left index finger with the direction of the magnetic field and their left middle finger in line with the current flow. The resulting thumb orientation which is perpendicular to both the index and middle finger indicates the direction of the force [12].

Electric Motor Operating Principles

The primary function of electric motors is to generate torque[9]. This torque is generated by taking advantage of the electromagnetic principles introduced in *Fundamental Electromagnetic Theory*. In SPM motors, torque is developed as a result of the interactions between the magnetic fields developed by the permanent magnets and windings in the stator. To understand how this interaction develops torque consider two scenarios where a permanent magnet (PM) is contained within a stationary ring of ferrous material. [5]

One scenario consists of a simple ring whereas the other contains a ring with two tabs (See Figure 17). The PM is free to rotate about its centre and is positioned such that its rotational axis is coincident with the centre of the ring. The PM and the ring are separated by an airgap. Since the force experienced due to magnetic attraction is greater when the airgap is smaller, it is evident that in the case of a simple ring, a consistent attraction force is experienced irrespective of the angular position of the magnet. In this case, the magnet experiences zero net force and thus zero torque. This relationship means that the PM has no preferred rest position. [5]

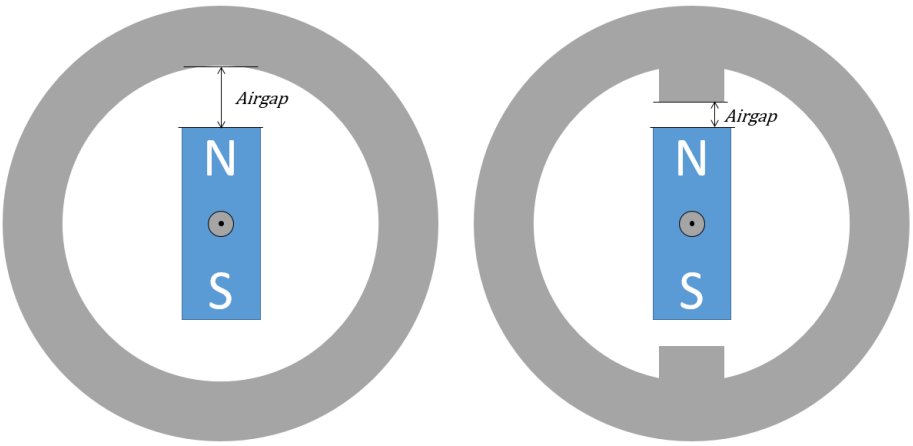


Figure 17: Magnet free to spin in simple ring and ring with two poles

However, when two equally sized tabs, or poles, are introduced in the ring, the force is no longer constant and becomes a function of the angular position of the PM (See Figure 18). When rotated, the magnet would tend to align itself in the direction with the strongest magnetic field where the airgap is smallest. Therefore, if the magnet is externally rotated it will experience a stronger force of attraction when aligned with the

[9] Torque is defined as a twisting force experienced when a tangential load ($F[N]$) is applied to a point at a distance ($r[m]$) from the torque axis. $T = Fr\ [N.m]$ [12]

poles in the ring. This force has a tangential component, with the magnitude a function of the angular position, which results in a net torque experienced by the magnet. The torque experienced by the magnet can be described as a function of the angular position and, as illustrated in Figure 18, can be approximated as sinusoidal. [5]

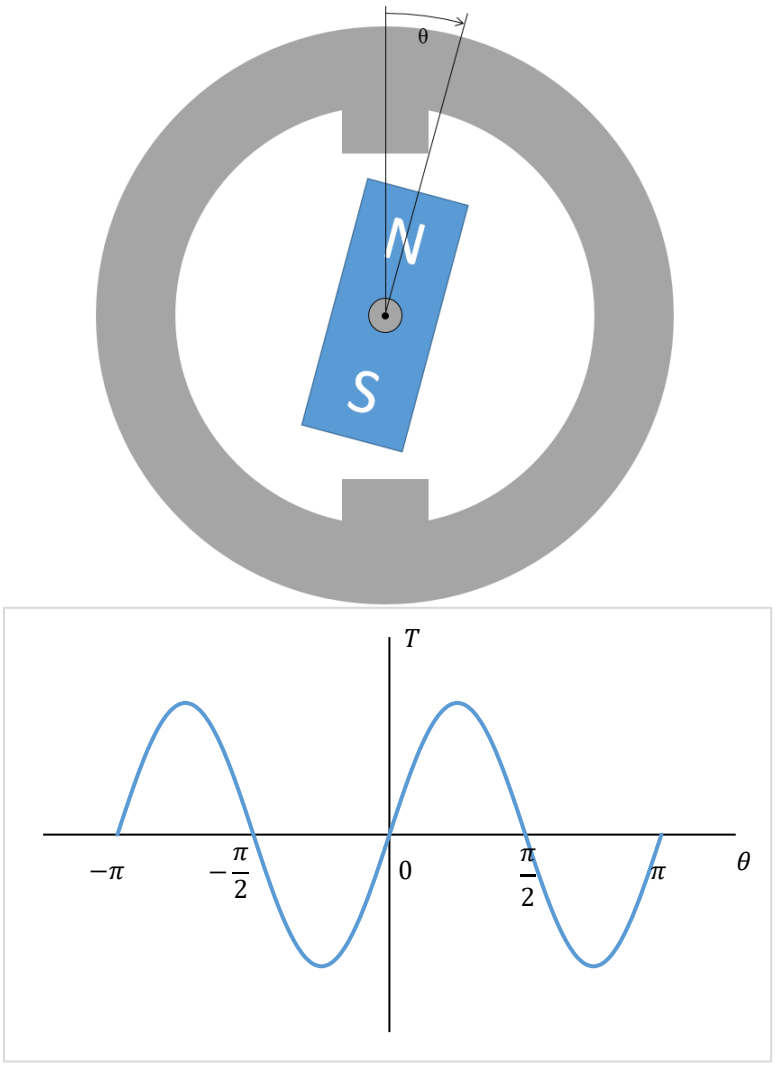


Figure 18: Torque variation with angular position experienced by magnet in two-pole ring [5]

The aforementioned torque is experienced because of the saliency in the stator and is defined as reluctance torque, if desired, and cogging torque if it serves to hinder the motors performance [5].

By leveraging the principles of electromagnetics, it is possible to improve and control the torque production by making use of electromagnets. Windings can be formed by wrapping current carrying conductors around the tabs (See Figure 19). The current flow will induce a magnetic field in the iron ring which will interact with the PM to enhance the torque production. This component of the torque is defined as mutual or

alignment torque [5]. The current flow direction can be controlled to manipulate the magnetic field direction to optimise the torque production based on the position of the magnet by making use of both the attractive and repulsive force phases to generate torque [5]. This concept can be extended to generate multi-pole stators which allow the PM to rotate completely with torque control available. [5]

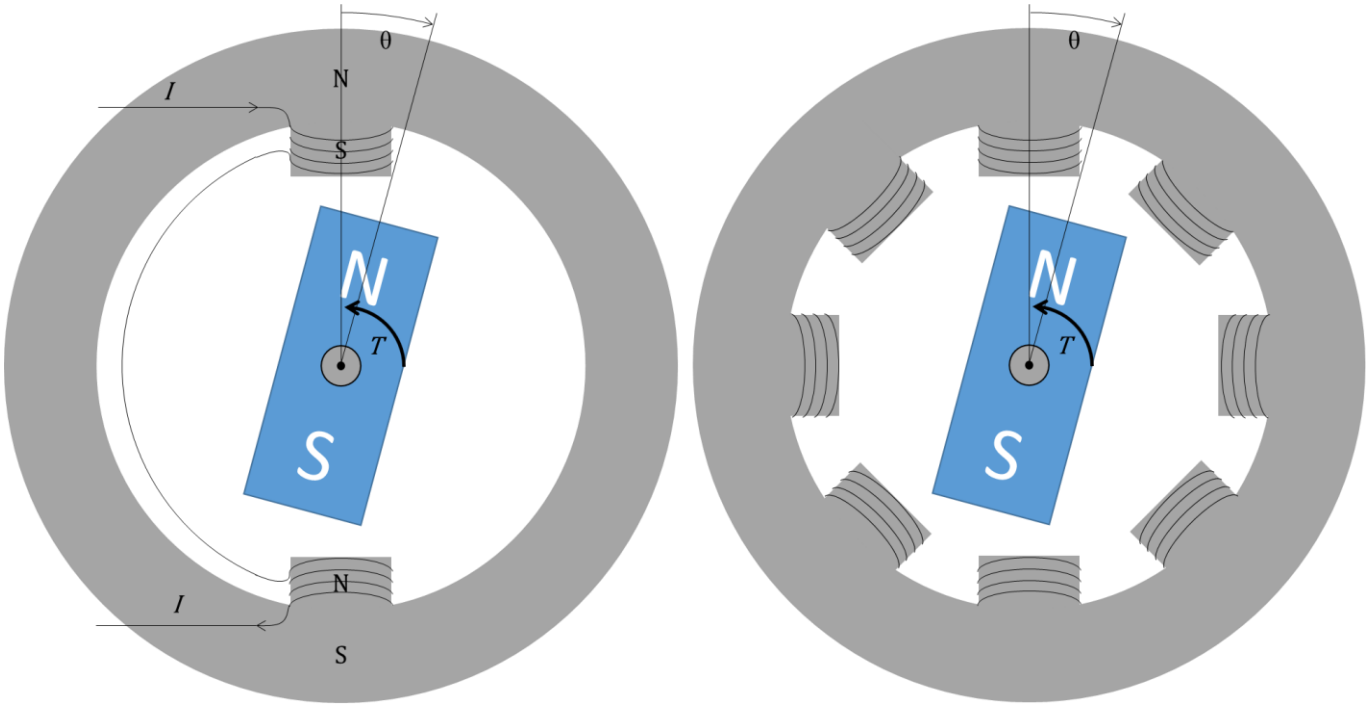


Figure 19: Current carrying conductor introduced to generate mutual/alignment torque component and extended multi-pole stator

The multi-pole stator illustrated in Figure 19 is an example of a 3-phase 3-pole pair stator. Two and three phase motors are common place as they minimise the requirement for additional power electronics necessary for control [5]. The sample motor has a 2-pole magnet (1-pole pair[10]); however, it is possible to construct the rotor with two to over fifty magnet poles [5]. Increasing the number of magnets tends to increase the torque production with constant electrical current, however the optimal number of magnet poles is based on geometrical and material factors. [5]

[10] A magnet pole pair can be defined as one north magnetic pole and one south magnetic pole facing the air gap. [4]

SPM Motor Performance

The design of an SPM motor begins with an understanding of its application and output requirements. The performance and characteristic parameters included in Table 1 are typically considered as the high-level driving parameters which are used as a basis for SPM motor design [3].

Table 1: High-level design parameters in electric motor design

Parameter	**SI Units**
Maximum Power Output	W
Maximum Speed	rpm
Constant Power Speed Range	rpm/rpm
Motor sizing consideration (e.g. Torque Per Unit Rotor Volume)	Nm/m^3
Number of Magnet Pole Pairs	-
Airgap Length	m
Voltage Input (DC)	V
Rotor Magnet Outer Diameter	m

When designing a motor, the first parameters that must be defined are the maximum power output and maximum rotational speed. To appreciate the relationship between power, torque and rotational speed it is necessary to understand the torque and power output characteristics of an SPM motor. Figure 20 illustrates the typical ideal torque and power curves of an SPM motor [32].

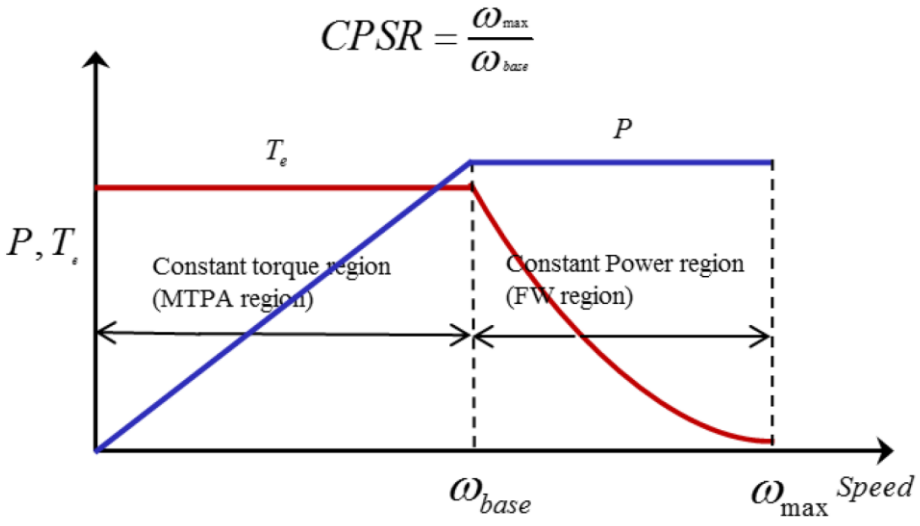


Figure 20: Typical SPM motor power and torque versus speed characteristics [32]

It is evident that the power and torque curves can be separated into two regions, namely; the constant-torque and constant-power regions. These regions are separated at the base speed (ω_b) of the motor which

represents the speed at which maximum torque and power are produced [33]. The relationship between the power and torque curves can be approximately described by the following [34]:

$$P = \omega T \tag{15}$$

$P - Power\ output\ [W]$

$\omega - Rotor\ angular\ velocity\ \left[{}^{rad}/_{s}\right]$

$T - Torque\ at\ \omega\ [Nm]$

Initially, in the constant-torque region, the power increases as the rotational speed is increased until the base rotational speed is achieved (See Figure 20). After this point the constant-power region is entered and for the expression to hold true, torque must decrease as the rotational speed increases. [32]

The CPSR (constant power speed range/ratio) is used to relate the maximum rated output speed with the base speed of the motor and is expressed as follows [19]:

$$CPSR = \frac{\omega_{max}}{\omega_b} \tag{16}$$

$CPSR - Constant\ power\ speed\ range/ratio\ [-]$

$\omega_{max} - Maximum\ rated\ output\ speed\ of\ the\ motor\ (highest\ speed\ where\ Power\ is\ at\ maximum)\ \left[rpm\ OR\ {}^{rad}/_{s}\right]$

$\omega_b - Base\ speed\ of\ motor\ (Power\ and\ Torque\ at\ maximum)\ \left[rpm\ OR\ {}^{rad}/_{s}\right]$

A fundamental aspect of motor design is related to motor sizing. Since the mechanical torque developed by a shaft is directly related to its physical size ($T_m = Fr$) [5], the relationship between a motor's torque output and its size is important. The following expression provides an understanding of the relationship between torque and an SPM motor's size [35]:

$$T = k{D_R}^2 L_R \tag{17}$$

$T - Torque\ [Nm]$

$k - Motor\ constant\ \left[{}^{N}/_{m^2}\right]$

$D_R - Rotor\ diameter\ [m]$

$L_R - Axial\ rotor\ length\ [m]$

As a motor is extended in terms of length, the torque output increases linearly. For example, if the torque output of a motor of length L_R is T_L, the torque produced by the same motor extended to $2L_R$ will produce a torque of $2T_L$. [35]

The relationship between the torque and the rotor diameter is influenced by multiple factors. From a purely mechanical point of view the torque developed by a shaft is $T_m = Fr$ [5]. Therefore, the torque produced has a linear relationship with the rotor diameter. However, the force experienced by the shaft is a function of the rotor diameter as well. This notion is made clear when considering the outer surface area of the rotor which supports the PMs. This is driven by the rotor circumference $(R_{circum} = \pi D)$ where an increase in diameter allows for additional magnets to be introduced. It can be approximated that the ability to produce magnetic force increases linearly with an increase in diameter [5]. The combination of these two factors leads to the approximated diameter squared factor in the torque expression. [35]

A consequence of the direct relationship between the torque output and motor size is the use of a rating parameter based on a motors torque per unit rotor volume. From (17) the torque output can be related to rotor volume [35]:

$$V_R = \frac{\pi {D_R}^2}{4} L_R \tag{18}$$

$V_R - Volume\ of\ rotor\ with\ diameter\ D\ and\ length\ L\ [m^3]$

Therefore,

$$\frac{4}{\pi} V_R = {D_R}^2 L_R \text{ and } \quad T = k{D_R}^2 L_R$$

$$\therefore T = k\frac{4}{\pi} V_R$$

And since k is a constant

$$T = kV_R$$

Therefore,

$$T \propto kV_R$$

The energy required to generate this torque is dependent on the magnetic energy available and generated in the electrical machine. To better understand the magnetic energy in an electrical machine it is necessary to investigate how the magnetic field is distributed within it and how the spatial relationship between the different components influences the distribution. [5]

There are two common analytical methods used to approximate the magnetic field distribution within an electric motor, namely: Magnetic circuit analysis (MCA) and finite element analysis (FEA). [5]

MCA can be used to resolve an electromagnetic problem into a magnetic circuit which is analogous with electrical circuit problems [5]. The analytical methods used when solving magnetic circuit problems are similar to the methods used when analysing electrical circuits [5]. This can be considered as a macroscopic analysis option.

Electromagnetic FEA makes use of a finite element model (FEM) containing a discretised geometrical mesh and loading information representative of the physical case. The magnetic field, and other properties, are determined at discrete nodes along the mesh [5]. Effectively, FEA breaks up a complex magnetic field distribution problem into a small number of pieces and determines the properties at each node to solve the problem. The development of electromagnetic FEA software and the increase in available computational resource has increased the usage of FEA for electric motor design and validation. However, for first phase design and approximation, FEA is still considered too complex, resource intensive and other analytical approximation methods are preferred [5]. This can be considered as the microscopic approach.

For this reason, additional emphasis is placed on the investigation into MCA techniques which can provide a macro perspective of the problem. MCA is based on two fundamental equations, one for magnetic flux density (See (3)) and the other for magnetic field intensity (See (4)) [5]. These expressions are used to develop an analogy with electrical circuit analysis. The expression for *MMF* detailed in (9) is analogous with Ohm's law in electrical circuit analysis, with the comparison presented in Table 2:

Table 2: Magnetic circuit analysis analogy with electrical circuit analysis [5]

$EMF = IR$	$MMF = \emptyset R$
$EMF - Electromotive\ Force\ [V]$	$MMF - Magnetomotive\ Force\ [A]$
$I - Current\ [A]$	$\emptyset - Magnetic\ Flux\ [T.m^2\ OR\ Wb]$
$R - Resistance\ [\Omega]$	$R - Reluctance\ \left[{}^{A}/_{Wb}\ OR\ H^{-1}\right]$

This fundamental expression for the analogy defines MCA which can be completed with the aid of schematics similar to those used in electrical circuit analysis. Figure 21 illustrates an example of how MCA is applied to an *MMF* source generated by a current carrying conductor wrapped around magnetic core material (Detailed in Figure 15) in comparison with an electrical circuit representing a battery, or *EMF*

source, within an electrical circuit. The tools used to solve and analyse electrical circuits apply in a similar manner to MCA problems (e.g., Kirchhoff's current and voltage laws) [5].

Modelling an *MMF* source from a permanent magnet is slightly more complicated. Since a magnetic material exhibits different magnetic properties dependent on its inherent molecular makeup plus elements influenced by exposure to an external field, the magnets field density is made up of two components [5]. During operation, the permanent magnet is exposed to the magnetic field induced in the windings which influences its operating properties [5]. The magnetic field density produced by the permanent magnet can be approximately expressed as follows [5]:

$$B_m = B_r + \mu_R \mu_0 H_m \tag{19}$$

$\mu_R - Relative\ recoil\ permeability\ [-]$

$H_m - Field\ intensity\ of\ external\ environment\ (Negative\ quantity)\ \left[{}^{N}/_{m^2}\right]$

This refined field density provides the basis for the permanent magnet circuit model of which an example for a rectangular block magnet is illustrated in Figure 22. The example model can be expressed as follows [5]:

$$\emptyset = \emptyset_r + P_m MMF_m \tag{20}$$

$$\text{Where, } \emptyset_r = B_r A_m \ \&\ P_m = \frac{1}{R_m} = \frac{\mu_R \mu_0 A_m}{L_m}$$

$A_m - Cross\ sectional\ area\ of\ magnet\ face\ in\ the\ magnetised\ direction\ [m^2]$

$MMF_m - Magnetomotive\ force\ of\ the\ magnet\ [A]$

$P_m - Magnet\ leakage\ permeance\ [H]$

$L_m - Length\ of\ magnet\ in\ magnetised\ direction\ [m]$

In most SPM motors, the PM's used are often in the shape of an arc and radially magnetised (See Figure 23) [5]. In this instance, a similar methodology can be followed to provide the following changes to the magnet circuit model [5]:

$$\emptyset = \emptyset_r + P_m MMF_m \tag{21}$$

Where, $\emptyset_r = B_r A = B_r L \theta_m$ & $P_m = \frac{1}{R_m} = \frac{\mu_R \mu_0 L \theta_m r_i}{L_m}$ & $L_m \ll r_i$

$L - Depth\ of\ magnet\ in\ direction\ or\ arc\ centreline\ [m]$

$r_i - Internal\ radius\ of\ magnet\ [m]$

$\theta_m - Angular\ span\ of\ magnet\ arc\ [H]$

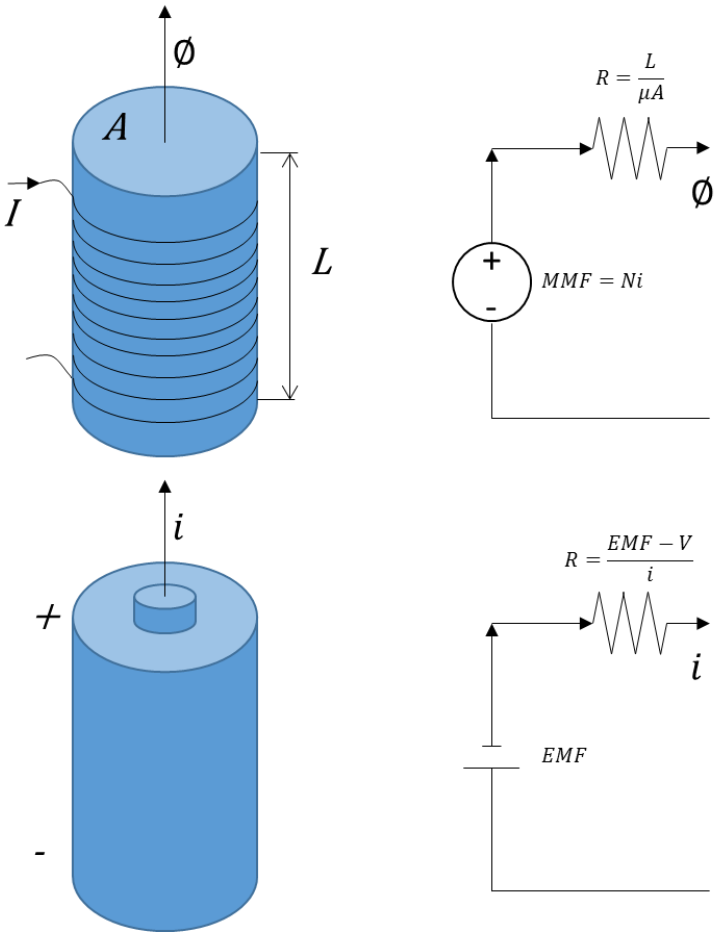


Figure 21: Comparison of magnetic circuit and electrical circuit schematics

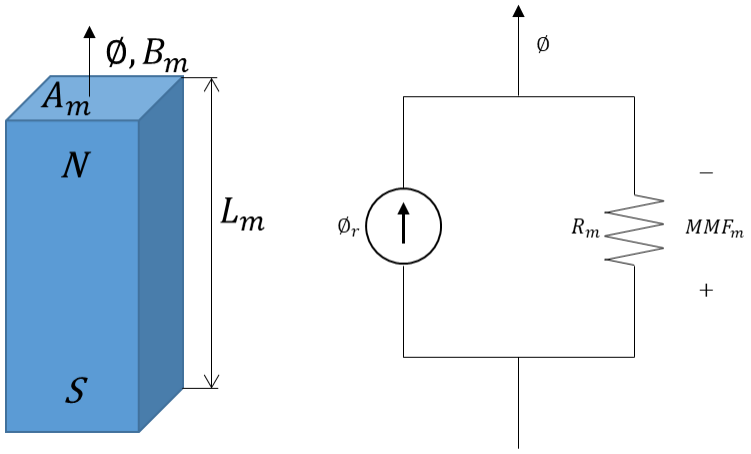


Figure 22: Magnetic circuit schematic for permanent magnet

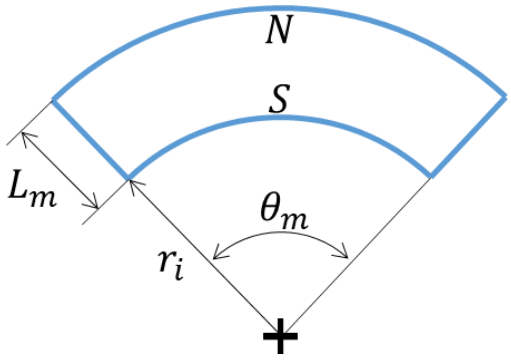


Figure 23: Radially magnetised arc-shaped permanent magnet

To apply the MCA method to SPM motor design it is necessary to investigate techniques to deal with the flux flow through the airgap present between the rotor and stator. The flux flow through the airgap can be determined by evaluating the reluctance of the airgap and to include this in an MCA of the motor to evaluate the magnetic flux distribution through the machine [5]. To determine the airgap reluctance, it is necessary to investigate the flux flow lines within the airgap region (See Figure 24) [5]. This is typically difficult to determine analytically and FEA methods are preferred, however, to perform initial design calculations certain approximations can be made to simplify the analysis.

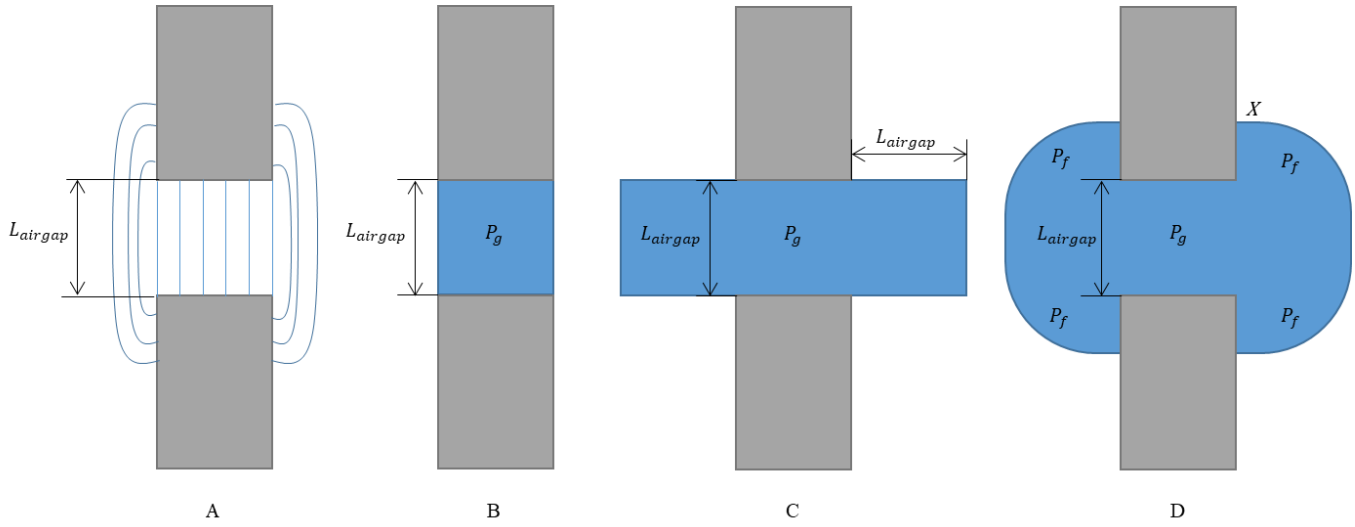


Figure 24: Airgap modelling schematics for magnetic circuit analysis

The difficulty in modelling the airgap flux lines is due to fringe effects experienced near the edges of the airgap [5]. Figure 24 A illustrates the magnetic flux flow between two magnetic materials between an airgap. Since the permeability of the air within the gap is the same as the permeability of air surrounding the magnetic blocks and airgap, the flux flows through fringe area. The flux lines illustrated in Figure 24 A are idealised and do not represent real conditions. [5]

The simplest model (Figure 24 B) ignores the fringe flux completely and assumes that the flux travels through the airgap only. Therefore, by using (6) and (8) the airgap permeance (P_{gA}) and reluctance (R_{gA}) can be determined as follows [5]:

$$P_{gA} = \frac{\mu_o A_{CS}}{L_{Airgap}} \;\&\; R_{gA} = \frac{L_{Airgap}}{\mu_o A_{CS}} \tag{22}$$

$L_{Airgap} - Length\ of\ the\ airgap\ [m]$

$\mu_o - The\ permability\ of\ the\ air\ is\ assumed\ equal\ to\ that\ of\ free\ space\ (\mu_0 = 4\pi \times 10^{-7})\ [{}^{H}/_{m}\ OR\ T \cdot {}^{m}/_{A}]$

$A_{CS} - Cross\ Sectional\ Area\ of\ magnetic\ blocks\ facing\ airgap\ [m^2]$

Figure 24 C represents a more accurate model since it takes into consideration an approximation of the fringe flux. This is done by extending the airgap flux model by a distance equivalent to the airgap itself, thereby increasing the flux flow area [5]. This approximation is generally accurate when the ratio of airgap

length to cross sectional area of magnetic blocks is small [5]. Using this model, the airgap permeance $\left(P_{gB}\right)$ and reluctance $\left(R_{gB}\right)$ can be determined as follows [5]:

$$P_{gB} = \frac{\mu_o A_{CS}^*}{L_{Airgap}} \;\&\; R_{gB} = \frac{L_{Airgap}}{\mu_o A_{CS}^*} \tag{23}$$

$A_{CS}^* - Extended\ cross\ sectional\ area\ of\ magnetic\ blocks + L_{Airgap} in\ both\ directions\ [m^2]$

Figure 24 D improves the approximation by modelling the fringe flux in a more accurate manner. In this model, the uniform flux density is modelled as per the first approximation with the permeance/reluctance of the fringe flux added in parallel [5]. If it is assumed that the fringe flux follows a circular arc from the one block up to a straight section which is parallel with the airgap flux and joins a second circular arc completing the flux line up to the second block, the total permeance $\left(P_{gC}\right)$ and reluctance $\left(R_{gC}\right)$ can be determined as follows [5]:

$$P_{gC} = P_g + 4P_f \;\&\; R_{gC} = R_g + 4R_f$$
$$\therefore P_{gC} = \frac{\mu_o A_{CS}^*}{L_{Airgap}} + 4 * \left[\left(\frac{\mu_o L_{Depth}}{\pi}\right) * \ln\left(1 + \frac{\pi X}{L_{Airgap}}\right)\right] \;\&\; R_{gC} = \frac{1}{P_{gC}} \tag{24}$$

$X - Extent\ of\ fringe\ flux\ along\ magnetic\ block\ which\ is\ generally\ assumed = 10L_{Airgap}\ [m]$

Due to the large relative permeability[11] of the rotor and stator core materials compared to the airgap between them, when performing MCA, it is evident that the air gap dominates the analysis [5]. This provides the basis for a useful simplification in assuming that the reluctance of the core materials is negligible and can be ignored. This simplifies the analysis significantly since majority of core materials have non-linear magnetic properties [5].

The MCA techniques can be applied as a tool for SPM motor design. In order to do so it is necessary to formulate a model representing a generic SPM motor. This model will be used as the basis for determining the flux flow through the unit. Consider the simplified SPM motor example illustrated in Figure 25. The MCA model in this case can be built by investigating the flux flow between a pair of magnets and the rotor and stator [5]. As illustrated in Figure 25 the flux flow will travel from the north pole of one of the magnets

[11] Relative permeability (μ_r) is defined as the permeability of a material relative to the permeability of free space. $\left(\mu_r = \frac{\mu}{\mu_o}\right)$. [5]

through the airgap, into the stator and form a loop to return by travelling back through the airgap, into the south pole of the adjacent magnet, and returns to the south pole of the original magnet after travelling through the rotor core [5].

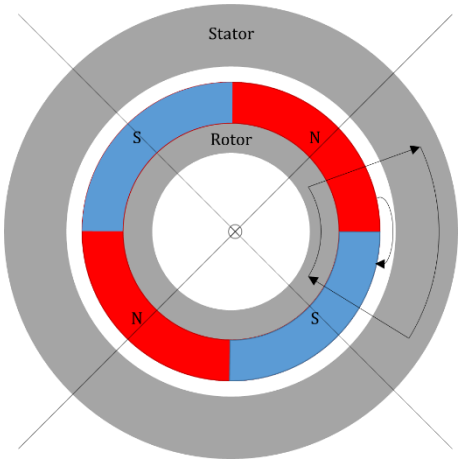


Figure 25: Simplified SPM motor for MCA analysis

Not all the flux flows as previously discussed. Some flux leaks through the airgap and travels directly into the South-pole of the adjacent magnet [5]. This magnet leakage flux is represented with the loop in Figure 25. This simplified representation of an SPM motor can be modelled using MCA techniques as shown in Figure 26 [5]. This model, which is represented in a linear frame of reference as opposed to the actual radial configuration, only considers two adjacent halves of the magnet defined by the appropriate angular spacing. [5]

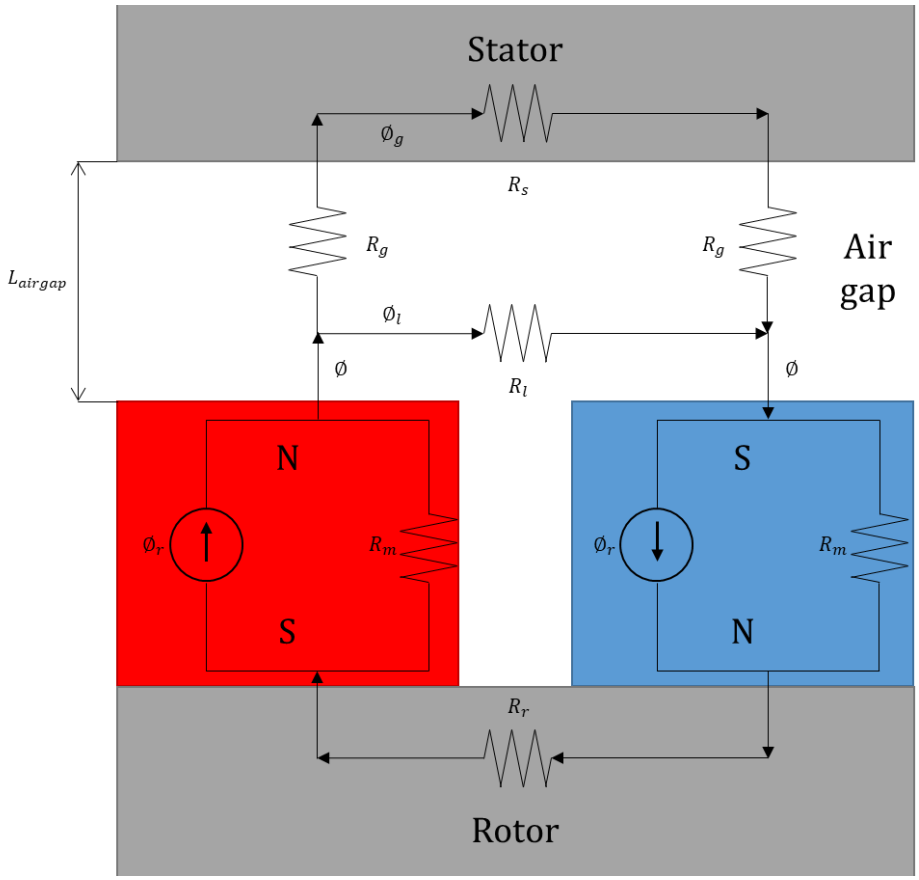


Figure 26: Magnetic circuit model for simplified SPM motor

This circuit can be simplified further to aid in dealing with the complexities associated in determining the leakage reluctance and the reluctance of the rotor and stator core materials which typically exhibit non-linear characteristics. [5]

The first simplification applied is to estimate the percentage of total flux that travels through the airgap which is reduced because of the leakage flux [5]. By introducing a leakage factor and applying this to the primary flux, it is possible to account for the leakage. This simplification allows one to avoid the complexity associated with modelling the leakage flux and the reluctance (R_l) more accurately [5]. The simplification is expressed as follows [5]:

$$\emptyset_g = K_l \emptyset_{tot} \tag{25}$$

$K_l - Leakage\ factor, typical\ values\ are\ 1.0 < K_l < 1.2\ [-]$

$\emptyset_g - Magnetic\ flux\ through\ airgap\ [T.m^2\ OR\ Wb]$

$\emptyset_{tot} - Total\ magnetic\ flux\ [T.m^2\ OR\ Wb]$

The second simplification that can be applied is to eliminate the stator and rotor core reluctances from the model [5]. It can be assumed that the stator core and rotor core material will have a much larger permeability than that of the airgap [5]. With this assumption, it is possible to remove the stator (R_s) and rotor (R_r) reluctance terms from the model and replace them with a reluctance factor that will increase the reluctance of the airgap to compensate for the simplification [5]. The simplification can be expressed as follows [5]:

$$R_g \rightarrow K_r R_g \tag{26}$$

$K_r - Reluctance\ factor, typical\ values\ are\ 0.9 < K_r < 1.0\ [-]$

$R_g - Reluctance\ of\ the\ airgap\ \left[{}^{A}/_{Wb}\ OR\ H^{-1}\right]$

The final simplification that can be applied is to replace the two magnet half models by a single magnet with twice the length [5]. This results in the reluctance increasing by a factor of two as well. By applying all the simplifications, it is possible to refine the magnetic circuit to the result presented in Figure 27. [5]

Based on the circuit model expressed in Figure 27, and using (22), (25) and (26) it is possible to determine the airgap magnetic properties. The total magnetic flux can be determined as follows [5]:

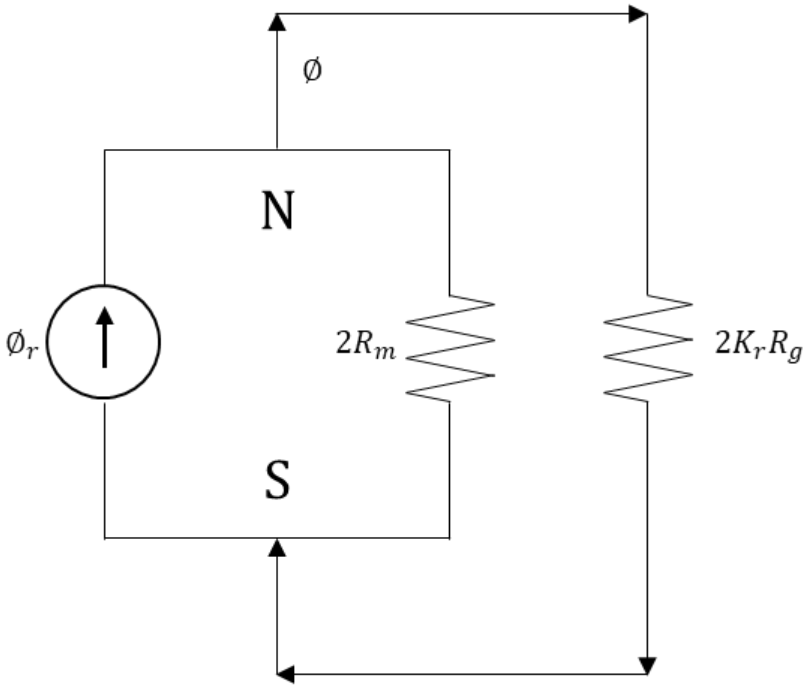


Figure 27: Simplified magnetic circuit for SPM motor analysis

$$\emptyset = \frac{2R_m}{2R_m + 2K_r R_g}\emptyset_r = \frac{1}{1 + K_r \frac{R_g}{R_m}}\emptyset_r$$

Where, $R_m = \frac{L_m}{\mu_R \mu_0 A_m}$ and $R_g = \frac{L_{Airgap}}{\mu_0 A_g}$

$$\therefore \emptyset_g = K_l \emptyset = \frac{K_l}{1 + K_r \frac{\mu_R L_{Airgap} A_m}{L_m A_g}}\emptyset_r \tag{27}$$

$A_g - Cross\ Sectional\ Area\ of\ magnetic\ blocks\ facing\ airgap\ [m^2]$

Introducing the flux concentration factor, flux density [(3)] and permeance coefficient it is possible to resolve the air gap flux density as follows [5]:

$$\therefore B_g = \frac{K_l C_\emptyset}{1 + K_r \frac{\mu_R}{P_c}} B_r \tag{28}$$

$$\text{Where, } C_\emptyset = \frac{A_m}{A_g} \text{ and } P_c = \frac{-B_m}{\mu_0 H_m} = \frac{L_m}{L_{Airgap} C_\emptyset} \tag{29}$$

$C_\emptyset - Flux\ concentration\ factor, ideally = 1.0\ [-]$[12]

$P_c - Permeance\ coefficient, usually\ > 4.0\ [-]$

The permeance coefficient introduced in (29) and (28) is a property that indicates the magnets operating point along its B-H curve [5]. This is described in further detail in *2.2.4 Permanent Magnets*.

Evaluating the air gap flux density [(28)] is an important step in SPM motor design since many geometrical features are dependent on its value. Since the leakage (K_l), flux concentration ($C_\emptyset$) and reluctance factors (K_r) are considered constant, the key parameters that dictate the air gap flux density are the remanence (B_r), relative recoil permeability[13] (μ_R) and the permeance coefficient (P_c). The remanence and relative recoil permeability are based on the material selection for the magnet and, once defined, are considered constant [24]. Thus, it can be concluded that the permeance coefficient plays a significant role regarding

[12] The flux concentration factor is expressed as the ratio of magnet area exposed to the airgap versus the airgap surface area itself. This can be used to indicate the ratio of airgap flux density to the flux density at the magnet surface. [40]

[13] The relative recoil permeability is equal to the gradient of the linear portion of the B-H curve found in the second quadrant. This provides a basis for determining the expected permeability after removal of the applied magnetic field ('H'). [24]

the airgap flux density. By increasing the permeance coefficient, achieved by increasing the ratio of magnet length to airgap length, the airgap flux density tends to its maximum. The maximum flux density is typically slightly less than the remanence because of the ideal flux concentration factor which is equal to 1. It is important to note that the relationship between the permeance coefficient and the air gap flux density is non-linear with the magnet remanence representing an asymptote. This means that diminishing air gap flux density gains are experienced when increasing the permanence coefficient, which typically requires larger and thus more costly magnets. [5]

If the investigation is applied to a full motor as illustrated in Figure 28 the total flux travelling through the airgap is:

$$\emptyset_{total} = B_g A_g = B_g 2\pi R_{ro} L_{st} \tag{30}$$

$R_{ro} - Outer\ radius\ of\ rotor\ including\ magnets\ [m]$

$L_{st} - Axial\ stack\ length\ of\ the\ motor\ [m]$

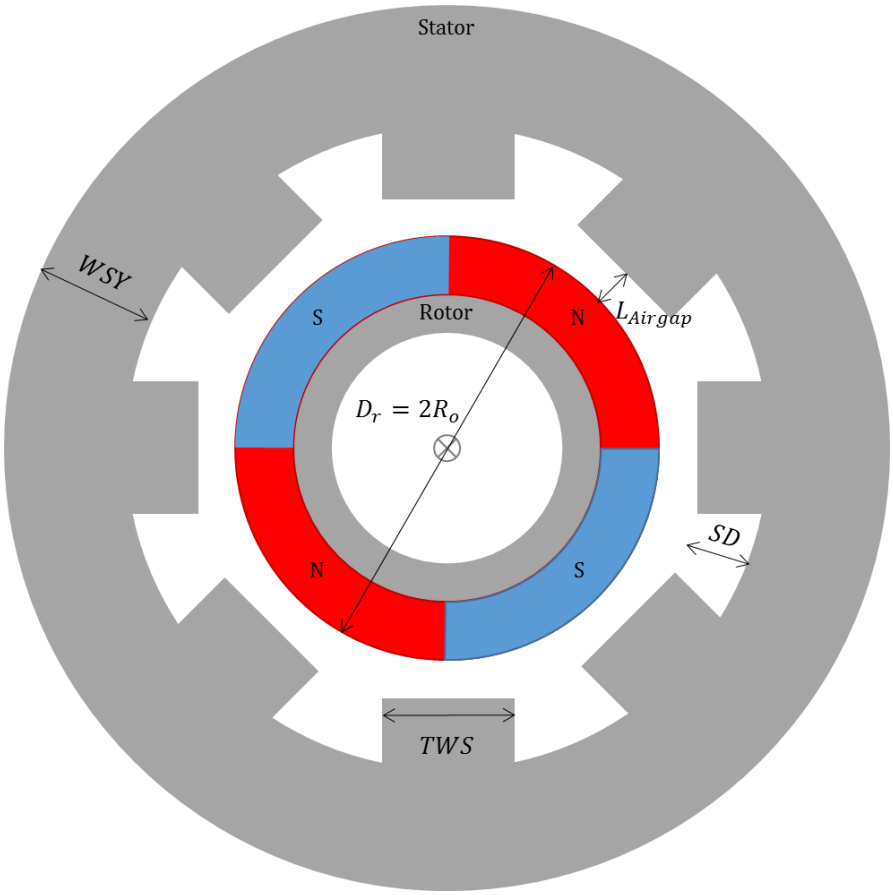


Figure 28: Full motor MCA analysis diagram

2.2.2 Stator Assembly

The stator assembly is defined as the stationary component of the PMAC motor. The stator is responsible for supporting the windings and provides the core material through which magnetic flux can travel. In cylindrical radial flux type motors, such as SPM units, the stator is cylindrical. Figure 29 is a great example of a PMAC motor stator assembly used in hybrid vehicle application [36]. As illustrated in the example, it is common to manufacture a stator with many individual teeth which interlock with each other. These teeth are designed to provide sufficient core material while at the same time providing a sufficiently large cut-out, or slot, to allow support for the windings. An insulator, which is often a formed plastic part, is placed in between the windings and the stator core material to avoid any potential electrical shorts between the windings and the stator tooth. [18]

The important factors to consider when designing the stator assembly are the stator configuration and tooth profile geometry, windings and core material selection. [18] [5]

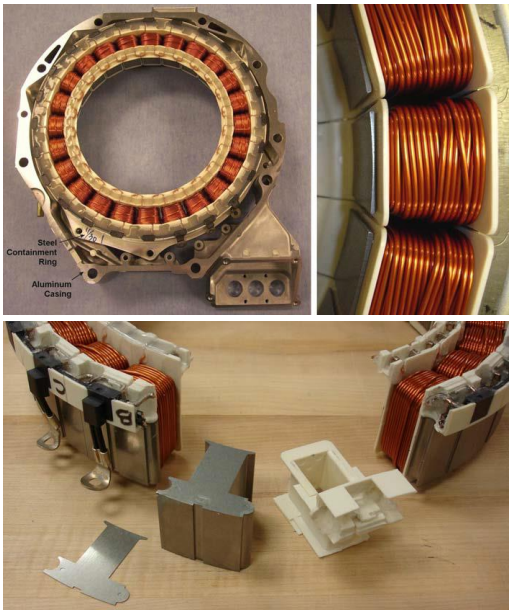


Figure 29: Honda Accord hybrid motor stator assembly [36]

Stator Configurations and tooth profile geometry:

There are a number of configuration options available for stator assembly design. Dependent on the type of radial flux unit being developed, there is an option to make use of an external stator and internal rotor configuration or an internal stator and external rotor configuration [18]. A comparison between the resulting stator for the two configurations is illustrated in Figure 30.



Figure 30: Internal and external stator configuration examples [37] [38]

Since the airgap length of an internal stator configuration motor is typically larger than that of an external stator configuration equivalent, the associated airgap flux density is lower [18]. For this reason, majority of high performance electric motors for hybrid and all electric vehicle application follow an external stator configuration. [5]

Considering the external stator configuration, there are a number of different options available for the design of the stator tooth profile. Table 3 illustrates a few common options for stator slot shapes which determine the stator tooth profile geometry [39].

Table 3: Common stator slot geometries [39]

	
Parallel tooth, Round bottom, Semi-closed slot	Parallel tooth, Arc-bottom, Semi-closed slot
	
Parallel slot, Square bottom, Open slot	Parallel slot, Round bottom, Semi-closed slot
	
Parallel slot, Square bottom, Semi-closed slot	Parallel tooth, Square bottom, Open slot

The different configurations have an influence on the magnetic flux distribution through the motor and ease of manufacture [39]. For simplicity, the investigation into the stator tooth profile geometry is completed on the parallel tooth arc-bottom semi-closed slot design.

The stator tooth geometry plays an important role in motor performance since it has a direct effect on the magnetic field distribution through the unit. Since the stator tooth is typically manufactured from ferromagnetic electrical steels, the geometrical design is important in order to ensure that saturation does not occur, thus avoiding a reduction in the air gap flux flow. The total flux flow through the overall airgap, as expressed in (30), divides equally amongst the stator teeth [5]. The flux flow through each tooth can be expressed as follows (See Figure 31) [5]:

$$\emptyset_t = \frac{\emptyset_{total}}{N_s} = \frac{B_g 2\pi R_{ro} L_{st}}{N_s} \tag{31}$$

$N_s - Number\ of\ stator\ slots\ [-]$

Therefore, the flux density that travels through the tooth body can be expressed as [5]:

$$B_t = \frac{\emptyset_t}{(TWS)K_{st}L_{st}} \tag{32}$$

$K_{st} - Lamination\ stacking\ factor\ [-]$ (Explained in more detail in Stator Core Material and Laminations)

$TWS - Stator\ tooth\ body\ width\ [m]$ (See Figure 31)

By using (31) and (32) the tooth body width can be expressed as [5]:

$$TWS = \frac{2\pi R_{ro} B_g}{N_s K_{st} B_t} \tag{33}$$

Typically, the tooth body width is determined as a factor of the tooth flux density. The tooth flux density is generally defined as a constant set by the designer. [5]

Similarly, half of the flux from each magnet travels through the stator yoke (See Figure 31). Thus, it is possible to express the flux density through the stator yoke as follows [5]:

$$B_{sy} = \frac{\emptyset_{total}/_2}{(WSY)K_{st}L_{st}} \tag{34}$$

$WSY - Stator\ yoke\ depth\ [m]$

Therefore, by using expressions (30) and (34) it's possible to express stator yoke depth as follows [5]:

$$WSY = \frac{\pi R_{ro} B_g}{2N_{pp}K_{st}B_{sy}} \tag{35}$$

$N_{pp} - Number\ of\ magnet\ pole\ pairs\ [-]$

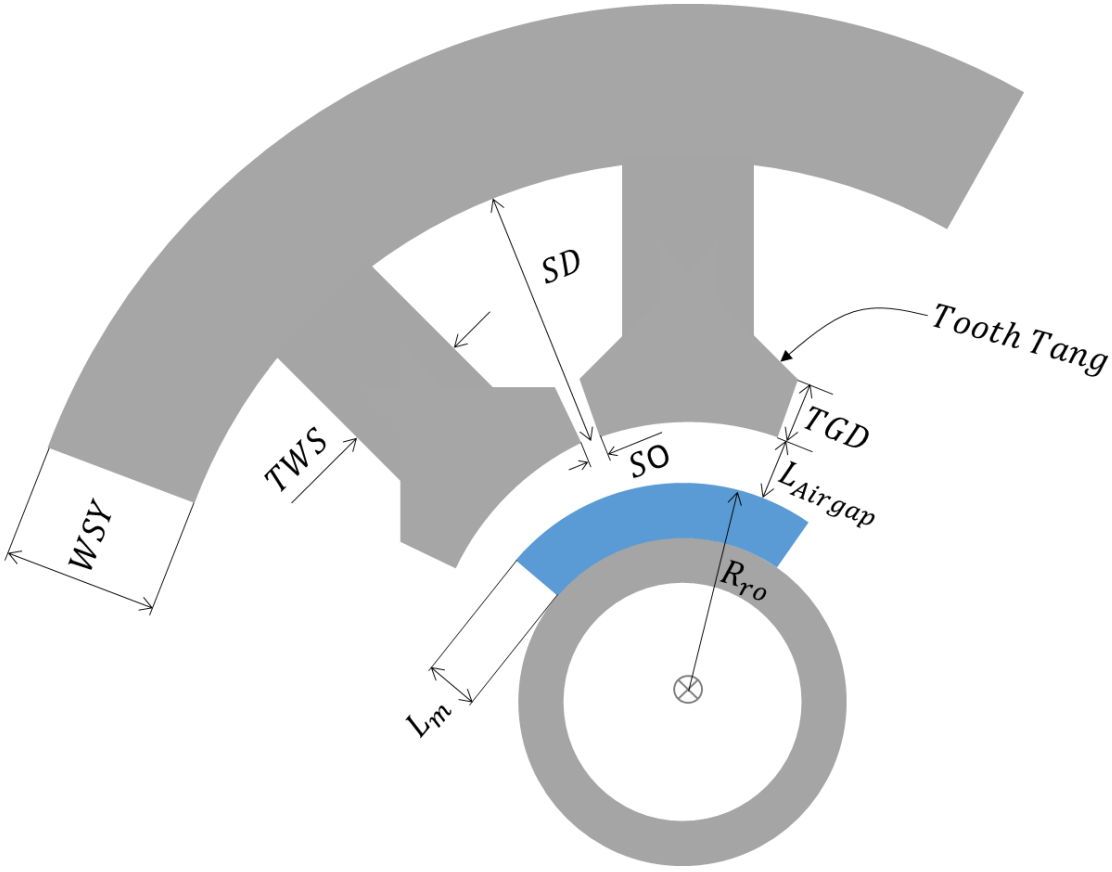


Figure 31: Stator tooth profile dimensions

Stator Core Material and Laminations

An important observation must be made when inspecting Figure 29 and that is with regards to the make-up of the stator tooth. The tooth is not a single piece of material but rather a stack of thin laminates that are pressed together to form a full tooth (See Figure 32 for a better illustration of stator tooth laminations). The

material used to produce the laminations is typically thin sheets of electrical steel which has high magnetic permeability and contains an insulating layer on either side of the sheet [5]. The reason for using a stack of laminations with insulation between each layer is to minimise the losses associated with eddy currents. [5]

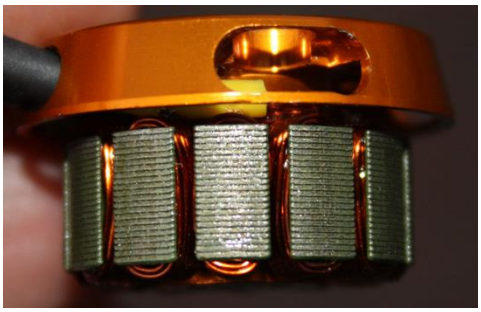


Figure 32: Small high-speed hobby motor stator assembly [40]

Increasing the resistivity of the core material will reduce eddy current generation which results in less power loss. The resistivity of the core can be increased significantly by introducing insulated layers of material. In addition, the resistivity can be further increased by introducing silicon into the steel [41]. For this reason, it is common to find silicon-iron (Si-Fe) electrical steel used in electric motors [41]. The losses associated with eddy currents induced in the stator core can be estimated using the following approximation [5]:

$$P_e = k_e h^2 f^2 B^2 \tag{36}$$

$P_e - Power\ loss\ associated\ with\ induced\ eddy\ currents\ [W]$

$k_e - Material\ specific\ constant\ [-]$

$h - Material\ thickness\ in\ plane\ perpendicular\ to\ flux\ flow\ [m]$

$f - Input\ current\ frequency\ [Hz]$

It is clear, therefore, that eddy current losses are proportional to the square of laminate thickness. Typical lamination thicknesses used in high performance motors vary between 0.05mm to 0.5mm [42]. However, the thickness depends on a balance between performance and cost. Thinner laminations tend to be more expensive to purchase and to manufacture [42].

Introducing the laminations to build up a tooth stack does decrease the amount of magnetic material available to carry flux. To compensate for this reduction a lamination stacking factor is used. This is defined

as the ratio of metal cross-sectional area to the total cross-sectional area of the stack and can be described as follows [5]:

$$K_{st} = \frac{A_{st}}{A_{total}} \tag{37}$$

$A_{st} - Cross\ sectional\ area\ of\ metal\ [m^2]$

$A_{total} - Cross\ sectional\ area\ of\ lamination\ stack\ [m^2]$

The lamination stacking factor typically varies between 0.8 and 0.99. [5]

The cost of the stator core is a factor of many elements including the material selection, lamination thickness and manufacturing methods. For this reason, it is difficult to provide an accurate cost estimate since many of these elements are dependent on factors such as tooling cost and number of units produced. General material costs provided by material suppliers are used as a basis. Appendix A: Materials Catalogue Database contains a supplier catalogue including data for suitable stator core materials. [43]

Windings

The windings that form part of the stator assembly are generally coils of insulated copper wire of a specified diameter. As described in *2.2.1 SPM Motor Operating Principles and Analytical Investigation (Performance)* the number of turns in the winding has a direct influence on the power output of the motor. Beyond these factors there are several different winding schemes available to motor designers [5]. The winding configuration is a factor of the number of stator slots and magnet poles of the motor with the ratio of slots per pole per electrical phase an important consideration [44]. The number of slots and poles, dependent on the number of phases, determines whether the motor is balanced or unbalanced [44]. A balanced motor has a slot to pole ratio that produces a symmetrical system. If a 3-phase environment is considered, a balanced winding scheme would be one where the back *EMF* of each phase is offset by 120° relative to each other [44]. Only balanced configurations will be considered feasible. A balanced winding scheme can be determined by evaluating the number of slots per phase per machine periodicity [44]. When this value is an integer, the winding configuration is balanced [44]:

$$\frac{N_s}{3 \times GCD(N_s, N_{PP})}\ is\ an\ integer \tag{38}$$

$GCD(a, b) - Greatest\ common\ divisor\ between\ a\ and\ b\ [-]$

Although possible to contradict, it is assumed that all slots will be filled. This means that the number of slots will always be a multiple of the number of phases. [5]

In general, a winding scheme is described by: the number of turns per coil; the number of magnet pole pairs and slots; and the winding layout [5]. The winding layout indicates the number of winding layers and the span of the coils, which is typically described in number of slot pitches. [5]

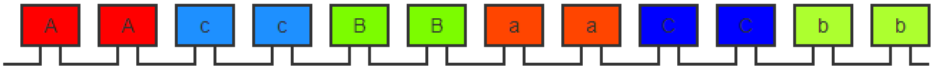
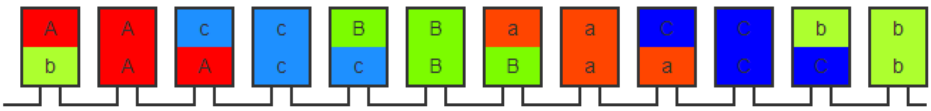
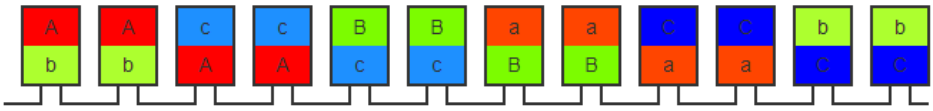
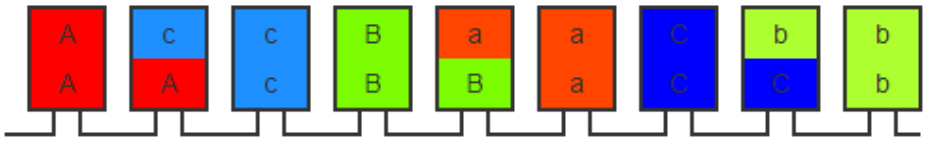
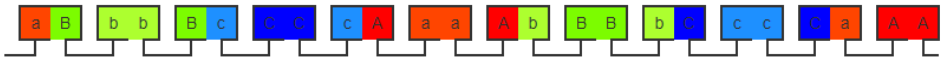
There are three primary classifications for the winding layout, namely: Integer-slot windings; Fractional-slot windings and Concentrated windings [5]. These classifications can be described by the slot per pole per phase value as shown below [5]:

$$N_{SPP} = N_s/2N_{PP}/N_{ph} \tag{39}$$

$N_{ph} - Number\ of\ electrical\ phases, confined\ to\ 3 - phase\ for\ scope\ of\ project$ [−]

A comparison between the different winding layouts can be seen in Table 4.

Table 4: Comparison between common winding layout configurations [45] [46] [47]

Classification	N_{SPP}	Example
Integer-slot	Integer value [45]	
		Single-layer 2-pole 12-slot integer slot winding with full pitch (6 slots)
		
		Double-layer 2-pole 12-slot integer slot winding with a reduced coil span compared to full pitch with one slot pitch
		
		Double-layer 2-pole 12-slot integer slot winding with a reduced coil span compared to full pitch with two slot pitches
Fractional-slot	Fractional and greater than 1 [46]	
		Double-layer 2-pole 9-slot fractional slot winding
Concentrated	Fractional and lower than or equal to 1 [47]	
		Single-layer 10-pole 12-slot concentrated winding
		
		Double-layer 10-pole 12-slot concentrated winding

The number of winding layers can either be single or double [48]. A single layer winding indicates that the individual slots contain windings belonging to a single coil only. Whereas double layer windings contain two coil sides per slot. This is illustrated in Figure 33. [48]



Figure 33: Single versus double layered windings [48]

Double layer windings are commonly found in SPM motors since the scheme is easily manufactured and maximises motor performance [5].

Another constraint that needs to be considered is the slot fill percentage. Due to manufacturing, wire profile shape and insulation constraints the stator slots cannot be completely filled by the windings (See Figure 34) [49]. The slot fill ratio, often referred to as the copper fill ratio, is calculated from the ratio of total conductor (copper) area to total slot area. [49]

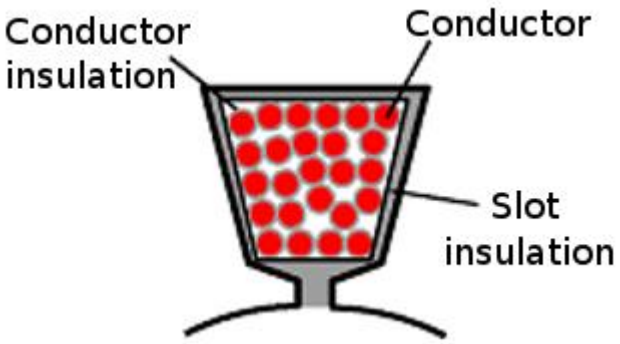


Figure 34: Stator slot winding fill factor [49]

It is possible to improve the slot fill factor; however, this is typically associated with greater material and winding costs. It is generally possible to achieve winding factors between 50%-60% at a midrange cost [5].

The cost of the windings is a factor of a number of elements including the winding material selection and manufacturing method. For this reason, it is difficult to provide an accurate cost estimate since many of the elements are dependent on factors such as tooling cost, complexity of winding scheme and number of units produced. General material costs provided by material suppliers are used as a basis. Appendix A: Materials Catalogue Database contains a supplier catalogue including data for suitable winding materials. [50]

2.2.3 Rotor Assembly

The rotor of a PMAC motor is the rotating component. The rotor assembly of an SPM motor consists of the rotor hub onto which the permanent magnets are mounted [18]. The magnets are typically bonded to

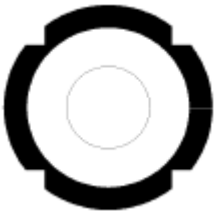
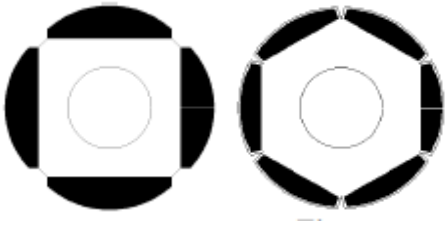
the rotor hub and a containment sleeve is placed over the magnets to ensure sufficient mechanical strength at high rotational speed [18].

The important factors to consider when designing the rotor assembly are the rotor configuration and magnet profile geometry and the rotor core material selection [18].

Rotor Configurations and magnet profile geometry:

Considering the internal rotor external stator configuration, there are a number of different options available for the design of the rotor assembly. Table 5 illustrates a few common options available for rotor hub and magnet shape definition [39].

Table 5: Common rotor magnet configuration geometries (SPM) [39]

	
Radially magnetised surface magnets, Arc-shaped	Parallel-magnetised surface magnets, Arc-shaped
	
Breadloaf type magnets (Nonsalient-pole)	Parallel-magnetised surface magnets, Rectangular

The different configurations represent varying performance versus cost trade-offs. Ideally, the airgap length and magnet length should be consistent along the rotor circumference, however, a magnet conforming to this arc shape is more costly to produce than the rectangular volume equivalent [5]. Majority of these magnet shapes are machined from a rectangular stock. It is also common to magnetise the permanent magnet after assembly onto the rotor hub. [5]

The permanent magnets are typically bonded to the rotor hub and reinforced with a containment sleeve [18]. To maintain the designed airgap length, it is imperative that the containment sleeve be as thin as possible whilst providing sufficient mechanical strength [51]. For this reason, it is common to find low

density high tensile metals and composite solutions being applied [51]. Figure 35 is an example of a carbon fibre composite sleeve used for high-speed application [51].



Figure 35: Carbon fibre composite rotor containment sleeve [51]

Rotor Core Material and Laminations

In a similar manner to that described in *Stator Core Material and Laminations*, the rotor core is made up as a series of laminates. This is to reduce the losses associated with eddy current formulation in the core iron. The materials used for the rotor core are similar to those used in the stator core and tend to be thin laminates of silicon-iron (Si-Fe) electrical steel.

The cost of the rotor assembly is a factor of a number of elements including the rotor core material selection, magnet containment material selection and manufacturing methods used. For this reason, it is difficult to provide an accurate cost estimate since many of the elements are dependent on factors such as tooling cost, manufacturing cost and number of units produced. Typically, the cost is dominated by the rotor hub component. For this reason general material costs for the rotor hub provided by material suppliers are used as a basis [52] [53] [54] [55]. Appendix A: Materials Catalogue Database contains mechanical properties for suitable rotor core materials [56].

2.2.4 Permanent Magnets

The permanent magnets of the motor are a fundamental component whose properties have a direct influence on performance. The permanent magnets produce the fundamental interaction field based on the orientation of magnetic domains (As described in Section *2.2.1 Fundamental Electromagnetic Theory*). The properties of a permanent magnet that must be considered when designing a PMAC motor are as follows: Residual induction or remanence; Coercive force and intrinsic coercivity; manufacturability and sensitivities to chemical and temperature changes. [7]

There are many different types of permanent magnet materials available, some common types are listed as follows [57]: Ferrite (Ceramic); Neodymium-Iron-Boron (NdFeB); Samarium Cobalt and Alnico. Most of these magnet types are available in both bonded and sintered form [57]. Bonded magnets are formed from powdered magnetic material bonded together using a non-magnetic resin. The introduction of the resin limits the performance of such units [57]. Therefore, it is more common to find sintered high-performance magnets [57].

Referring to the hysteresis loop introduced in *2.2.1 Fundamental Electromagnetic Theory*, permanent magnet materials are those that exhibit large hysteresis loops. Therefore, these materials tend to exhibit large residual induction or remanence properties. This means that the magnitude of the magnetic field strength remains substantial after the magnetisation process. [57]

An important property that can be extracted from the hysteresis loop is available when investigating the 2nd quadrant of the curve (An example can be seen in Figure 36. Reference Figure 9 if required). The operating point of most permanent magnets in SPM motors will tend to lie in the 2nd quadrant where the permeance value is between zero and infinity [5]. This means that the operating point will lie between the remanence or residual induction and the coercive force. The permeance coefficient (P_C) is defined as the magnitude of the slope of the line drawn from a point on the curve to the origin [5]. Several permeance coefficients and their respective representations can be seen in Figure 36. When the permeance coefficient is zero, the intersection with the curve will be at the coercive force and when the permeance coefficient is infinity, the intersection point will be at the remanence [5]. It is also clear from Figure 36 that the hysteresis loop changes with varying temperature. [24]

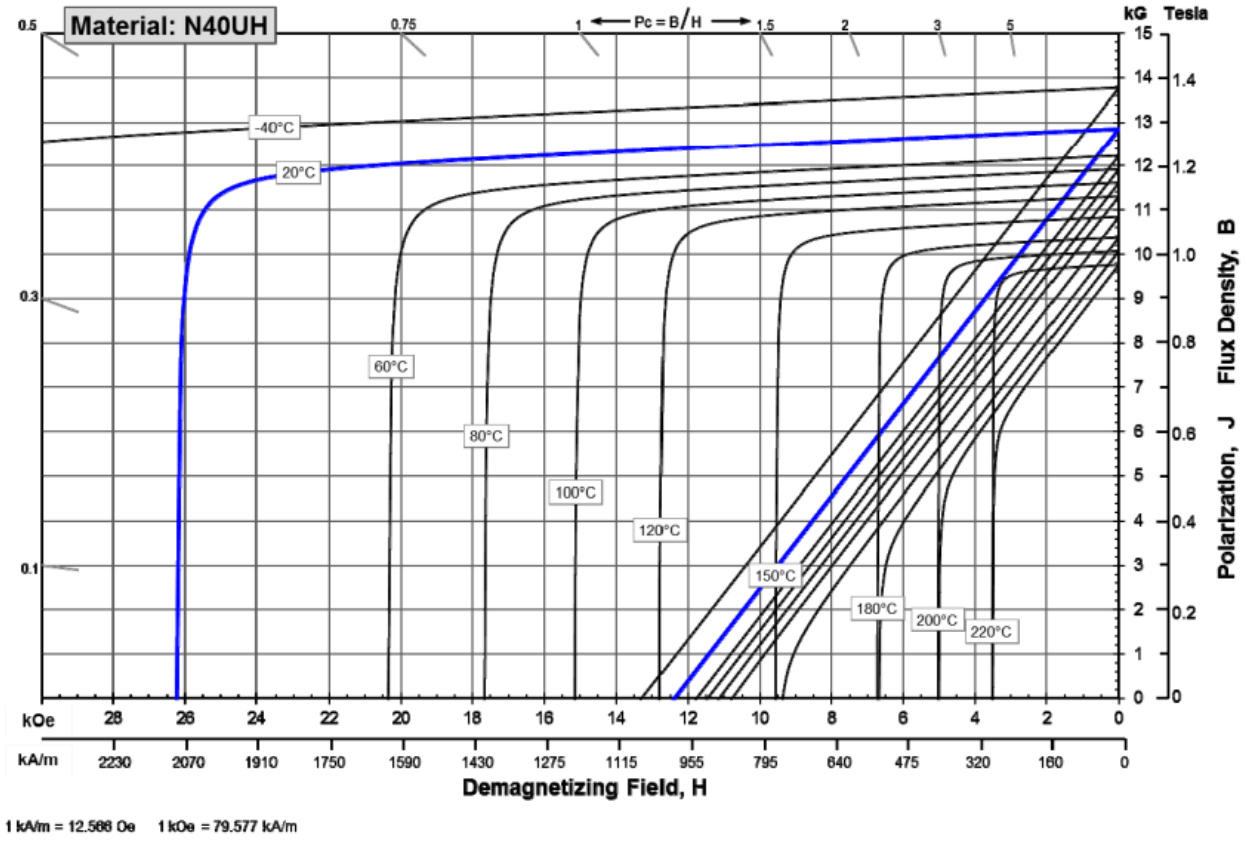


Figure 36: Sample demagnetisation curves at various temperatures for N40UH permanent magnet [24]

A comparison between several common permanent magnet material groups with their respective advantages, disadvantages and suitable applications can be seen in Table 6.

Table 6: Comparison of typical permanent magnet materials [57]

Magnet Material	Advantages	Disadvantages	Typical applications
Ferrite (Ceramic)	• Economical - high output-to-price ratio • High Hc and Hci compared to Alnico • Suitable for high temperature applications • Outstanding corrosion resistance	• Simple shapes only • Fragile (prone to chipping, cracking) • Expensive tooling for manufacture • Temperature sensitive with regard to flux output (generally useful to less than 150 °C) • Generally limited to use above -40 ºC (coercivity decreases as temperature decreases)	• DC PM motors (e.g. starter motors, blowers, window lifts and windshield wiper motors etc.) • Magnetos used on lawnmowers, garden tractors and outboard motors • DC brushless motors used in the electronics industry for remote controls, cooling fans, etc.
Neodymium-Iron-Boron (NdFeB)	• Very high magnetic energy for size • Widely available • Suitable to ambient temperature situations; strongest magnet material at and near room temperature • High coercivity (Hci) grades are available	• Subject to corrosion that can result in loss of energy or failure • Temperature sensitive (dependent on grade) • Requires heavy rare earth substitution for performance above 80 °C	• High performance applications • Computer rigid disc drives • Hammer-bank (dot matrix-type) printers • Speakers and headphones including ear buds and cell phone speakers • Hearing aid transducers • Microphone assemblies • Brushless DC, variable speed and servo-motors
Samarium Cobalt	• High Hc, Hci and BHmax • Temperature-stable (2 Kelvin to over 500ºC) • Powerful for their size • Good corrosion resistance	• Moderately expensive because of the samarium and cobalt content • Require careful handling to prevent chipping and breaking	• High performance • Traveling wave tubes • D.C. Motors, especially where temperature stability is vital, such as in satellite systems, aircraft generators, and small military-use motors • Sensors, especially for automotive applications • Linear actuators
Alnico	• Mechanically strong • Cast to a variety of shapes • Most temperature stable PMs • High Br and BHmax characteristics compared to ceramic magnets • Moderately corrosion resistant, often require no protective coating	• Can be brittle • Exhibit low coercivities	• Electron tubes, radar, traveling wave tubes • Separators, holding magnets, coin acceptors, clutches and bearings • Magnetos, motors, generators, gauges, controls, relays, watt-hour meters (bearings and dampeners) • Communications - receivers, telephones, microphones, bell ringers, musical instruments (guitar pickups) • Automotive sensors, loudspeakers, distributors

The cost of the permanent magnets is a factor of a number of elements including the magnet material selected and manufacturing methods used. For this reason, it is difficult to provide an accurate cost estimate since many of the elements are dependent on factors such as tooling cost, manufacturing cost including

material yield from the magnetic block and number of units produced. In addition, the raw material cost has experienced dramatic fluctuation over recent years [58] [59]. For this reason, it is difficult to provide an accurate estimate, however, a general indication of the cost can be determined by making use of the current cost of processed magnets, formed in simple generic shapes, and using this to evaluate an approximate cost per unit mass. Appendix A: Materials Catalogue Database contains a supplier catalogue including data for suitable magnets. [60]

2.2.5 Housing Components

The housing components that form part of the fundamental elements of an SPM motor are the main housing and the cover. The main housing provides structural support for majority of the components, includes features to mount the unit and protects the components from exposure to environmental factors. The cover is used to seal the final unit and provides support for one of the rotor bearings. [5]

Figure 37 is an example of an Integral Powertrain SPM motor which illustrates the housing components [61]. The motor in Figure 37 incorporates an axial mounting scheme as indicated by the orientation of the mounting lugs [61].



Figure 37: Example of Integral Powertrain Motor Housing Components [61]

There are two possible housing configurations considered within Integral Powertrain, namely: 2-Piece and 3-Piece configurations (See Figure 38) [3]. The 2-Piece configuration consists of a main housing component which is a cylindrical unit with an integrated cover, similar to a 'tin-can' shape plus a single cover piece to seal the unit [3]. The 3-Piece configuration consists of a simple cylindrical element plus two cover units used to seal the unit (See Figure 38) [3].



2-Piece Configuration 3-Piece Configuration

Figure 38: 2-Piece and 3-Piece motor housing configurations. [62] [63]

The structural integrity of the housing elements is important. This is because it houses the stator assembly, supports the rotor bearings and provides the features for mounting the unit. For this reason, it is common for the housing elements to be made from high tensile strength, low density materials such as aluminium. [3]

Since the stator assembly is inserted into the housing it is important to consider the electrical relationship between the windings of the stator and the housing. Should the enamel insulation coating the windings conductor degrade and become exposed, it is possible for the current to short circuit with another winding or the housing [64]. In order to prevent this, it is important to introduce additional levels of insulation protection. The methods available to improve electrical insulation protection are to encapsulate the stator assembly in an insulating material and to maintain specific minimum distances between the elements [65] [64].

Encapsulating a motor is a process of isolating the windings from the housing and other elements by means of either a pre-moulded insulator or by injecting insulating material into the stator and housing assembly

[3]. A set of pre-moulded insulators, which are often formed plastic components, will be placed into the housing before and after the stator assembly has been inserted, with the aim of isolating the windings from the walls and ends of the housing components [3]. The more effective option is to full encapsulate the stator assembly by means of injecting an epoxy-based resin into the housing after the stator assembly has been inserted (See Figure 39 for examples of fully encapsulated stator assemblies including section views of the full assembly and windings) [65]. This process is often referred to as potting. In addition to the comprehensive insulation protection, potting has the advantage of improving the thermal characteristics of the motor. The resins used in the potting process have thermal conductivity values far greater than that of air [65]. For this reason, high-performance motors are often potted in order to improve the electrical insulation and meet the thermal performance requirements [3].

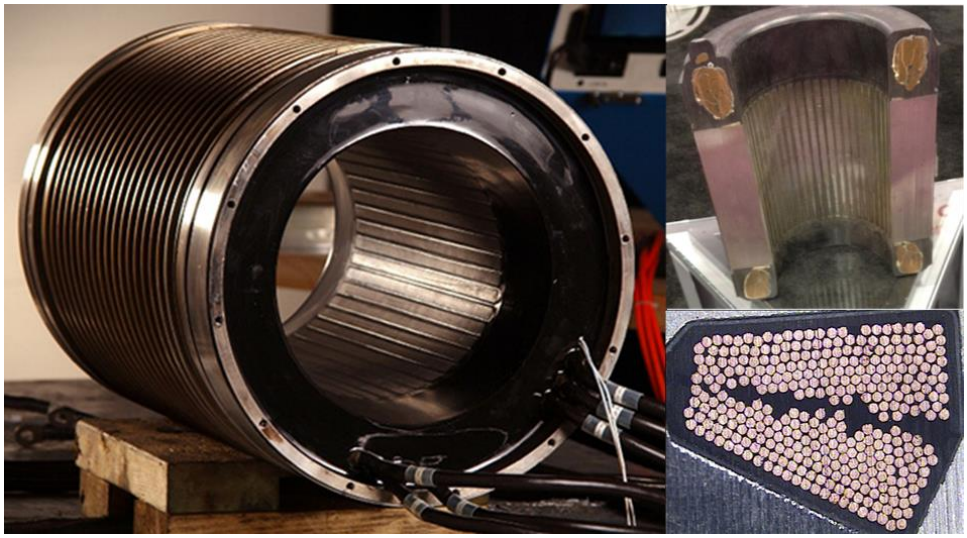


Figure 39: Examples of fully encapsulated stator assemblies including sectioned views [65] [66]

Electrical isolation can be improved further by ensuring that the minimum creepage and clearance distances between high voltage elements and housing components are maintained [3]. Creepage is defined as the shortest distance along the surface of an insulator between a high-voltage source and another conductive element (See Figure 40) [67]. The minimum creepage distance indicates the minimum distance, measured along an insulator, between conductive elements required to avoid failure by tracking [67]. Tracking refers to a breakdown of the insulator surface which forms paths for current to flow [67]. Clearance is defined as the straight-line minimum distance between conductive elements required to prevent an electrical short circuit across the insulation barrier (See Figure 40) [64].

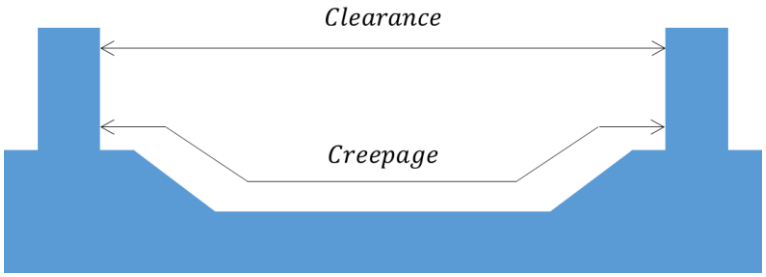


Figure 40: Creepage and clearance measurements across insulation barrier

The minimum creepage and clearance distances are a factor of the voltage conditions, operating environmental conditions and insulator material selection [64]. The British Standards Institution BS EN 60664-1:2007 defines a method for determining the minimum creepage and clearance values for phase-to-phase (Between windings in different phases) and phase-to-ground scenarios (Between windings and other conductive components such as the housing elements) [64].

The costs of the housing components is a factor of a number of elements including the material selection, treatment processes and manufacturing methods used. For this reason, it is difficult to provide an accurate cost estimate since many of the elements are dependent on factors such as tooling cost, manufacturing cost and number of units produced. For this reason general material costs for the typical housing materials from suppliers are used as a basis [52] [53] [54] [55]. Appendix A: Materials Catalogue Database contains mechanical properties for suitable housing component materials [56].

2.3 CATIA V5 and 3DExperience Platform – Automation Techniques

Integral Powertrain and Intrinsys make use of the CATIA V5 and 3DExperience engineering platforms. CATIA, which stands for Computer Aided Three-Dimensional Interactive Application, is a premium 2D and 3D CAD design and engineering software tool originally developed for use in the automotive and aerospace industries by Dassault Systèmes [68].

The CATIA platform is used as the basis for all electric motor mechanical design elements including the full CAD including tolerance information, linear structural analysis, engineering drawings, bill of materials for manufacture and fully associative and linked tooling designs.

The 3DExperience computer-aided engineering (CAE) tool is fully implemented into the 3DExperience product lifecycle management (PLM) system. The 3DExperience platform allows for full design lifecycle, manufacturing, BOM and change management [69]. The CATIA platform has various methods available

for generating intelligent and automated design models. The primary techniques available include the following:

- VB Scripting (Microsoft visual basic) and macros [70].
- CATIA CAA/RADE which is a CATIA add-on that provides users with the application programming interface (API) to develop C++ based code for custom applications [71].
- CATIA *Knowledgeware* design templates [72].

Majority of these methods allow for all the geometrical and other engineering parameters of the CAD models to be controlled and utilised in the automation process. To automate the CAD design process, it is necessary to link the design input parameters to output parameters which can be used to generate the CAD model. The input parameters will be based on the electric motor design requirements. These parameters will be controlled by a series of design rules which will consider general electric motor design principles and, if necessary, Integral Powertrain specific constraints to provide a set of output parameters. These output parameters will be linked to the CATIA platform to generate the CAD models. The CAD models will be able to provide an additional data output, including elements such as assembly mass/volume, which can be used to generate the outstanding desired output parameters such as the estimate cost.

Scripting for automation within the CATIA V5 and 3DExperience platforms can be achieved by using either IN-process or OUT-process applications [73]. IN-process applications are completed within the CAD design platform and can be written in Microsoft (MS) VB script or proprietary CATscript [73]. This limits the automation capability because of the single platform restriction. OUT-process applications allow for a foreign process, for example VB script generated in an external application, to call the CAD software, create or modify geometry and control most elements of the software [73]. This code can be written in VB, Windows scripting host, Windows explorer HTML or any Component Object Model (COM) application [73]. Figure 41 illustrates an example of different communication methods for automation available within the CAD platforms.

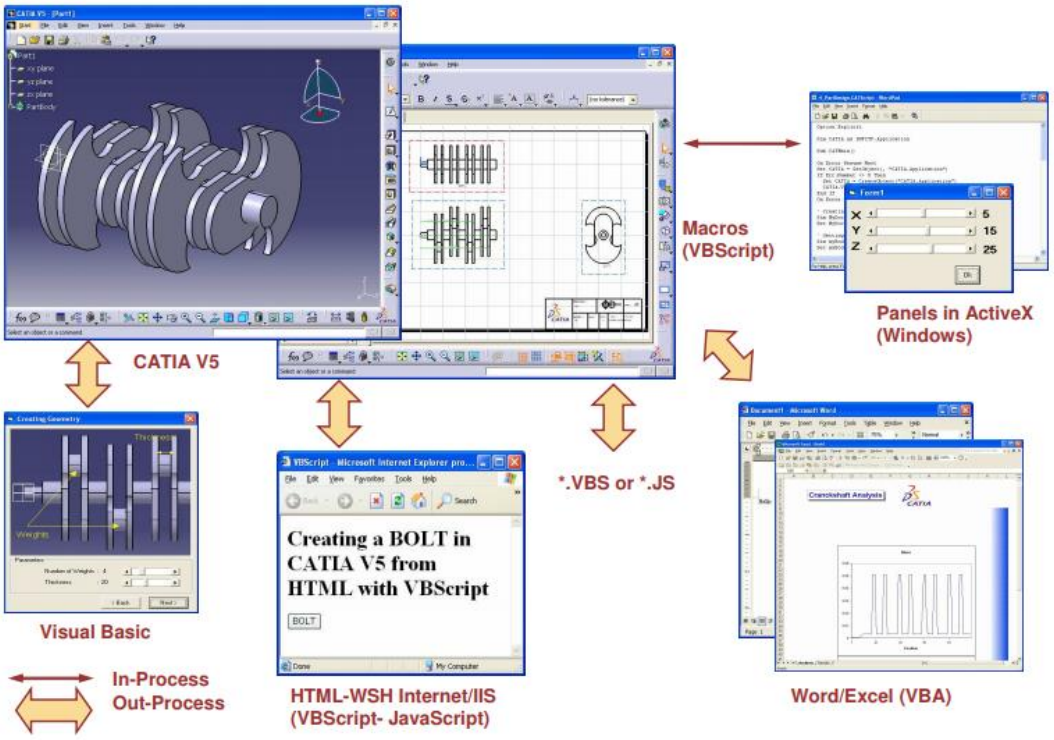


Figure 41: Examples of automation techniques within the Dassault Systemes software platforms [73]

Appendix B: CATIA V5 Automation Objects contains an extract from the standard library of automation objects available within the CATIA V5 platform [74]. This library provides important reference material for the development of an automation macro. Information pertaining to pre-defined CATIA V5 Visual Basic objects such as defined variables, properties and procedures is available in the library.

3 RESEARCH OBJECTIVES

The objectives of this research project are as follows:

- Investigate and develop the foundations for a software tool (AIEED) to aid in the first-level design development and costing phase of a new electric motor project.
- The objective of the tool is to reduce the response time, provide a product model and estimate cost for new electric motor enquiries.
- The tool will convert customer requirements data into geometrical design data, based on general electric motor design principles and design rules, to develop a first-level CAD model of the electric motor which will provide a basis for further detailed development of the final ‘delivered’ unit.
- The tool will output an estimate material cost of the electric motor based on the CAD model mass/volume and average material costs per unit mass/volume.

4 RESEARCH METHODS

To successfully fulfil the objectives of the research project it is necessary to acquire and synthesise the relevant knowledge and intelligence available through detailed investigation of literature, internal company 'know-how' and historical empirical data.

The initial phase of the AIEED tool development involves an extensive data and knowledge gathering exercise to collate the necessary intelligence that will be incorporated into the application. The AIEED will be used as a basis for the development of actual physical motors and will not remain a theoretical construct. It must, however, be clear that the tool is developed to create a first-level design model and as such, although the accuracy of the tool is important, there is a margin for error. The quality of the AIEED tool is primarily dependent on the logic implemented in order to develop the output. For this reason the quality of research, primarily obtained from published literature, historical project data and first principles theory, is of great importance.

After the appropriate intelligence has been gathered it is necessary to investigate methods of incorporating all the motor design knowledge and rules into a single utility or calculator. This tool will provide design parameter outputs as a result of input data based on the motor performance and specification as defined by the customer requirements. This phase of the AIEED tool development requires investigation into the logic necessary to build the tool such that the interface be simple enough for all users to run and be compatible with the formats required by the CAD design tool (CATIA V5 or 3DExperience).

Once the calculator is complete, it is necessary to investigate and evaluate an interfacing method between the calculator output data and the CAD design package. This requires the development of a CAD template model that is driven by the output parameters from the calculator.

Once the CAD has been integrated into the AIEED tool it is necessary to extract further data from the CAD model including the mass and volume. The AIEED tool is required to make use of the mass, volume and additional data to calculate a cost estimate for the e-motor. Once the AIEED tool can successfully generate a CAD model and estimate unit cost of an electric motor based on a customer's performance requirements, it is necessary to perform an overall verification process.

The original project schedule can be seen in Appendix C: Project Schedule.

5 CRITERIA FOR VALIDATION AND VERIFICATION

The AIEED tool is verified at multiple stages during the development phase. This includes verifying the design calculator utility periodically during its development to ensure accurate data generation. Verification stages are also included during the CAD template build to ensure that the template be robust and avoid improper behaviour as a result of invalid data entry. Similar verification processes will take place during the development of the estimate material cost calculator. The verification checks ensure that progress is monitored throughout the duration of the project to ensure the development of an accurate and stable software tool.

The scope of the project does not include the full validation of the tool. The tool can be validated in future by evaluating the accuracy of the output data. The accuracy of the application can be evaluated by executing a series of tests based on input data from past projects and comparing the output geometry and cost estimate data with the respective actual physical data. The criteria for validation would include a number of factors such as geometrical accuracy, performance characteristics, unit mass and cost. A list of criteria that could be included in a future validation activity can be seen below:

- Motor maximum output speed.
- Motor maximum torque output.
- Magnet stack length.
- Stator outer diameter and inner diameter.
- Stator tooth profile and dimensions such as yoke depth, tooth width.
- The motor mass or power density.
- The motor materials cost.
- Total time of response to new motor enquiries.

6 AIEED DEVELOPMENT PROCESS

The foundations of the AIEED tool are developed based on the principles presented in *2 Literature Review*. The tool was developed in different stages with iterative processes between each stage. The foundations of the tool were built using the following methodology:

1. Calculator build: The first phase of the tool build is the development of a calculator to convert input data (performance and specific dimensional parameters) to output design data. The calculator incorporates all the relevant fundamental SPM motor design theory required to fully define the geometrical aspects of an SPM motor.
2. Design model template build: The second phase of the tool is to develop a series of generic 3D CAD model templates for each major component of the motor. The model templates are developed in a generic manner to enable a robust tool.
3. Interface calculator and design model: The third phase of the tool development is to link the design calculator with the 3D model templates. The data (input and output) from the calculator is interfaced with the design template to automate the CAD build process. This phase involves macro development required to automate the CAD build process.
4. Determine material cost and build final assembly: The fourth phase of the tool development is to introduce a reverse link between the calculator and the models to extract volume data required to estimate the overall mass and material cost of the unit.
5. Final compilation: The final phase of the tool build is to incorporate all the elements together into a single utility. This utility allows for the development of a first-level CAD model of an SPM motor based on high-level parameters and provides an estimate material cost.

The development of the foundations of the tool were not performed in a strictly sequential approach and many of the phases were involved in an iterative development process. However, investigation into the methodology followed at each phase is provided in the following sections.

The development process is explained using sample data representative of a previous hybrid vehicle motor project. This dataset provides a basis for validation and verification.

6.1 Development Platform Decisions

To begin building the AIEED tool it is necessary to establish the development environment with which each phase will be built. It is important to ensure that the development environment selected for each phase

be compatible with each other. Since the design software is dictated by Integral Powertrain's requirements it is compulsory for the tool to be compatible with either the CATIA V5 or 3DExperience CAD packages.

Despite the additional features and more modern technology, the 3DExperience modelling tool requires access to a full PLM platform. For this reason, it is inconvenient to develop on the 3DExperience platform as a separate development workspace is required to be setup on the commercial 3DExperience platform. CATIA V5, which can operate as a standalone CAD package, has very similar modelling functionality compared to the 3Dexperience platform. For this reason, CATIA V5 is used as the modelling platform for the AIEED tool.

In terms of ensuring compatibility between the calculator and the design application it is beneficial to use a more generic solution as opposed to a proprietary option which may be exclusive to its particular environment. For this reason, CATIA specific tools such as *Knowledgeware* are avoided and options such as CAA RADE (C++) and VB scripting environments are preferred.

The calculator can be developed on several platforms. However, in order to maintain compatibility, it is required that the platform support C++ or VB scripting. Since all users at IP have Microsoft (MS) Office, MS Excel has been selected as the platform for the calculator. MS Excel is a suitable development platform as it supports VB script and provides sufficient capability to perform the necessary computation. Macros can be developed in MS Excel and CATIA V5 using common VB script. A number of these scripts can be developed to satisfy majority of the automation requirements. This could include pushing commands from the MS Excel spreadsheet to CATIA V5 for the CAD build and pushing data from CATIA V5 to MS Excel for the material cost estimates.

The AIEED tool is developed in CATIA V5-6R2016 SP3 and MS Excel 2013. Figure 42 illustrates the high-level data flow and interaction between the components of the AIEED tool.

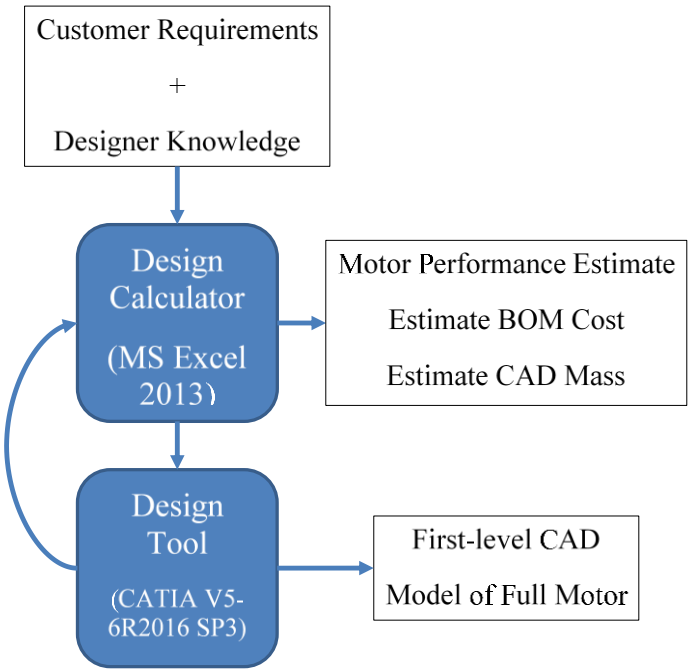


Figure 42: AIEED Tool: High-level data flow and interaction diagram

6.2 Design Calculator Build

The design calculator, developed on MS Excel, is a tool that converts the input performance and geometrical requirements of the motor into design output data. The calculator is the fundamental aspect of the AIEED tool as it contains the necessary electric motor design theory. The development of the calculator begins with identifying the input variables.

The calculator is structured in a number of different worksheets. The first sheet contains a page for all the inputs (customer requirements), the second sheet contains all the output data (performance plus geometrical parameters). There are also several additional sheets containing material information, constants and other sub-component information. A general user will only have to interact with sheets one and two for general operation.

By investigating permanent magnet motor design by Hanselman [5] and Soong [35] and considering the typical requirements data requested by customers, a number of inputs have been defined for the calculator. These inputs have been split up into different categories. The primary set of inputs are classified as performance and characteristics parameters. Table 7 contains an extract from the calculator and indicates the list of the performance inputs and their respective the following performance and characteristic parameters are used when designing a new motor.

Table 7: Calculator inputs: Performance and characteristics (Sample values)

Customer Requirements - INPUTS				
Section	**Parameter**	**Symbol**	**Units**	**Value**
Performance	Maximum Power Output	Pmax	kW	135
	Maximum Speed	nMax	rpm	19,000
	Constant Power Speed Range	CPSR	rpm/rpm	2.950
	Torque Per Unit Rotor Volume	rMPerRotorVolume	Nm/l	153.000
	Number of Magnet Pole Pairs	NPP	-	6
	Airgap Length	LAirgap	mm	2.500

The first performance parameters required are the expected maximum power output (P_{max}) and maximum rotational speed (n_{max}) of the unit. In addition to this, in order to describe the operating characteristics of the motor it is necessary to define constant power speed range $(CPSR)$ of the motor. With these parameters, it is possible to determine the maximum torque output.

To begin sizing the unit, it is useful to consider making use of a sizing parameter. By investigating (17) and (18), it is possible to relate the torque output of the motor to the rotor volume. For this reason, the torque per unit rotor volume is defined as an input parameter $(rM_{PerRotorVolume})$.

An important input variable that is included is the number of magnet pole pairs (N_{PP}) to be used in the motor and the airgap length (L_{Airgap}) between the rotor outer diameter (Including the magnets) and the stator internal diameter.

From the performance input information received it is possible to determine the maximum torque output. Using (15), (16) and investigating the typical CPSR curve illustrated in Figure 20 it is possible to show that the maximum torque be determined as follows:

$$P = \omega T \text{ and } CPSR = \frac{\omega_{max}}{\omega_b}$$

$\therefore T_{max} = \frac{P_{max}}{\omega_b}$, Since the operating speed at maximum torque is ω_b (Limit of constant torque region) and

$$\omega_b = \frac{\omega_{max}}{CPSR}$$

$$\therefore T_{max} = \frac{P_{max} CPSR}{\omega_{max}}$$

As indicated in Table 8 the maximum torque output of the motor is presented in the *Performance* section of the calculator output. Included in the output list for reference is the maximum rotational speed represented in radians per second.

Table 8: Calculator outputs: Performance

OUTPUTS				
Section	**Parameter**	**Symbol**	**Units**	**Value**
Performance	Maximum Speed	nMax_rads	rad/s	=nMax*(2*PI()/60)
	Max Torque Output	MMax	Nm	=(Pmax*1000*CPSR)/(nMax_rads)

The second phase of the calculator build introduces material properties and specific dimensional parameters related to each sub component of the motor. Table 9 represents an extract from the calculator indicating the input parameters required for material selection, permanent magnet definition, stator and winding properties and rotor specification.

Table 9: Calculator inputs: Materials, Magnets, Stator & Windings and Rotor (Sample values)

Section	Parameter	Symbol	Units	Value
Materials	Magnet Material Selection	MagMat	-	Generic PM
	Winding Material Selection	WinMat	-	Generic Cu
	Stator Material Selection	StaMat	-	Iron (Stator)
	Housing Components Material Selection	HouMat	-	Aluminium (Housing)
	Rotor Material Selection	RotMat	-	Aluminium (Rotor Hub)
Magnets	Magnet Length	LM	mm	10.000
	Lamination Stacking Factor	Kst	-	0.990
	Leakage Factor	Kl	-	0.980
	Reluctance Factor	Kr	-	1.100
	Residual Induction	Br20degC	T	1.350
	Relative Permeability	Mu_r	-	0.980
Stator & Windings	Stator tooth slot depth	SD	mm	20.000
	Tooth Tang Depth	TGD	mm	2.000
	Stator tooth slot opening	SO	mm	3.500
	Peak flux density through Stator Yoke	By_pk	T	1.470
	Peak flux density through Stator Tooth	Bt_pk	T	1.690
	Number of Winding Turns	nTurns	-	40
	Number of slots per pole per phase	Nspp	-	0.5
	Slot Fill, Gross	SFg	-	0.550
	Cu Winding Resistivity	Rho_Cu_20C	Ω·m	1.720E-08
Rotor	Rotor Magnet Outer Diameter	DR	mm	174.000
	Number of Rotor Spokes	nRotorSpokes	-	3
	Rotor Hub Web Thickness	WebThk	mm	5.000
	Rotor Hub Web Draft Angle	WebAng	deg	2.0
	Resolver Rotor Mount Bolt Thrd Length	ResBoltLen	mm	16.000
	Resolver Rotor Mount Bolt Thread	ResThrd	-	M8
	Resolver Rotor Mount C-Bore Length	ResCboreLen	mm	12.300
	Resolver Rotor Mount C-Bore Diameter	ResCboreDia	mm	15.700
	Rotor Spline Length	RSLength	mm	27.500
	Rotor Spline Lead-in Angle	RLAng	deg	30.000

Material selection is completed by means of a drop-down list containing options for each component material (See Figure 43). This includes a list for: permanent magnet material, winding material, stator material, rotor material and housing components material. The list is generated based on a materials database stored in a separate worksheet in the document.

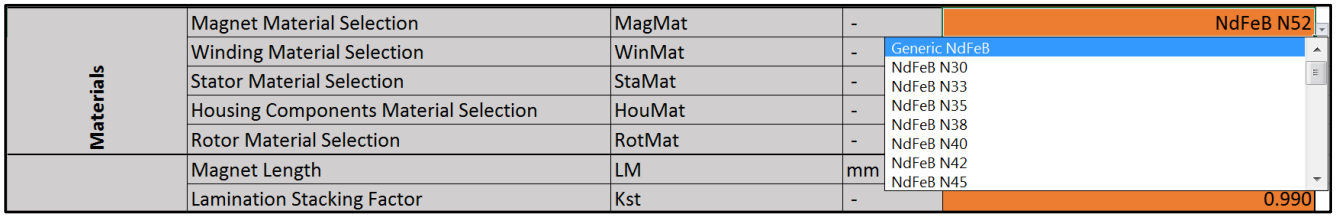


Figure 43: Calculator inputs: Permanent magnet material selection drop-down list

The materials database contains a number of properties important for the evaluation of geometrical parameters of the motor and to estimate the material cost. Table 10 indicates the material properties included in the materials database. The database is easy to manipulate, and additional materials can be added by including additional lines of data. Ideally the materials database definition should be controlled by a materials administrator. Restriction controls can be implemented using the standard MS Excel protection options.

Table 10: Calculator inputs: Material properties

Material Category	Permanent Magnet	Winding	Stator Core	Rotor Core	Housing Elements
Properties	Density [kg/m^3] Cost [£/kg] Resistivity [Ωm] Relative Permeability [-] Residual Inductance/Remenance [T] Coercive Field [A/m]	Density [kg/m^3] Cost [£/kg] Resistivity [Ωm]	Density [kg/m^3] Cost [£/kg] Resistivity [Ωm]	Density [kg/m^3] Cost [£/kg] Resistivity [Ωm]	Density [kg/m^3] Cost [£/kg]

Once the material selection has been completed, certain parameters such as those highlighted blue in Table 9, will be automatically populated. This activity is completed by using a *LOOKUP* function in MS Excel which allows for automatic field population based on the material selection defined. This reduces potential error as the calculator will always use the material information from the materials database and does not allow for manual entry by the user. An important example of this is with regards to the residual induction input value which is dependent on the magnet material selected and cannot be entered independently of the material selection.

In addition to the magnetic material properties such as residual induction $(B_{r20degC})$ and relative permeability (μ_r), it is also necessary to define the magnet length (in the magnetised direction) (L_m). The

magnet length is defined as a user input variable in order to provide designers with a level of control over the magnet size and subsequently cost. By using the magnetic circuit analysis techniques presented in *2.2 Surface Permanent Magnet Alternating Current Motor Design Principles* it is possible to approximate the airgap flux density which is required to determine certain geometrical features. To evaluate the airgap flux density, it is necessary to include factors such as the leakage factor (K_l), reluctance factor (K_r) and lamination stacking factor (K_{st}). These inputs are grouped in the *Magnets* section. Another important factor that is required for the motor sizing and performance design is the rotor magnet outer diameter (D_R) (See Figure 28). This is included as an input under the *Rotor* category.

With the input data presented and using (18), (28) and (29) it is possible to determine the airgap flux density (B_g), rotor volume (V_R) and rotor length (L_{Rotor}) as follows:

$$B_g = \frac{K_l C_\emptyset}{1+K_r \frac{\mu_R}{P_c}} B_r \text{ and } P_c = \frac{L_m}{L_{Airgap} C_\emptyset}$$

Assuming that the flux concentration factor is ideal ($C_\emptyset = 1$):

$$P_c = \frac{L_m}{L_{Airgap}}$$

$$\therefore B_g = \frac{K_l}{1 + K_r \frac{\mu_R L_{Airgap}}{L_m}} B_{r20degC}$$

And,

$$V_R = \frac{\pi {D_R}^2}{4} L_R = \frac{T_{max}}{rM_{PerRotorVolume}}$$

$$\therefore L_R = \frac{4V_R}{\pi {D_R}^2}$$

As indicated in Table 11 the airgap flux density and rotor length are presented in the *Rotor & Magnets* section of the outputs list of the calculator. Included in the output list for reference is the permeance coefficient (P_c) and rotor volume.

Table 11: Calculator outputs: Rotor and Magnets

Section	Parameter	Symbol	Units	Value
Rotor & Magnets	Airgap Flux Density	Bg	T	=Br20degC*((Kl*1)/(1+Kr*(Mu_r/Pc)))
	Permeance Coefficient	Pc	-	=(LM/(1*LAirgapMagnetic))
	Rotor Volume	VR	l	=MMax/rMRatedPerRotorVolume
	Rotor Length (Stack Length)	LR	mm	=VolRotor*4/PI()/dRotorMagnetOD^2*1000000

With all necessary high-level performance parameters defined and the motor size established it is possible to begin defining the stator and winding elements. As indicated in Table 9, additional input information is required to complete the stator and windings design. The stator tooth and slot profile is determined using several input parameters, namely; stator tooth slot depth (SD); stator tooth tang depth (TGD) and the stator tooth slot opening (SO) (Refer to Figure 31). To complete the stator tooth profile, the theory presented in *2.2.2 Stator Assembly* is used. Due to magnetic saturation, the stator tooth body width (TWS) and stator yoke depth (WSY) can be determined. The designer can insert suitable values for peak flux density through the stator yoke $\left(B_{SY_pk}\right)$ and tooth$\left(B_{T_pk}\right)$. With these constants and using (33) and (35), the stator tooth profile can be completed by using the following:

$$TWS = \frac{2\pi R_{ro} B_g}{N_s K_{st} B_t}$$

And

$$WSY = \frac{\pi R_{ro} B_g}{2N_{pp} K_{st} B_{sy}}$$

$$\therefore TWS = \frac{\pi D_R B_g}{2N_s K_{st} B_{T_pk}} \text{ and } WSY = \frac{\pi D_R B_g}{4N_{pp} K_{st} B_{SY_pk}}$$

In addition, the full stator outer diameter $(OD)$and inner diameter (ID) can be determined as follows (See Figure 28):

$$OD = 2\left(L_{Airgap} + SD + WSY\right) + D_R \text{ and } ID = 2L_{Airgap} + D_R$$

The stator assembly definition is completed with user defined inputs for the number of turns in the windings (n_{turns}) and the gross slot fill percentage $\left(SF_g\right)$ (This is used for mass determination only). The copper winding resistivity is indicated as well and can be used for estimating power losses through the unit (See Table 9). This figure is pulled from the materials database.

The outputs for the stator definition can be seen in Table 12. This includes the stator outer and inner diameter, the yoke depth, tooth width and the number of slots. The number of slots (N_s) is determined using the number of slots per pole per phase $\left(N_{spp}\right)$, the number of magnet pole pairs (N_{PP}) and (39) as follows:

$$N_{SPP} = N_s / 2N_{PP} / N_{ph}$$

Therefore, applying the restriction that the motor is in a 3-phase environment $\left(N_{ph} = 3\right)$ and contains concentrated double layer windings $(N_{SPP} \leq 1)$

$$N_s = 3 \times N_{SPP} \times 2N_{PP}$$

As represented in Table 12 the stator and winding output parameters are found in the *Stator* section of the calculator outputs.

Table 12: Calculator outputs: Stator

Section	Parameter	Symbol	Units	Value
Stator	Stator OD	OD	mm	=(LAirgapMagnetic+yoke_depth+Slot_depth)*2+dRotorMagnetOD
	Stator ID	ID	mm	=2*LAirgapMagnetic+dRotorMagnetOD
	Yoke Depth	WSY	mm	=(PI()*dRotorMagnetOD*Bg)/(2*2*NPP*Kst*By_pk)
	Tooth Width	TWS	mm	=(2*PI()*dRotorMagnetOD*Bg)/(2*Ns*Kst*Bt_pk)
	Number of stator slots	Ns	-	=3*Nspp*2*NPP

The primary rotor dimensions are defined, but in order to develop a more complete first-level model additional input information is required. These are listed in the *Rotor* section of the calculator inputs (See Table 9). Additional packaging input parameters are included in the *Packaging Consideration* category (See Table 13) which are required to build up the structural aspects of the motor. These parameters are explained in context with the model in *6.3 Design Model Template Build*.

Table 13: Calculator inputs: Packaging considerations and Mass (Sample values)

Section	Parameter	Symbol	Units	Value
Packaging Considerations	Number of Mounting Lugs	nMountingLugs	-	4
	Mounting Lug Bolt Spec	BoltSize	-	M10
	Mounting Bolt PCD Offset	MBoltPCDOffset	mm	10.000
	Mounting Lug Fillet Radius	MLugFilR	mm	10.000
	Housing Minimum Thickness	MinThk	mm	3.000
	Bearing Race OD	bRaceOD	mm	55.000
	Bearing Race ID	bRaceID	mm	35.000
	Bearing Length	bLength	mm	13.000
	Resolver OD	ResOD	mm	62.000
	Resolver Length	ResLength	mm	4.500
	Min Insulator Thickness	InsMinThk	mm	1.500
Mass	Magnet Density	Rho_Magnet	kg/m^3	7,800.000
	Windings Density	Rho_copper	kg/m^3	8,920.000
	Stator Density	Rho_stator	kg/m^3	7,650.000
	Housing Density	Rho_Housing	kg/m^3	2,700.000
	Rotor Hub Density	Rho_RotorHub	kg/m^3	6,500.000

The material mass information (density) for each component material is listed in the *Mass* inputs section (See Table 13). This information is extracted from the materials database and is used when determining the estimate mass and subsequently estimate cost of the unit. The mass output and cost estimates are indicated in the outputs sheet in the *Mass & Cost* section (See Table 14). This will be described in greater detail in *6.4 Automating the Modelling Process.*

Table 14: Calculator outputs: Mass and Cost

Section	Parameter	Symbol	Units	Value
Mass & Cost	Power Density	Power_density	kW/kg	=Pmax/TotalMass
	Stator CAD Mass	StatorMass	kg	FROM CAD
	Rotor CAD Mass	RotorHubMass	kg	FROM CAD
	Housing CAD Mass	HousingMass	kg	FROM CAD
	Magnets CAD Mass	MagnetsMass	kg	FROM CAD
	Windings CAD Mass	WindingsMass	kg	FROM CAD
	Total Estimate CAD Mass	CAD_Mass	kg	FROM CAD
	Total Estimate Material Cost	CAD_Cost	£	FROM CAD AND MATERIAL COSTS

6.3 Design Model Template Build

The input and output data from the calculator provides sufficient information to fully define a first-level design model of the motor. The motor model includes an assembly with the following primary components: stator; rotor; magnets representation; windings representation and the housing elements (housing and cover). The model is developed in a manner that is feasible for representation whilst applying certain simplifications. For example, the laminations contained within the rotor and stator stacks have not been modelled individually but rather represented as a single body.

A CATIA V5 template model of each component is defined. Each of these template models is defined with a global axis system in mind and contain a skeleton structure including a series of planes used to define the axial position of key features. This skeleton structure contains a common set of elements that are used as a basis for positioning particular features of the motor. For example, features such as the rear and front of the magnet, rotor and stator stack are included. By designing the model with a global axis system, it is simpler to manage the positioning of the components within the final motor assembly. With the generic positioning and skeleton model approach it is possible to begin developing the template models for each individual component.

6.3.1 Stator Template Model

The first model to be developed is the stator core. The stator assembly contains several components including the stator core stack, the individual windings, individual tooth insulators and additional insulating elements. The stator model, however, is representative of the stator stack only. As mentioned previously, the model is a simplified representation of the laminated stack and is modelled as a single solid. Figure 44 illustrates the stator template model.

The stator model can be generated by defining the appropriate stator tooth geometry and extruding this profile in the axial direction until the required stack length has been achieved. To control the stack length, the reference planes from the skeleton geometry are used as constraints. Once complete, the single tooth solid can be copied in a rotational direction about the motor axis to complete the stator model with the correct number of slots defined.

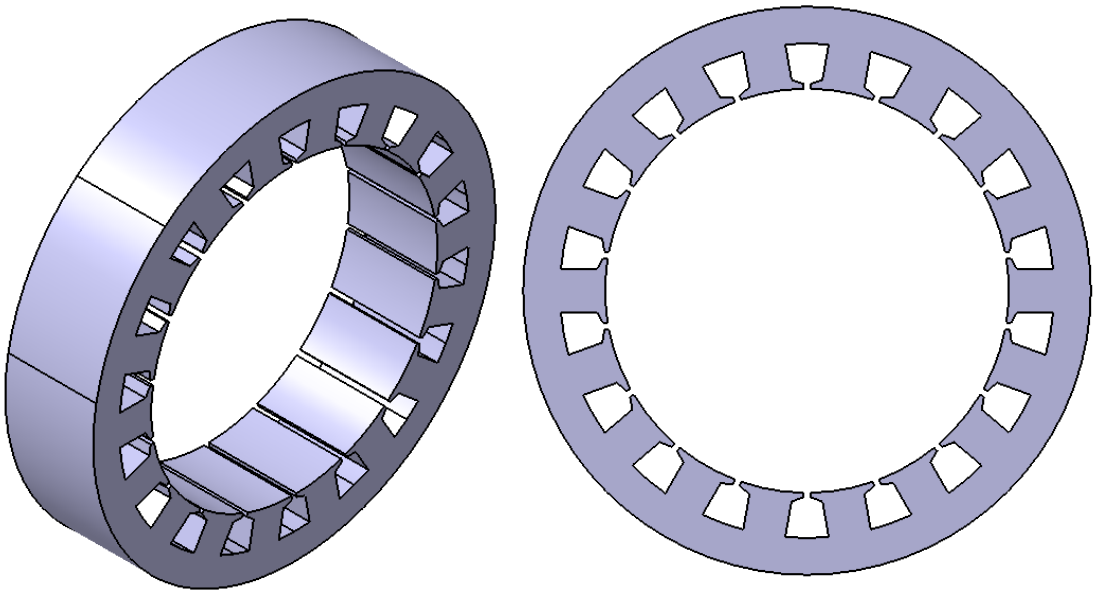


Figure 44: Stator template model

The most important aspect of the stator model is the stator tooth profile. For simplicity, the stator tooth profile is restricted to the *Parallel tooth, Arc-bottom, Semi-closed slot* option as described in Table 3. A representation of the stator tooth sketch which drives the stator tooth model can be seen in Figure 45. The dimensions driving the geometrical features of the profile are controlled by the parameters from the calculator. This interaction is described in *6.4 Automating the Modelling Process*.

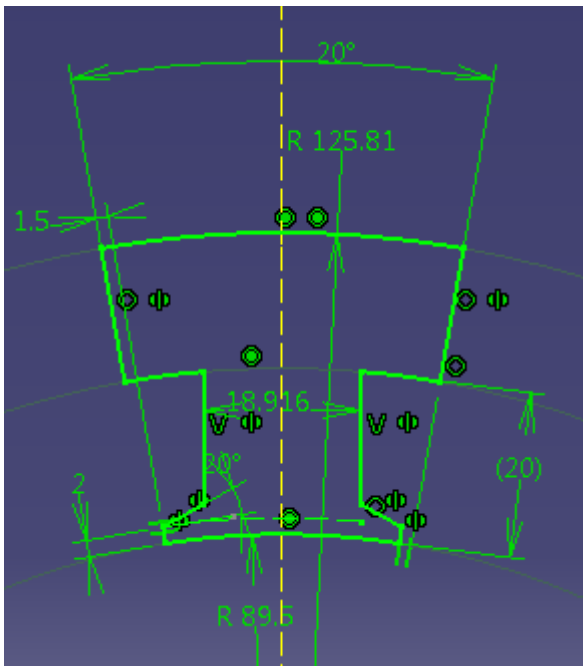


Figure 45: Stator template model: Tooth profile sketch (Sample dimensions)

6.3.2 Windings Representation Template Model

The windings representation is a simplified model which illustrates the volume occupied by the windings. In reality, the windings are typically coils of wire wrapped around individual stator tooth stacks with a rigid insulator between them. However, for simplicity, the windings and stator have been modelled separately. In addition, the windings consist of coils of insulated wire with a circular profile. Instead of attempting to model the windings in detail including each turned wire, a volume representation has been developed instead. This simplification improves computational performance since the system is not required to render the detail associated with each coil of the windings. Figure 46 is an illustration of the winding representation template model.

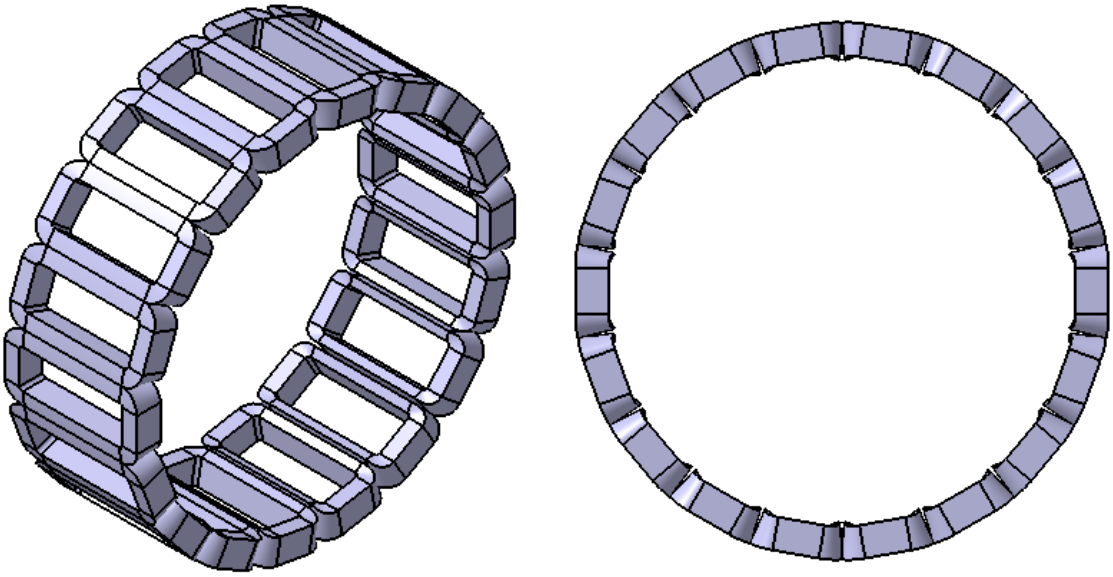


Figure 46: Windings representation template model

This model is developed as follows. Initially a duplicate of the stator tooth profile sketch is included as reference. This is used to determine the maximum volume available in the slots to accommodate the windings. An offset is placed on the slot portion of the tooth profile (See Table 13 for $InsMinThk$ parameter in calculator). This offset is applied to take into account the material that forms part of the stator tooth insulator, which is not modelled (See Figure 47). This profile is extruded along the motor axial direction to the extent of the stack. This is controlled by the reference planes defined in the skeleton geometry.

Additional operations are included to represent the end windings. The profile for the end windings no longer must conform to the stator slot geometry and as such is represented in a more natural rectangular form. These portions are joined together with a swept volume to represent the bends at the corners of the windings.

A minimum bend radius of 2mm is maintained. Once a quarter model of the winding volume is complete, a series of mirror and rotational pattern operations are performed to complete the full winding template model.

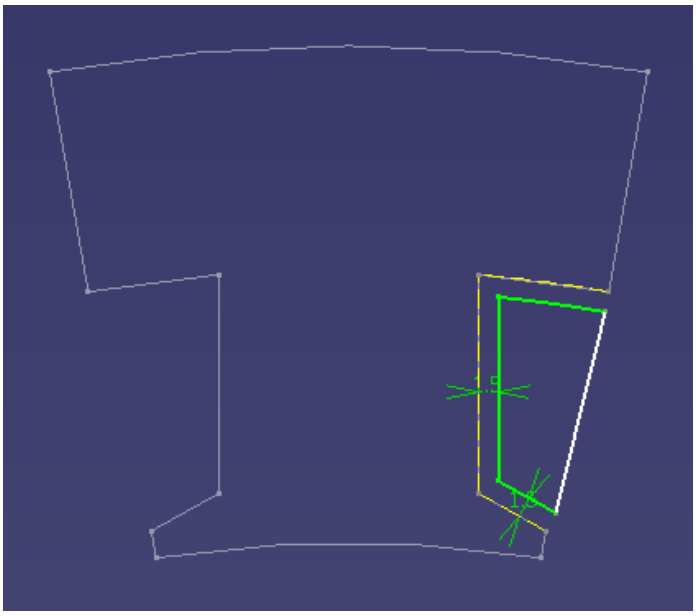


Figure 47: Windings representation template model: Windings volume profile sketch

All significant dimensions used to define the winding model are driven from the calculator and is explained in more detail in *6.4 Automating the Modelling Process*.

6.3.3 Rotor Template Model

The rotor template model contains sufficient detail to be used as a first-level design iteration which is suitable for customer presentation. The rotor model contains detail to include the following: permanent magnets support, spokes for mechanical support, resolver mounting support features, interfacing spline support features and bearing support features. The parameters that drive these features are included as input variables in the calculator.

Figure 48 contains an illustration of the rotor template model. The model is developed in a robust manner by making use of as few sketch profiles as possible. The primary sketch determines the major dimensions of the rotor (See Figure 49). The additional dimensions illustrated in Figure 50 are defined by input parameters from the calculator (See Table 9). The profile illustrated in Figure 49 is revolved around the motor axis to produce the base model. Once revolved, additional dress-up operations are applied to introduce the rotor spokes and resolver mounting support features. As indicated by the yellow lines in

Figure 49, certain elements of the rotor profile sketch are constrained to elements of the skeleton geometry. This controls the axial offset of certain features (e.g. bearing planes etc.).

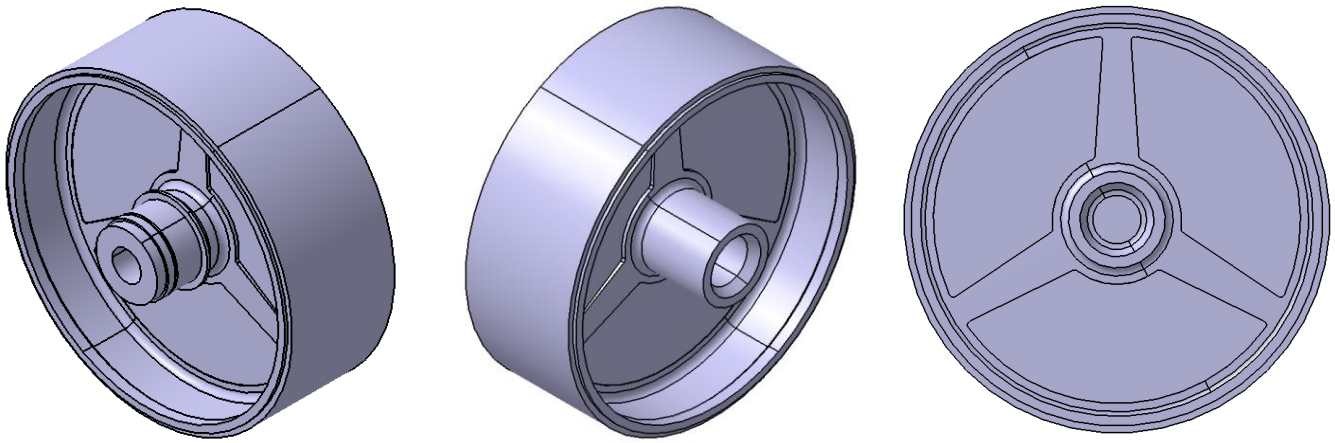


Figure 48: Rotor template model

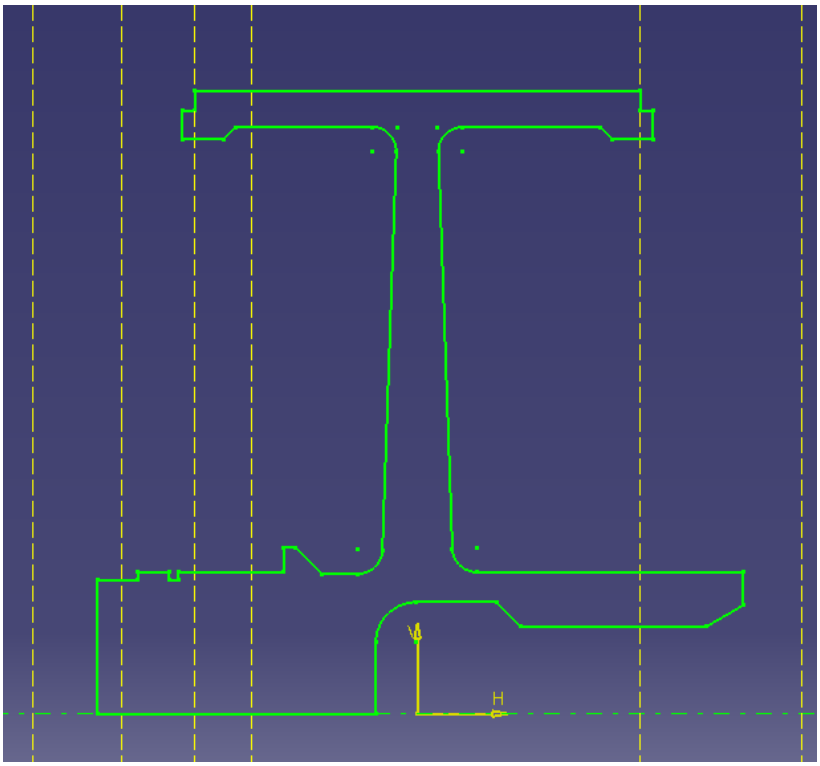


Figure 49: Rotor template model: Rotor profile sketch

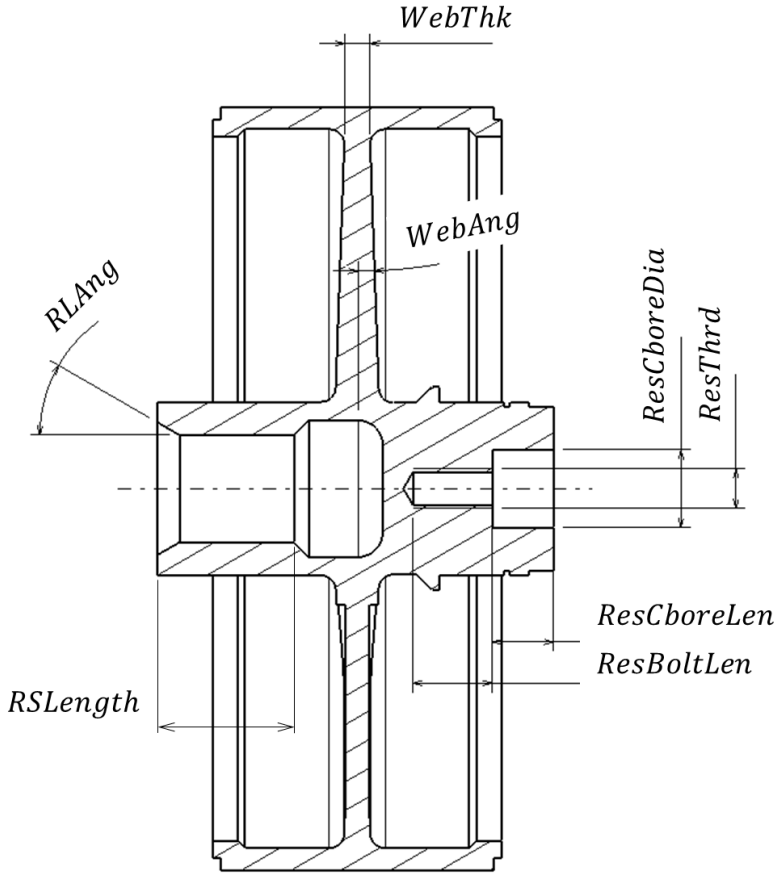


Figure 50: Rotor template model: Additional rotor detail dimensions

All the dimensions used to define the rotor template model are driven from the calculator. The interface between the geometry and the parameters is discussed in *6.4 Automating the Modelling Process*.

6.3.4 Permanent Magnets Representation Template Model

The permanent magnets representation template model is a simple representation of all magnet poles used in the motor. The magnet configuration is limited to the *radially magnetised surface magnets, arc-shaped*-type as described in Table 5. Figure 51 illustrates the template model. The model is developed with a profile sketch which defines the shape of a single magnet stack. This sketch is extruded in the axial direction of the motor to the length of the stack. The stack length is again controlled by planes in the skeleton geometry which is defined by the calculator data. A rotational pattern operation is performed to complete the full magnet model.

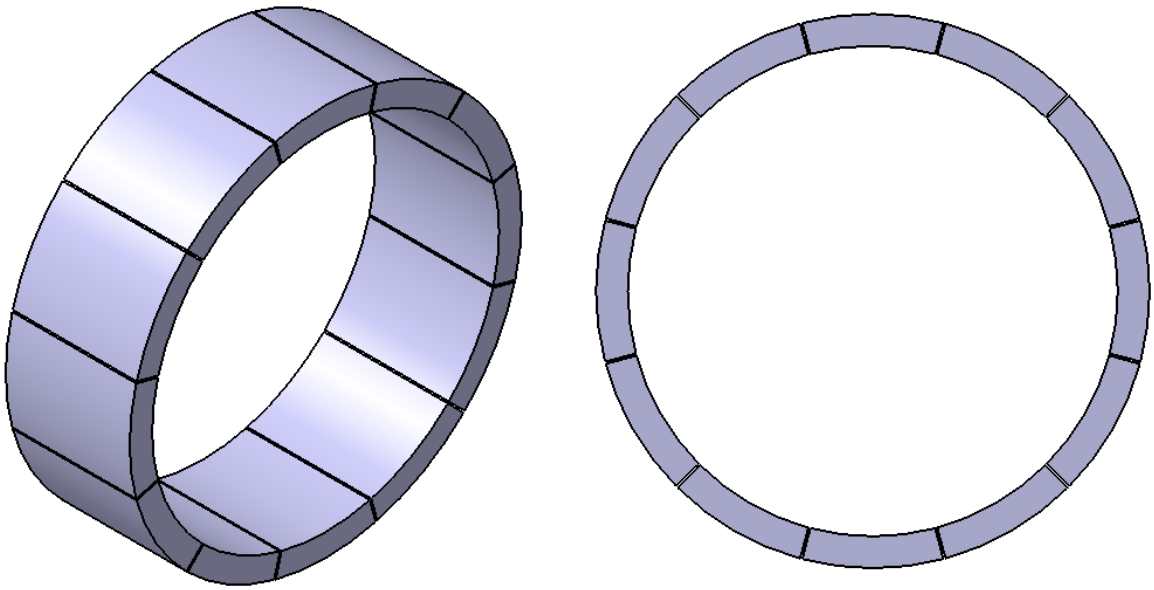


Figure 51: Permanent magnets representation template model

The profile of the magnet stack can be seen in Figure 52. This is representative of an arc-shaped magnet which is magnetised in the radial direction. The profile dimensions are controlled by parameters in the calculator for the number of pole pairs, magnet length and the rotor magnet outer diameter (See Table 9). The interface between the geometry and the parameters is discussed in *6.4Automating the Modelling Process*.

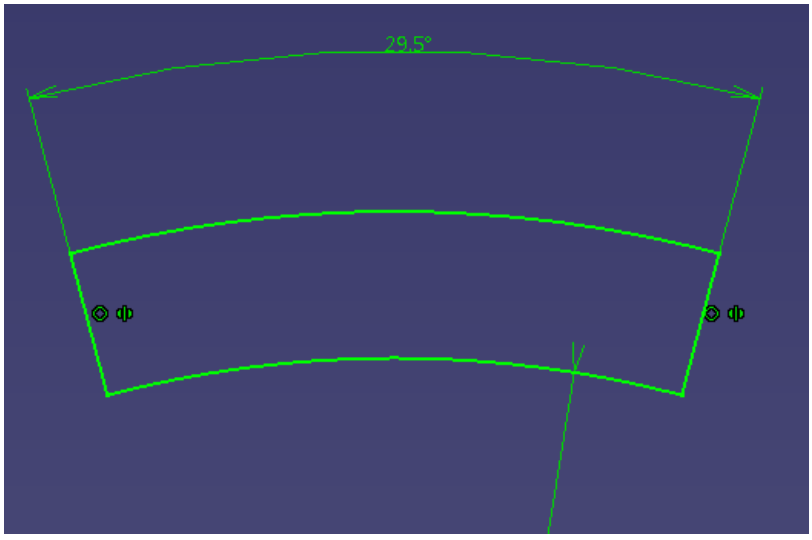


Figure 52: Permanent magnets representation template model: Magnet profile sketch

6.3.5 Housing Template Model

The housing model is required to house the stator assembly (stator and windings representation), support the rotor via bearings, support the resolver and provide mounting lugs to interface with the rest of the drivetrain. The foundations of the AIEED tool support 2-piece housing configuration only and for this reason, the housing model is created with a 'tin-can' shape as described in *2.2.5 Housing Components*.

As illustrated in Figure 53, the housing template model contains sufficient detail to include the following: support for stator assembly, bearing support features, resolver mounting support features and mounting lugs to suit the customer application. The parameters that drive these features are available from the calculator (See *6.2 Design Calculator Build*).

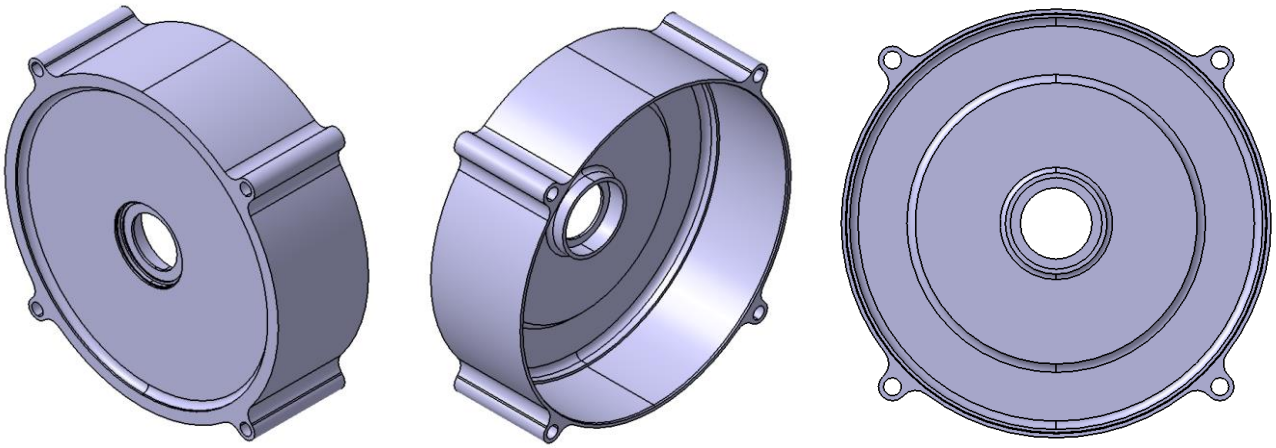


Figure 53: Housing template model

The housing model template is built from a primary revolved profile. Figure 54 illustrates the primary profile sketch that defines the main body of the housing. This profile contains the details for features required to house the stator, provide sufficient clearance for the end windings, support the rotor bearings and provide a platform to mount the resolver. The parameters that define the dimensions of the sketch are driven from the calculator. The *Packaging Considerations* section (See Table 13) of the calculator inputs provides sufficient data to fully define the housing (See Figure 55 for an illustration used to identify the additional parameters).

Parameters to control the bearing race outer diameter, the bearing length, the resolver outer diameter and the resolver length and are defined in the primary profile sketch and are identified in Figure 55. The profile sketch is controlled in the motor axial direction by applying constraints between certain sketch elements and planes in the skeleton geometry set.

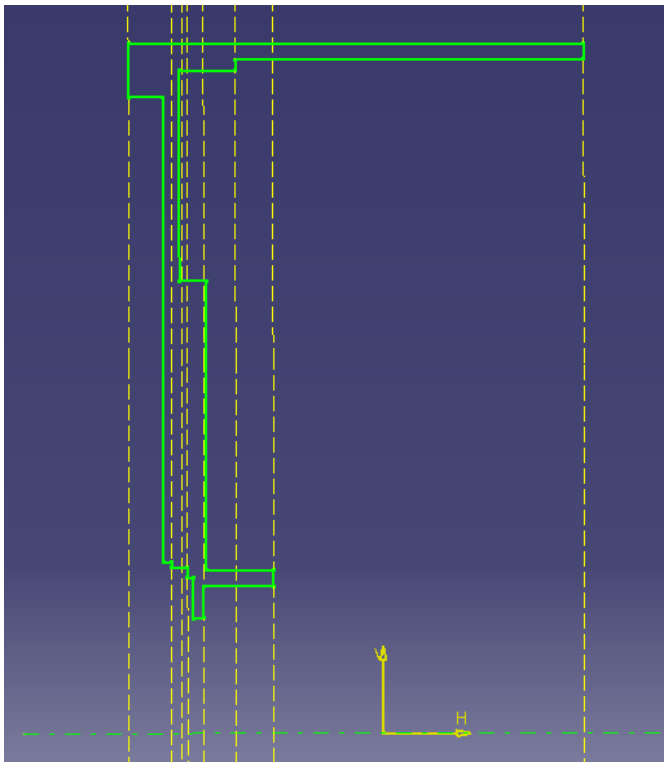


Figure 54: Housing template model: Housing profile sketch

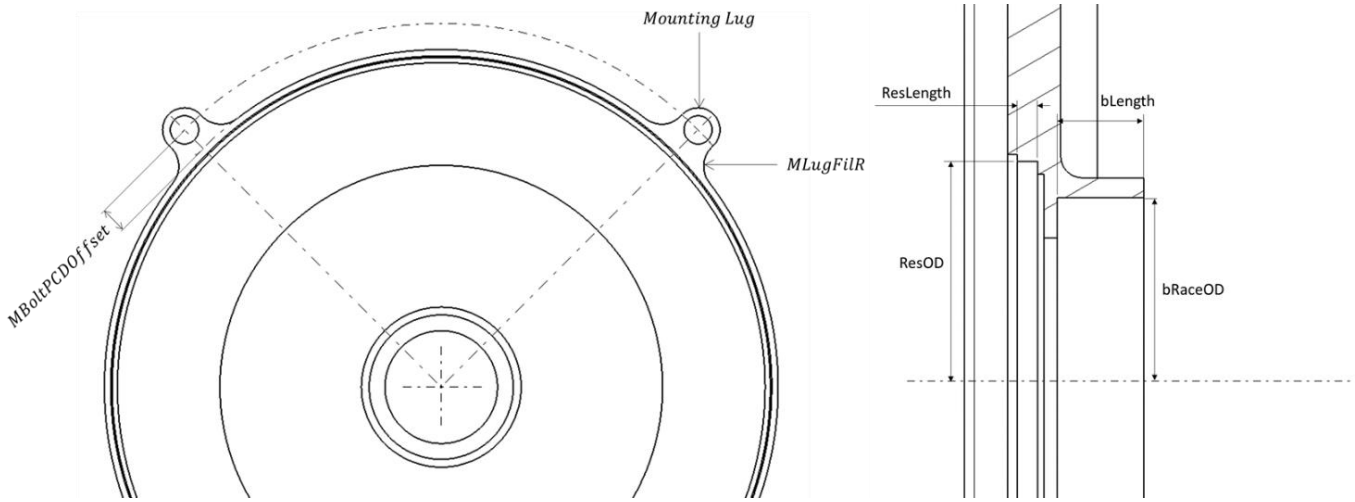


Figure 55: Housing template model: Additional housing detail dimensions

The mounting lugs are added with additional operations. The lugs are orientated such that mounting is limited to the axial direction only. The option to support radial mounting is not supported in the model. To develop the mounting lugs, a single lug is defined using a sketch. This sketch is dimensioned according to the parameters available in the calculator which can be described using Figure 55. To support the mounting

bolt, an operation is applied to the single mounting lug which creates a clearance hole. Once complete, the single mounting lug, with the clearance hole, is copied using a rotational pattern feature. This allows for several mounting lugs to be created in an equi-spaced arrangement. Additional dress-up features are applied to complete the model.

All the parameters that drive the template dimensions are defined in the calculator with the interface between the two elements described in *6.4Automating the Modelling Process*.

6.3.6 Cover Template Model

The cover model, developed in a similar manner to the housing model, provides support for the second rotor bearing, as well as sealing the motor whilst providing clearance for the front-end windings. The model contains mounting lugs in the same arrangement as the housing model. As illustrated in Figure 56, the cover template model contains the features required to support the front bearing, seal the motor and support the mounting arrangement.

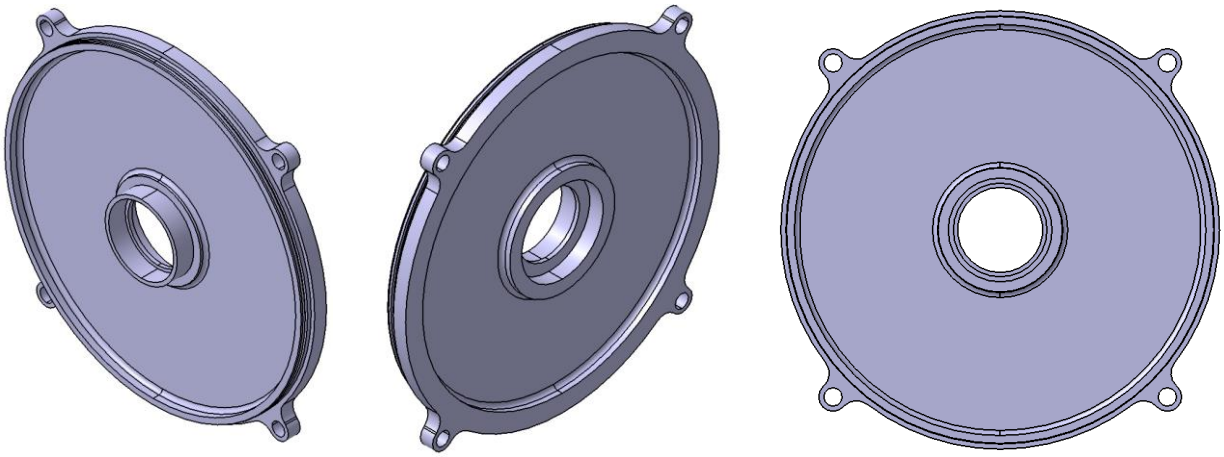


Figure 56: Cover template model

The primary solid is modelled based on a revolved profile as illustrated in Figure 57. As with the other template models, the primary profile illustrated in Figure 57 contains majority of the features required and makes use of the skeleton model methodology to constrain certain sketch elements along the axial direction. The mounting lug detail is replicated as defined in the housing model (See Figure 55).

All the parameters that drive the dimensions are extracted from the calculator with the interface between the calculator and the model template described in *6.4 Automating the Modelling Process*.

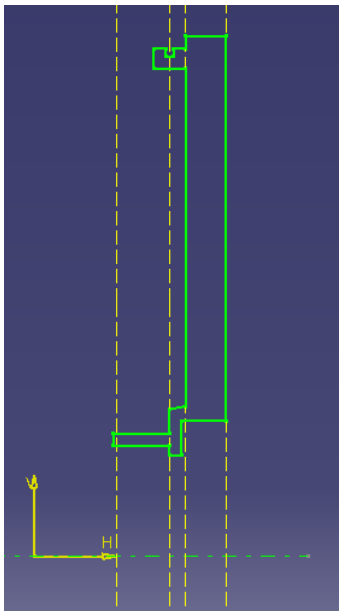


Figure 57: Cover template model: Cover profile sketch

With all the individual component models completed, it is possible to build up the overall assembly. The sample assembly model can be seen in Figure 58.

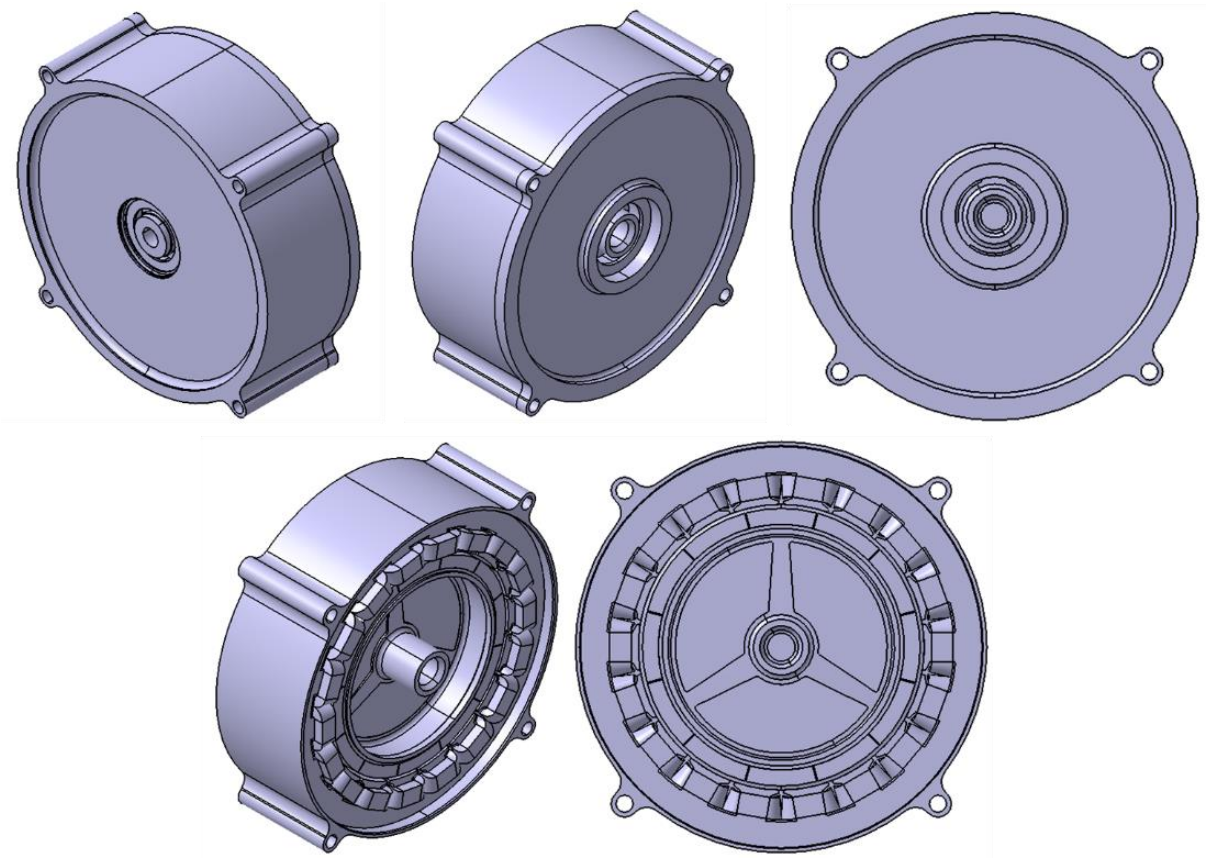


Figure 58: Full motor assembly template model (Sample parameters)

6.4 Automating the Modelling Process

The model templates of each component have been created and the parameters that define the dimensions have been determined in the calculator. With the objective of automating the CAD model build, it is necessary to link the appropriate parameters from the calculator to the geometry defined in the templates. Since both MS Excel (the calculator development environment) and CATIA V5 (the CAD model development environment) support MS visual basic, the interface between the two elements is facilitated through a series of macros written in VB script.

After providing MS Excel with the necessary CATIA V5 object libraries and references it is possible to control CATIA V5 using commands initiated from MS Excel. Since the calculator is developed in MS Excel and contains the bulk of the processed data, it was decided that the scripts be developed in the VBA editor based in MS Excel.

A very useful macro recording feature available in CATIA V5 facilitates the development process. It was decided that instead of attempting to build a script to replace the parameters in the template models with those defined in the calculator it would be simpler and more robust to issue the CAD model build operation commands directly from the calculator using the appropriate parameters upfront. The fundamental methodology adopted to interface the calculator with the design models and to automate the CAD build is as follows:

1. Enable macro recording in CATIA V5.
2. Replicate the template model build process, using the same methodology described in *6.3 Design Model Template Build* in CATIA V5.
3. Record each step of the model build process for each component of the motor.
4. Copy the recorded VB script from the CATIA environment into the MS Excel VBA editor.
5. Introduce design variables in the VB script that extract parameter data from the calculator.
6. Edit the recorded VB script (from CATIA V5) with the objective of replacing the generic variables that define the model geometry with the appropriate design variables introduced in step 5.
7. Test the code stability and functionality at each phase of the script development.
8. Introduce code with the intention of improving robustness.
9. Improve robustness by making use of data validation techniques available in MS Excel. This will reduce the range of possible input variables, thereby limiting the possibility of inserting invalid parameters (e.g. a negative number of mounting lugs).

10. Compile the full CAD build scripts for each component.
11. Compile an assembly script to create a product including all the sub-components of the motor.
12. Create a single script that calls each individual component script and the assembly script to complete the full motor build with a single macro.

Following the above methodology provides the basis upon which the AIEED tool is built.

In addition to the core component build and assembly build scripts, additional pieces macros have been included in the tool with the aim of improving the user experience. For example, code is built into each component build script to automate the model save operation.

All the macros can be executed from within the MS Excel based calculator by means of labelled push buttons as illustrated in Figure 59. The macros available in the AIEED tool, with a brief description of each, are listed in Table 15.

Table 15: AIEED Macros and their description

Macro Name	Description
Build Housing	Creates a model of the housing to the specifications defined in the calculator
Build Cover	Creates a model of the cover to the specifications defined in the calculator
Build Stator	Creates a model of the stator to the specifications defined in the calculator
Build Windings	Creates a model of the windings representation to the specifications defined in the calculator
Build Rotor	Creates a model of the rotor to the specifications defined in the calculator
Build Magnets	Creates a model of the magnets representation to the specifications defined in the calculator
FULL MOTOR BUILD	Initiates the full motor build which includes the build of each component and the final assembly operation
Build Assembly	Assembles the components. Only works if the components have been created and saved in their working directory
Reset Mass	Clears the *Mass* fields in the outputs sheet of the calculator
Reset Directory	Clears the *Working Directory* field in the calculator
Change Directory	Allows user to redefine the working directory with the aid of a pop-up navigation window

Project Code	TEST			Change Directory	Instructions:
Working Directory	C:\Users\gminucci\Desktop\Test			Reset Directory	1) Complete all input fields (orange)
Build Housing	**Build Windings**	Build Assembly	Reset Mass	**FULL MOTOR BUILD**	2) Press **FULL MOTOR BUILD** to complete CAD build process
Build Cover	**Build Rotor**				3) Go to OUTPUTS to see **Mass** and **Cost** estimates
Build Stator	**Build Magnets**				4) Go to **Info** for additional instructions and revision information
Customer Requirements - INPUTS					
Section	**Parameter**		**Symbol**	**Units**	**Value**

Figure 59: Macro buttons available in AIEED tool

To manage the design data, a working directory selection tool is included to assist the designer in selecting an appropriate working directory to which all developed models will be saved. This is executed by selecting the *Change Directory* button.

Each component build VB script contains generic code that ensures CATIA V5 is open. If not, the script will issue a command to open the program. The macros also contain code to define the appropriate CATIA V5 settings for the modelling session. This is included to ensure consistent and robust operation.

In addition, a basic part numbering utility is included in the script as well. This extracts data from part numbering cells in the calculator workbook and renames the components accordingly (See Figure 60).

Project Code	TEST			
Working Directory	C:\Users\gminucci\Desktop\Test			
Part Numbering	Housing Section Code	Housing_SectionCode	-	100
	Cover Section Code	Cover_SectionCode	-	150
	Stator Section Code	Stator_SectionCode	-	200
	Winding Section Code	Winding_SectionCode	-	250
	Rotor Section Code	Rotor_SectionCode	-	300
	Magnets Section Code	Magnet_SectionCode	-	400

Figure 60: AIEED Tool: Part numbering fields

The mass and material cost estimates are completed by initiating the *FULL MOTOR BUILD* macro. Once the full motor assembly has been created, the script initiates code which extract the CAD volume of each component. The volumes are used in conjunction with the density information available in the calculator (dependent on the material selection from the library) to determine the mass of each component. The cost is determined based on an average cost per unit mass which is also included in the materials database. The overall unit mass and cost are included in the *Mass & Cost* section of the outputs sheet of the calculator and are determined as follows:

$$M_{total} = M_{Stator} + M_{Rotor} + M_{Housing} + M_{Magnets} + M_{Windings}$$

The mass of each component can be determined by finding the product of the component volume, extracted from the CAD model, and the density of the component material, available from the materials database. However, since the windings CAD model represents the volume available for the windings, multiplication by the slot fill factor (SF_g) provides a more accurate estimate of the windings mass.

$$\therefore M_{total} = (\rho V)_{Stator} + (\rho V)_{Rotor} + (\rho V)_{Housing} + (\rho V)_{Magnets} + SF_g(\rho V)_{Windings}$$

&

$$Cost_{total} = C_{Stator}M_{Stator} + C_{Rotor}M_{Rotor} + C_{Housing}M_{Housing} + C_{Magnets}M_{Magnets} + C_{Windings}M_{Windings}$$

$M_x - Mass\ of\ component\ x\ [kg]$

$V_x - CAD\ volume\ of\ component\ x\ [m^3]$

$\rho_x - Density\ of\ component\ material\ x\ [kg/m^3]$

$C_x - Average\ cost\ per\ unit\ mass\ of\ component\ material\ x\ [£/kg]$

In addition to the mass and cost estimates being inserted into the spreadsheet, a message box opens on screen to indicate the values. An example of the message box can be seen in Figure 61.

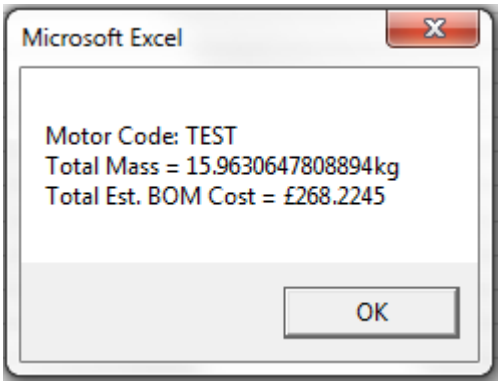


Figure 61: AIEED tool: Sample estimate mass and material cost message box

The foundations of the full AIEED tool containing the calculator and all CAD build macros can be seen in Appendix D: AIEED Tool. The appendix contains the MS Excel document and a video to demonstrate the functionality of the tool. Appendix E: AIEED Tool – VBA Code contains a document with the full VBA code used in the foundations of the AIEED tool.

6.5 AIEED Tool Verification and Validation

The scope of the project does not provide for a full verification and validation activity. However, to improve robustness, it is necessary to implement some level of data checking to avoid failed computation. The method that has been followed to provide this level of data verification is to limit the range of the individual data fields such that invalid entries are avoided. For example, entering a negative value for a dimension is not possible.

The data inputs are restricted by making use of the *Data Validation* options available in MS Excel. The tool allows for the definition of validation criteria on specific cells in the worksheet based on a number of criteria. The data validation criteria applied to the input cells of the foundations of the AIEED tool, including a description of the criteria, can be seen in Table 16.

Table 16: Data validation criteria applied to input data

Section	Parameter	Data Validation Criteria			Description
		Type	Range	Units	
Performance	Maximum Power Output	Whole number	0-1500	kW	Typical IP range [3]
	Maximum Speed	Whole number	0-300,000	Rpm	Typical IP range [3]
	Constant Power Speed Range	Decimal	0.500-4.000	-	Typical range [19]
	Torque Per Unit Rotor Vol.	Whole number	> 10	Nm/l	Positive integer open to designer
	Number of Magnet Pole Pairs	List	2,3,4,5,6,7,8,9,10		Integer values within recommended range (1-25) [5]
	Airgap Length	Decimal	0.05-10.00	mm	Typical IP range [3]
Materials	Magnet Material Selection	List	Materials catalogue		
	Winding Material Selection	List	Materials catalogue		
	Stator Material Selection	List	Materials catalogue		
	Housing Components Material Selection	List	Materials catalogue		
	Rotor Material Selection	List	Materials catalogue		
Magnets	Magnet Length	Decimal	1.0-100.0	mm	Typical IP range [3]
	Lamination Stacking Factor	Decimal	0.8-1.0	-	Typical range [5]
	Leakage Factor	Decimal	0.9-1.0	-	Typical range [5]
	Reluctance Factor	Decimal	1.0-1.2	-	Typical range [5]
	Residual Induction	RESULT	Materials catalogue		
	Relative Permeability	RESULT	Materials catalogue		
Stator & Windings	Stator tooth slot depth	Decimal	> 2	mm	Positive value open to designer
	Tooth Tang Depth	Decimal	0.2-5.0	mm	Typical IP range [3]
	Stator tooth slot opening	Decimal	2.0-50.0	mm	Typical IP range [3]
	Peak flux density through Stator Yoke	Decimal	1.000-2.300	T	Typical range [5]
	Peak flux density through Stator Tooth	Decimal	1.000-2.300	T	Typical range [5]
	Number of Winding Turns	Whole Number	1-100	-	Typical IP range [3]
	Number of slots per pole per phase	Decimal	0.2-1.0	-	Limited to Concentrated Windings
	Slot Fill, Gross	Decimal	0.2-1.0	-	Positive value within acceptable range
	Cu Winding Resistivity	RESULT	Materials catalogue		
Rotor	Rotor Magnet Outer Diameter	Decimal	75.0-300.0	mm	Typical IP range [3]
	Number of Rotor Spokes	List	2, 3, 4, 5, 6, 7, 8	-	Positive integer value range
	Rotor Hub Web Thickness	Decimal	1.0-10.0	mm	Simplified range
	Rotor Hub Web Draft Angle	List	0, 0.5, 1, 1.5, 2, 2.5, 3 deg		Simplified range
	Resolver Rotor Mount Bolt Thread Length	Decimal	5.0-50.0	mm	Acceptable range based on bolt spec range
	Resolver Rotor Mount Bolt Thread	List	M4, M5, M6, M7, M8, M10, M12, M14, M16		Range of ISO metric thick pitch bolts
	Resolver Rotor Mount C-Bore Length	Decimal	5.0-20.0	mm	Clearance depth range related to bolt size range [75]

	Resolver Rotor Mount C-Bore Diameter	Decimal	8.0-26.0	mm	Clearance hole range related to bolt size range [75]
	Rotor Spline Length	Decimal	5.0-50.0	mm	Reasonable design range [75]
	Rotor Spline Lead-in Angle	Decimal	10.0-45.0	deg	Reasonable design range [75]
Packaging Considerations	Number of Mounting Lugs	List	2, 3, 4, 5, 6, 7, 8, 9, 10		Positive integer value range
	Mounting Lug Bolt Spec	List	M4, M5, M6, M7, M8, M10, M12, M14, M16		Range of ISO metric thick pitch bolts
	Mounting Bolt PCD Offset	Decimal	5.0-20.0	mm	Limited range to avoid unwanted result
	Mounting Lug Fillet Radius	Decimal	2.0-10.0	mm	Limited range to avoid large value
	Housing Minimum Thickness	Decimal	1.0-6.0	mm	Reasonable design range [75]
	Bearing Race OD	Decimal	20.0-300.0	mm	Typical range from supplier catalogue [76]
	Bearing Race ID	Decimal	10.0-200.0	mm	Typical range from supplier catalogue [76]
	Bearing Length	Decimal	4.0-30.0	mm	Typical range from supplier catalogue [76]
	Resolver OD	Decimal	25.0-132.0	mm	Typical range from supplier catalogue [77]
	Resolver Length	Decimal	2.0-10.0	mm	Typical range from supplier catalogue [77]
	Min Insulator Thickness	Decimal	0.2-3.0	mm	Typical IP range [3]
Mass	Magnet Density	RESULT	Materials catalogue		
	Windings Density	RESULT	Materials catalogue		
	Stator Density	RESULT	Materials catalogue		
	Housing Density	RESULT	Materials catalogue		
	Rotor Hub Density	RESULT	Materials catalogue		
Part Numbering	Housing Section Code	N/A			
	Cover Section Code	N/A			
	Stator Section Code	N/A			
	Winding Section Code	N/A			
	Rotor Section Code	N/A			
	Magnets Section Code	N/A			

Should a parameter be inserted that does not conform to the validation restrictions applied, an error message appears indicating that the value is invalid and provides the range of valid inputs. An example of the error message can be seen in Figure 62.

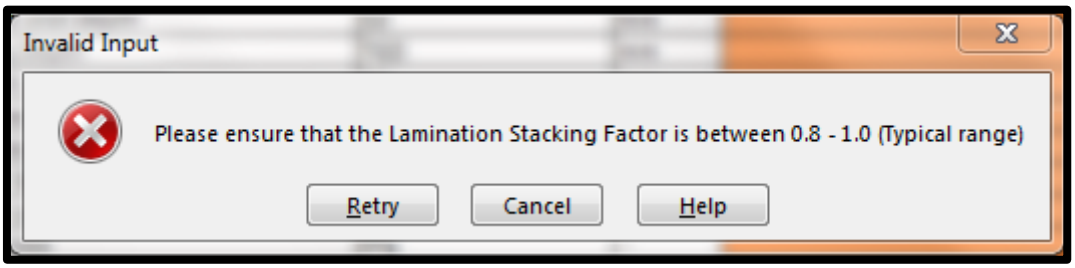


Figure 62: Data validation: Example of invalid input data entry error message

In addition to the data validation criteria, helpful images are included as comments in necessary cells. This includes diagrams to assist in when defining the parameters. An example of how these images are displayed is illustrated in Figure 63.

DR	mm	174.000
nRotorSpokes	-	3
WebThk	mm	5.000
WebAng	deg	2.0
ResBoltLen	mm	16.000
ResThrd	-	M8
ResCboreLen	mm	12.300
ResCboreDia	mm	15.700
RSLength	mm	27.500
RLAng	deg	30.000
nMountingLugs	-	4
BoltSize	-	M10
MBoltPCDOffset	mm	10.000
MLugFilR	mm	10.000
MinThk	mm	3.000
bRaceOD	mm	55.000
bRaceID	mm	35.000
bLength	mm	13.000
ResOD	mm	62.000
ResLength	mm	4.500
InsMinThk	mm	1.500

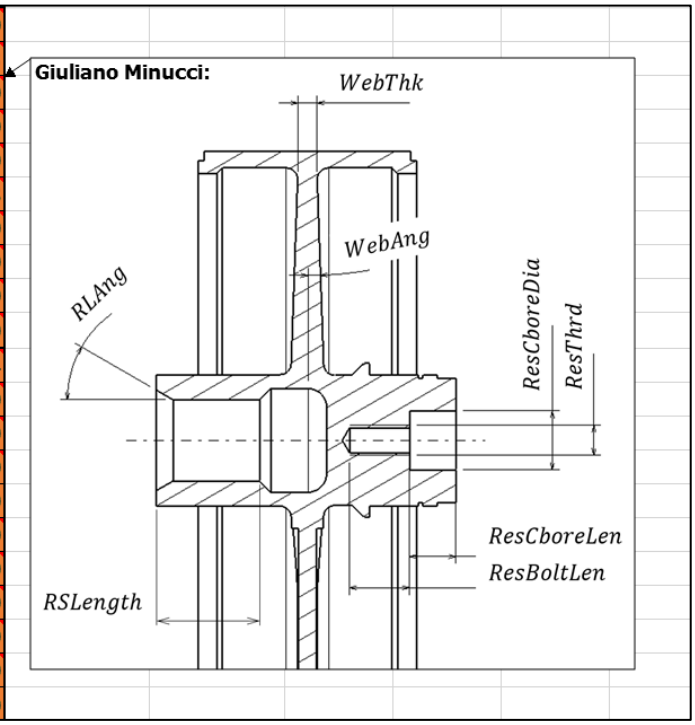


Figure 63: Example of parameter description diagram included in AIEED tool

The limited data verification provides a single layer of robustness and does not consider the relationships between the various input parameters. The verification technique is specific to the individual parameters and only considers the value in isolation. For this reason, if two related dimensions are defined in a manner that would lead to an impossible result, the system is not able to identify this and executing the motor build macro would lead to a failed computation. To improve the robustness of the AIEED tool a more comprehensive verification process is required.

A possible validation technique that can be used to evaluate the accuracy of the AIEED tool is to compare the results with data from past projects. However, due to intellectual property protection it is not possible to perform this validation for the purposes of the project. To validate the foundations of the tool it is necessary to complete a comparison activity with historical project data.

7 CONCLUSIONS

The foundations of a software tool (AIEED) used to improve the time and quality of response to new motor enquiries has been developed. The foundations of the AIEED tool are built into a Microsoft Excel document which contains the necessary logic required to convert customer requirements data into geometrical design data. A series of macros are included in the tool which allow for the automated generation of a first-level CAD model of the motor, including the following components; stator, windings, rotor, magnets, housing and cover. The CAD models are developed on the CATIA V5 design platform. In addition, the tool makes use of the CAD model to determine the estimate material cost of the unit based on average materials cost per unit mass defined in the materials database stored in the tool.

The foundations of the tool include support for the following motor specifications:

- SPM PMAC cylindrical radial flux motors only (external stator and internal rotor).
- The units are designed for 3-phase supply only.
- The winding configuration is limited to concentrated double layer option only.
- There is no option to include rotor skew.
- Parallel tooth, arc-bottom, semi-closed stator slot profiles only.
- Arc-shaped radially magnetised surface magnet rotor configuration option only.
- The mounting scheme is axial only. The option to mount radially is not supported.
- The housing is limited to a 2-Piece configuration option only.

Individual macros are available to build each sub-component independently of each other, however, the mass and material cost estimate is only performed when generating the full motor assembly. Although full validation and verification has not been completed for the foundations of the AIEED tool, certain restrictions have been placed on the range of input data. This basic level of data verification aims to minimise the potential for invalid inputs.

The foundations of the AIEED tool enables IP to respond to new motor enquiries in a far more effective and efficient manner. After customer requirements have been gathered, the AIEED tool can be used to develop a first-level CAD design model and estimate material costs in a matter of minutes. This is significantly faster than the current manual processes which take around 3-4 weeks. Since the foundations of the tool only supports a limited range of motor specifications and a full validation phase has not been completed, it is currently estimated that the tool is capable of reducing new project enquiries' response time

by around 75%. In addition, the CAD model that is generated can be shared with customers in order to improve the quality and value of the response.

The foundations of the AIEED tool can be used to improve the costing and initial design phase of a motor enquiry. However, to fully realise these benefits, it is necessary to expand the tool to support additional motor types and specifications as well as package the foundations into a single, easy-to-use utility.

8 RECOMMENDATIONS FOR FUTURE WORK

The scope of the project does not include a final AIEED development phase to package the project into a single standalone software tool. In addition to this, the full verification and validation of the AIEED tool foundations is out-of-scope. Recommendations for future work include compiling the functionality into a single tool, final code verification and validation and extending the functionality of the AIEED tool to include support for multiple PMAC motor types and a greater variety of options regarding motor configuration and specification. The following future work is recommended:

- Incorporate all the foundational elements of the AIEED tool into a package that can run within a single environment (Figure 64 illustrate an example of the potential layout of the final AIEED tool). An option is to build the tool directly into CATIA V5 so that the working environment remain consistent from the requirements input phase through to the model build and material cost estimate phase.
- Further testing and verification of the existing AIEED code. The project brief limited the extent to which the code was verified, it is therefore necessary to test and debug the code to improve its robustness. This includes extending the verification to consider the relationships between different parameters and not only the individual parameters in isolation.
- A full validation activity is to be performed. This could include comparing the results of the AIEED tool to historical project data to evaluate its accuracy.
- Test and adapt code to work on different releases of MS Excel and CATIA V5. The foundations of the tool have been built to work on MS Excel 2013 and CATIA V5-6R2016 SP3 and no additional testing has been performed on older and newer releases of either package.
- Extend the application scope to include support for the following:
    - Internal Permanent Magnet (IPM) AC motors.
    - Alternative stator winding configurations (Distributed, Integer-slot, fractional-slot, single layer etc.).
    - Allow for rotor skew.
    - Additional stator slot profile options.
    - Additional rotor and magnet configuration options.
    - Multi-phase arrangements (Not just 3-phase).
    - Radial mounting arrangements.

- Electrical insulation considerations in the housing design. This includes incorporating a model and material costs for the stator encapsulation (potting) and provision for minimum clearance and creepage factors.

- Extend the application functionality to include the following:
  - Definition and generation of the electrical termination components such as the busbars and star termination ring.
  - High-voltage and low-voltage connectors. Include options for connectors such that representations are built into the final CAD model and their respective mass and cost factors are included in the final approximation.
  - Motor cooling considerations. The tool can include a thermal characteristics calculator that can be used to approximate thermal conditions in the motor and develop coolant jacket representations in the models. This can be developed for stator and rotor cooling options.
  - 2D-Inductance computation to allow for more accurate electromagnetic specification calculation.
  - Introduce winding wire diameter considerations and support for multi-strand windings plus precision wound options.
  - Additional analytical work regarding estimate losses (Hysteresis, eddy, power, core and harmonic) to provide a more accurate performance estimate of the motor. This will also allow for computation of the motor efficiency.
  - Influence of temperature on magnetic properties of permanent magnets. This is currently ignored and would provide for more accurate performance and sizing estimates if included.
  - Introduce expected motor load-cycle information. This can allow for more accurate estimates based on specific operating requirements.
  - Include full detail and definition of rotor spline specification.
  - Introduce elements of structural analysis in the calculator. A first level stress calculation on certain components can be incorporated into the tool. For example, a stress calculation on the rotor hub in order to evaluate the safety factor of its design. This would allow for a first phase evaluation before a more detailed stress analysis is performed.
  - Incorporate aspects of finite element analysis for more accurate magnetic distribution evaluation. This could include a basic FEA computation or preparation and integration with an established electric motor simulation package.

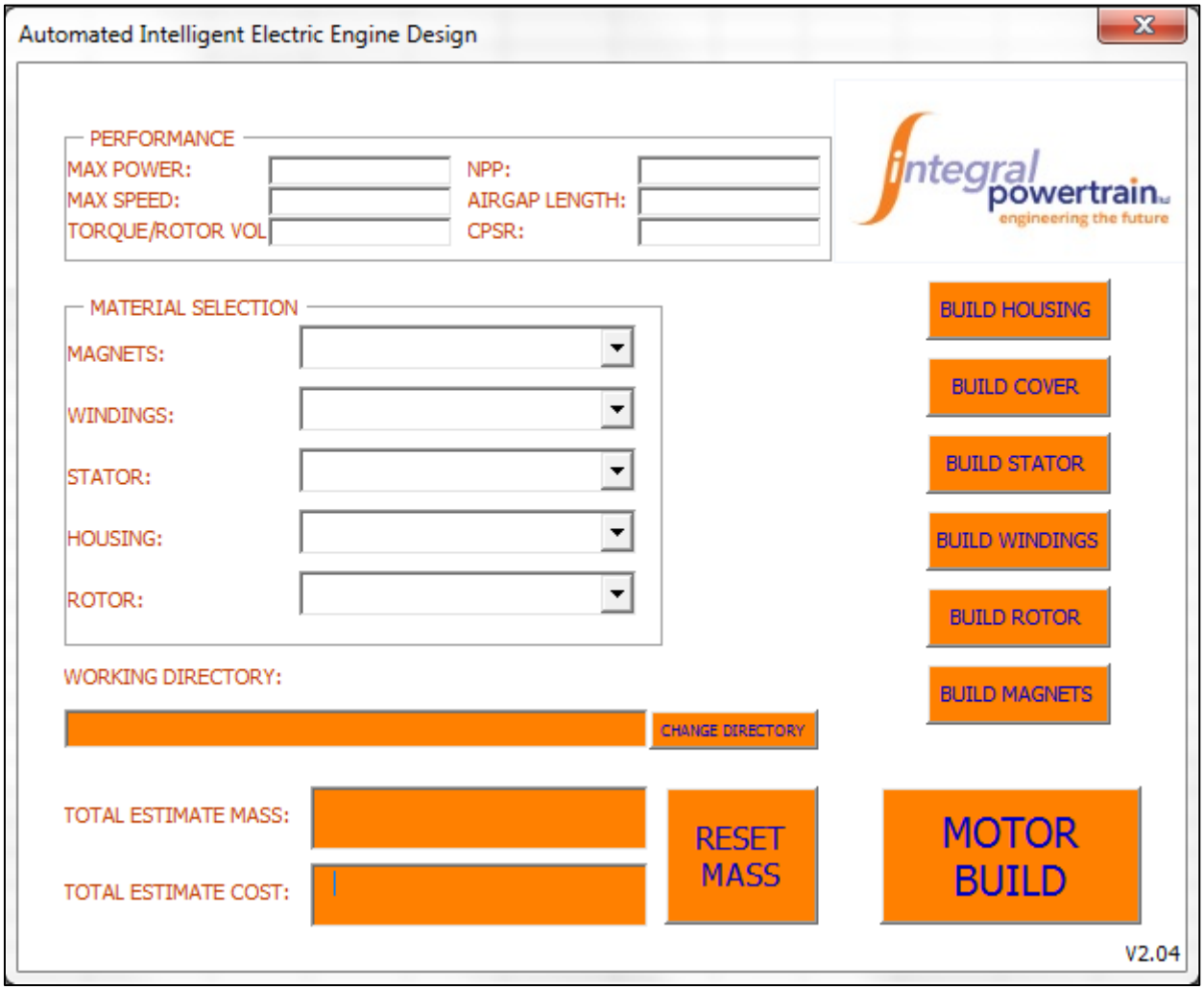


Figure 64: Possible layout of the final AIEED tool

REFERENCES

[1] Integral Powertrain, “Introduction to IP,” [Online]. Available: http://www.integralp.com/introduction-to-ip. [Accessed 04 April 2017].

[2] Integral Powertrain, “e-Drive Systems,” http://www.integralp.com/edrive, [Online]. Available: http://www.integralp.com/edrive. [Accessed 23 April 2017].

[3] A. Cherrington, Interviewee, *Chief Engineer of Design and Analysis.* [Interview]. 28 February 2017.

[4] M. O. Thurston, Handbook of Electric Motors, 2nd ed., 2004.

[5] D. D. Hanselman, Brushless Permanent Magnet Motor Design, 2nd ed., Orono, Maine: MAGNA PHYSICS PUBLISHING, 2003.

[6] N. A. Patil , “Field Weakening Operation of AC Machines for Traction Drive Applications,” The University of Tennessee, Knoxville, Knoxville , 2009.

[7] J. L. Kirtley, “Class Notes 6: DC(Commutator) and Permanent Magnet Machines,” in *Electric Machines*, Cambridge, Massachusetts, Massachusetts Institute of Technology - Department of Electrical Engineering and Computer Science, 2005, pp. 8-13.

[8] G. Pellegrino, A. Vagati, P. Guglielmi and B. Boazzo, “Performance Comparison Between Surface-Mounted and Interior PM Motor Drives for Electric Vehicle Application,” *IEEE TRANSACTIONS ON INDUSTRIAL ELECTRONICS,* vol. 59, no. 2, pp. 803-811, 2012.

[9] M. A. Rahman, *Status Review of Advances in Hybrid Electric Vehicles,* Newfoundland : Memorial University of Newfoundland and St. John’s, 2014.

[10] Georgia State University, “Coercivity and Remanence in Permanent Magnets,” Georgia State University, 2005. [Online]. Available: http://hyperphysics.phy-astr.gsu.edu/hbase/Solids/magperm.html. [Accessed 13 September 2017].

[11] Nidec, “Nidec's Technical Capabilities - Brushless Motors,” Nidec, [Online]. Available: http://www.nidec.com/en-NA/technology/capability/brushless/. [Accessed 22 February 2017].

[12] J. W. Jewett and R. A. Serway, Physics for Scientists and Engineers with Modern Physics, Belmont, CA: Thomson, 2008.

[13] Integral Powertrain, “Integral Powertrain Linkedin Profile,” [Online]. Available: https://www.linkedin.com/company/integral-powertrain. [Accessed 23 April 2017].

[14] L. Teschler , “IPM motors get bigger role in appliance energy efficiency,” 06 January 2013. [Online]. Available: http://machinedesign.com/news/ipm-motors-get-bigger-role-appliance-energy-efficiency. [Accessed 23 04 2017].

[15] HAMACO Industries Corporation, “Motor Technology,” [Online]. Available: http://www.hamaco-ind.com/motor_technology/. [Accessed 20 April 2017].

[16] A. Kronberg, “Design and Simulation of Field Oriented Control and Direct Torque Control for a Permanent Magnet Synchronous Motor with Positive Saliency,” Uppsala Universitet, Uppsala, 2012.

[17] C. Jaszczolt, “Control Engineering,” 01 January 2017. [Online]. Available: https://www.controleng.com/single-article/understanding-permanent-magnet-motors/345972809e774096c1b1eeec350f0168.html?tx_ttnews%5BsViewPointer%5D=1. [Accessed 17 September 2017].

[18] A. G. Kladas and K. I. Laskaris, “Internal Permanent Magnet Motor Design for Electric Vehicle Drive,” *IEEE TRANSACTIONS ON INDUSTRIAL ELECTRONICS,* vol. 57, no. 1, pp. 138-145, 2010.

[19] Y.-k. Chin, “A Permanent Magnet Synchronous Motor for an Electric Vehicle - Design Analysis,” Department of Electrical Engineering - Royal Institute of Technology Sweden, Stockholm, 2004.

[20] E. L. C. Arroyo, “MODELING AND SIMULATION OF PERMANENT MAGNET SYNCHRONOUS MOTOR DRIVE SYSTEM,” UNIVERSITY OF PUERTO RICO, MAYAGÜEZ CAMPUS, 2006.

[21] S. Jurkovic and E. G. Strangas, “Comparison of PMAC Machines for Starter-Generator Application in a Series Hybrid-Electric Bus,” *International Journal of Vehicular Technology,* vol. 2011, no. 1, p. 11, 2011.

[22] Dowling Magnets, “What is a Magnetic Field?,” 13 December 2016. [Online]. Available: http://www.dowlingmagnets.com/blog/2015/what-is-a-magnetic-field/. [Accessed 21 September 2017].

[23] Electronics Tutorials, “Magnetic Hysteresis,” [Online]. Available: http://www.electronics-tutorials.ws/electromagnetism/magnetic-hysteresis.html. [Accessed 12 October 2017].

[24] Arnold Magnetic Technologies, “What is the Magnetic Hysteresis Loop,” 2015. [Online]. Available: http://www.arnoldmagnetics.com/wp-content/uploads/2017/10/FINAL_Tech-Library_Tech-Notes_Hysteresis-Loop.pdf. [Accessed 12 October 2017].

[25] Arnold Magnetic Technologies, “Arnold Magnetics Technical Publications,” 09 March 2011. [Online]. Available: http://www.arnoldmagnetics.com/Portals/0/Fileshttp://www.arnoldmagnetics.com/wp-content/uploads/2017/12/FINAL_Tech-Library_Tech-Publications_-Glossary-Magnetics-Industry.pdf. [Accessed 12 October 2017].

[26] J. Belcher, P. Dourmashkin, R. Redwine, B. Knuteson, G. Roland, B. Wyslouch, B. Wecht, E. Katsavounidis, R. Simcoe, J. Formaggio, A. Neely, M. Strafuss, E. Hudson and S.-B. Liao, Physics II: Electricity and Magnetism, Boston: Massachusetts Institute of Technology, 2007.

[27] Supermagnete, “Supermagnete Frequently Asked Questions,” Supermagnete, [Online]. Available: https://www.supermagnete.de/eng/faq/How-do-you-calculate-the-magnetic-flux-density. [Accessed 15 November 2017].

[28] J. L. Kirtley, “Class Notes 6: Magnetic Circuit Analog to Electric Circuits,” in *Introduction to Power Systems*, Cambridge, Massachusetts, Massachusetts Institute of Technology - Department of Electrical Engineering and Computer Science, 2011, pp. 1-9.

[29] F. D. Tombe, “Lenz’s Law,” *The General Science Journal,* vol. 54, pp. 1-5, 2008.

[30] Y. S. Lai and Y. K. Lin, “Back-EMF Detection Technique of Brushless DC Motor Drives for Wide Range Control,” *IECON 2006 - 32nd Annual Conference on IEEE Industrial Electronics,* pp. 1006-1011, 2006.

[31] R. Karam, F. B. Kneubil and M. R. Robilotta, “Forces on a current-carrying wire in a magnetic field: the macro–micro connection,” *European Journal of Physics,* vol. 38, no. 5, 2017.

[32] L. Muyang, “Flux-Weakening Control for Permanent-Magnet Synchronous Motors Based on Z-Source Inverters,” Marquette University, Wisconsin, 2014.

[33] S. Meier, “Theoretical design of surface-mounted permanent magnet motors with field-weakening capability,” *Royal Institute of Technology Department of Electrical Engineering Electrical Machines and Power Electronics ,* 2002.

[34] J. K. Nisbett and R. G. Budynas, Shigley's Mechanical Engineering Design, New York: McGraw-Hill, 2011.

[35] W. L. Soong, “Sizing of Electrical Machines,” 26 September 2008. [Online]. Available: http://www.eleceng.adelaide.edu.au/research/power/pebn/. [Accessed 15 October 2017].

[36] M. Olszewski, “Evaluation of 2005 Honda Accord Hybrid Electric Drive System,” US Department of Energy - Energy Efficiency and Renewable Energy - FreedomCAR and Vehicle Technologies, Washington, D.C., 2006.

[37] Auto Ignition Limited, “Electrical Stators,” [Online]. Available: http://www.autoignition.in/electrical-stators.htm. [Accessed 14 July 2017].

[38] RM Stator, “Kit Stator + Regulator Rectifier + High Performance CDI Box + External Ignition Coil For Yamaha YFM 400 Kodiak 2000 2001,” [Online]. Available: https://www.rmstator.com/en_ca/products/kit-stator-regulator-rectifier-high-performance-cdi-box-external-ignition-coil-for-yamaha-yfm-400-kodiak-2000-2001-rm23012. [Accessed 12 July 2017].

[39] CD-adapco, “PC-BDC 9.1 User's Manual,” Computational Dynamics Ltd., "CD-adapco", New York, 2011.

[40] Ron, “Electric Bike - Motor Tech: Learn the Terms-Part 1,” 14 May 2014. [Online]. Available: https://www.electricbike.com/motor-tech-learn-the-terms-part-1/. [Accessed 23 November 2017].

[41] S. Constantinides, “Thin Gage Silicon-Iron for Motors, Generators, Transformers and Inductors,” 10 June 2011. [Online]. Available: http://www.arnoldmagnetics.com/wp-content/uploads/2017/10/Thin-Gauge-Silicon-Iron-Constantinides-WMM-2010-psn-hi-res.pdf. [Accessed 20 October 2017].

[42] eMetor, “Lamination Thickness,” eMetor.org, 2017. [Online]. Available: https://www.emetor.org/glossary/lamination-thickness/. [Accessed 15 October 2017].

[43] Cogent - A Tata Steel Enterprise, “Electrical Steel - Download catalogues, datasheets and ISO Certificates,” 2016. [Online]. Available: https://cogent-power.com/cms-data/downloads/Cogent NO brochure 2016.pdf. [Accessed 16 January 2018].

[44] eMetor, “Unbalanced Winding,” eMetor.org, [Online]. Available: https://www.emetor.org/glossary/unbalanced-winding/. [Accessed 05 October 2017].

[45] eMetor, “Integer-slot winding,” eMetor.org, [Online]. Available: https://www.emetor.org/glossary/integer-slot-winding/. [Accessed 05 September 2017].

[46] eMetor, “Fractional-slot winding,” eMetor.org, [Online]. Available: https://www.emetor.org/glossary/fractional-slot-winding/. [Accessed 05 September 2017].

[47] eMetor, “Concentrated winding,” eMetor.org, [Online]. Available: https://www.emetor.org/glossary/concentrated-winding/. [Accessed 2017 September 5].

[48] eMetor, “Number of winding layers,” eMetor.org, [Online]. Available: https://www.emetor.org/glossary/number-of-layers/. [Accessed 05 October 2017].

[49] eMetor, “Slot fill factor,” eMetor.org, [Online]. Available: https://www.emetor.org/glossary/slot-fill-factor/. [Accessed 05 September 2017].

[50] Essex, “ROUND ENAMELLED WIRE - Round Wire Brochure,” April 2016. [Online]. Available: essexeurope.com/uploadedFiles/EssexEurope/Products/Round_Enamelled_Wires/Round_Enamelled_Wire/PRODUCT TECHNICAL DATASHEETS.pdf. [Accessed 15 January 2018].

[51] CirComp, “Products - Composite Sleeves,” CirComp, 2017. [Online]. Available: http://www.circomp.de/composite-sleeves.html. [Accessed 06 September 2017].

[52] Info Mine, “InfoMine - Aluminium Price Trend,” [Online]. Available: http://www.infomine.com/investment/metal-prices/aluminum/5-year/. [Accessed 30 January 2018].

[53] Iron Foundry, “Cast Iron Price Calculator,” [Online]. Available: http://www.iron-foundry.com/cast-iron-price-calculator.html. [Accessed 30 January 2018].

[54] Alibaba, “Alibaba - Aluminium Billet,” [Online]. Available: https://www.alibaba.com/showroom/aluminum-billet.html. [Accessed 30 January 2018].

[55] IndiaMart, “Aluminium Billet,” [Online]. Available: https://dir.indiamart.com/impcat/aluminum-billets.html?biz=10. [Accessed 30 January 2018].

[56] MatWeb - Material Property Data, “MatWeb,” [Online]. Available: http://www.matweb.com/. [Accessed 2018 January 2018].

[57] Arnold Magnetic Technologies, “Permanent Magnet Applications,” 2015. [Online]. Available: http://www.arnoldmagnetics.com/wp-content/uploads/2017/10/TN_0204_rev_150715.pdf. [Accessed 15 December 2017].

[58] C. Elworthy, Interviewee, *Purchasing and Quality Manager - Integral Powertrain.* [Interview]. 30 January 2018.

[59] G. Erskine, Interviewee, *Sales Manager - Arnold Magnetic Technologies.* [Interview]. 30 January 2018.

[60] Arnold Magnetic Technologies, “Neodymium Iron Boron Catalog,” 21 October 2015. [Online]. Available: http://www.arnoldmagnetics.com/wp-content/uploads/2017/10/Catalog-151021.pdf. [Accessed 25 November 2017].

[61] Integral Powertrain, “Integral e-drive - Our Electric Drives - High Torque SPM,” Integral Powertrain Ltd, [Online]. Available: https://integralp.com/integral-e-drive/. [Accessed 23 December 2017].

[62] Integral Powertrain, “Integral e-drive - Our Electric Drives - Heavy Duty IPM,” Integral Powertrain Ltd, [Online]. Available: https://integralp.com/integral-e-drive/. [Accessed 23 December 2017].

[63] McLaren Applied Technologies, “E-Motor 120kW/130Nm,” McLaren Technology Group, [Online]. Available: https://www.mclaren.com/appliedtechnologies/products/item/e-motor-120kw-130nm/. [Accessed 23 December 2017].

[64] British Standards Institution, *Insulation coordination for equipment within low-voltage systems. Principles, requirements and tests (BS EN 60664-1:2007),* 2007.

[65] EFI Polymers, “Motors / Stator Epoxy & Potting,” EFI Polymers, [Online]. Available: http://www.efipolymers.com/applications/electrical-potting/motors/. [Accessed 23 December 2017].

[66] Motorsolver, “STATOR ENCAPSULATION SERVICE USING THERMAL CONDUCTIVE POTTING MATERIALS,” Motorsolver, [Online]. Available: https://motorsolver.com/mfg-services/stator-encapsulation/. [Accessed 23 December 2017].

[67] N. Parkman, “Electrical breakdown by tracking,” *Proceedings of the IEE - Part B: Electronic and Communication Engineering,* vol. 109, no. 22, pp. 448-453, 1962.

[68] Dassault Systemes, “CATIA,” [Online]. Available: https://www.3ds.com/products-services/catia/. [Accessed 24 April 2017].

[69] Dassault Systemes, “The 3DExperience Platform,” [Online]. Available: https://www.3ds.com/products-services/3dexperience/. [Accessed 24 April 2017].

[70] Dassault Systemes Academy, “CATIA V6 Automation Essentials Training,” [Online]. Available: https://academy.3ds.com/en/learn/catia-v6-automation-essentials. [Accessed 24 April 2017].

[71] Dassault Systemes, “CAA-RADE Solutions,” [Online]. Available: https://www.3ds.com/products-services/catia/products/v5/portfolio/domain/CAA_RADE/. [Accessed 25 April 2017].

[72] Dassault Systemes, “Knowledgeware Training Guide,” [Online]. Available: http://www.catia.com.pl/tutorial/knowledgeware.pdf. [Accessed 24 April 2017].

[73] Dassault Systemes, “CATIA V5 Training: Automation,” Dassault Systemes, 2009.

[74] Dassault Systemes, “CATIA V5-6R2016 Automation.chm - CAA V5 Basic Help,” Dassault Systemes, Paris, 2011.

[75] R. G. Budynas, J. K. Nisbett and J. E. Shigley, Shigley's Mechanical Engineering Design, London: McGraw-Hill, 2008.

[76] SKF, “MRC Hybrid Ceramic Ball Bearings Catalogue,” 2011. [Online]. Available: http://www.skf.com/binary/30-229377/MRC-hybrid-ceramic-ball-bearings.pdf. [Accessed 23 November 2017].

[77] Tamagawa Seiki Co. Ltd., “Singlsyn VR Type Resolver Catalogue,” [Online]. Available: https://www.tamagawa-seiki.com/assets/img/downloads/pdf/resolver-synchro/1570N14EJ.pdf. [Accessed 30 November 2017].

[78] G. J. Atkinson, “HIGH POWER FAULT TOLERANT MOTORS FOR AEROSPACE APPLICATIONS,” Newcastle University - School of Electrical, Electronic and Computer Engineering , Newcastle, 2007.

[79] N. Weisenberger, VB Scripting for CATIA V5, 2012.

[80] A. El Shahat, A. Keyhani and H. El Shewy, “Sizing a High Speed PM Generator for Green Energy Applications,” *Journal of Electrical Systems,* vol. 6, no. 4, pp. 501-516, 2010.

[81] C. Wester, “Motor Protection Principles,” [Online]. Available: https://www.l-3.com/private/ieee/Motor%20Protection%20Principles.pdf. [Accessed 23 June 2017].

APPENDICES

A. Materials Catalogue Database
B. CATIA V5 Automation Objects
C. Project Schedule
D. AIEED Tool
E. AIEED Tool – VBA Code

APPENDIX A: MATERIALS CATALOGUE DATABASE

The materials defined in the materials database are based on the following supplier information

Stator Core:

The properties of the electrical steel used to manufacture the stator core can be seen below. The data is extracted from the Cogent non-oriented electrical steel catalogue [43]. Additional data can be seen in the catalogue. [43]

Non-grain oriented electrical steel magnetic properties

Our extensive range of industry standard electrical steel grades all conform to EN10106 and IEC 60404-8-4 and are used in rotating machines of all sizes, as well as small transformers and a variety of other electromagnetic applications.

We have a comprehensive range of data on the magnetic, mechanical and physical properties of electrical steels which can be provided on request.

Table 1: Magnetic Properties

SURA Grade	Thickness (mm)	Maximum specific total loss at 50 Hz		Minimum magnetic polarization at 50 Hz			Conventional Density
		J=1.5T	1.0T*	H=2500	5000	10000 A/m	
		W/kg	W/kg	T	T	T	kg/dm³
M210-35A	0.35	2.10	0.90	1.49	1.60	1.70	7.60
M230-35A	0.35	2.30	0.95	1.49	1.60	1.70	7.60
M235-35A	0.35	2.35	0.95	1.49	1.60	1.70	7.60
M250-35A	0.35	2.50	1.00	1.49	1.60	1.70	7.60
M270-35A	0.35	2.70	1.10	1.49	1.60	1.70	7.65
M300-35A	0.35	3.00	1.20	1.49	1.60	1.70	7.65
M330-35A	0.35	3.30	1.30	1.49	1.60	1.70	7.65
M230-50A	0.50	2.30	1.00	1.49	1.60	1.70	7.60
M250-50A	0.50	2.50	1.05	1.49	1.60	1.70	7.60
M270-50A	0.50	2.70	1.10	1.49	1.60	1.70	7.60
M290-50A	0.50	2.90	1.15	1.49	1.60	1.70	7.60
M310-50A	0.50	3.10	1.25	1.49	1.60	1.70	7.65
M330-50A	0.50	3.30	1.35	1.49	1.60	1.70	7.65
M350-50A	0.50	3.50	1.50	1.50	1.60	1.70	7.65
M400-50A	0.50	4.00	1.70	1.53	1.63	1.73	7.70
M470-50A	0.50	4.70	2.00	1.54	1.64	1.74	7.70
M470-50HP	0.50	4.70	2.20	1.63	1.71	1.81	7.70
M530-50A	0.50	5.30	2.30	1.56	1.65	1.75	7.70
M530-50HP	0.50	5.30	2.30	1.63	1.71	1.81	7.80
M600-50A	0.50	6.00	2.60	1.57	1.66	1.76	7.75
M700-50A	0.50	7.00	3.00	1.60	1.69	1.77	7.80
M800-50A	0.50	8.00	3.60	1.60	1.70	1.78	7.80
M310-65A	0.65	3.10	1.25	1.49	1.60	1.70	7.60
M330-65A	0.65	3.30	1.35	1.49	1.60	1.70	7.60
M350-65A	0.65	3.50	1.50	1.49	1.60	1.70	7.60
M400-65A	0.65	4.00	1.70	1.52	1.62	1.72	7.65
M470-65A	0.65	4.70	2.00	1.53	1.63	1.73	7.65
M530-65A	0.65	5.30	2.30	1.54	1.64	1.74	7.70
M600-65A	0.65	6.00	2.60	1.56	1.66	1.76	7.75
M600-65HP	0.65	6.00	2.60	1.63	1.72	1.82	7.80
M700-65A	0.65	7.00	3.00	1.57	1.67	1.76	7.75
M800-65A	0.65	8.00	3.60	1.60	1.70	1.78	7.80
M600-100A	1.00	6.00	2.60	1.53	1.63	1.72	7.60
M700-100A	1.00	7.00	3.00	1.54	1.64	1.73	7.65
M800-100A	1.00	8.00	3.60	1.56	1.66	1.75	7.70
M1000-100A	1.00	10.00	4.40	1.58	1.68	1.76	7.80

1. J̄ represents the peak magnetic polarisation in Tesla. H̄ represents the peak magnetic field strength in A/m.

Windings:

The properties of the magnetic wire used to make up the stator windings can be seen below. The data is extracted from the Essex round enameled copper wire product catalogue [50]. Additional data can be seen in the catalogue. [50]

ENAMELLED WIRE: TABLE OF DIMENSIONAL CHARACTERISTICS



COPPER							STANDARD WIRES				SELF-BONDING WIRES		
				Resistance load per unit length			GRADE 1		GRADE 2		bondcoat increase	GRADE 1B	GRADE 2B
Ø (mm)	Tolerance ± mm	Cross-section (mm^2)	Mass g/m	Min. Ω/m	Rated nominal Ω/m	Max. Ω/m	(D-d) mm min.	D mm max.	(D-d) mm min.	D mm max.	mm min.	D mm max.	D mm max.
*0,160	0,003	0,02011	0,1787	0,8122	0,8502	0,8906	0,012	0,182	0,023	0,199	0,010	0,197	0,209
0,170	0,003	0,02270	0,2018	0,7211	0,7531	0,7871	0,013	0,194	0,025	0,205	0,010	0,210	0,221
*0,180	0,003	0,02545	0,2262	0,6444	0,6718	0,7007	0,013	0,204	0,025	0,217	0,010	0,220	0,233
0,190	0,003	0,02835	0,2521	0,5794	0,6029	0,6278	0,014	0,216	0,027	0,228	0,011	0,233	0,245
*0,200	0,003	0,03142	0,2793	0,5237	0,5441	0,5657	0,014	0,226	0,027	0,239	0,011	0,243	0,256
0,212	0,003	0,03530	0,3138	0,4669	0,4843	0,5026	0,015	0,240	0,029	0,254	0,012	0,258	0,272
*0,224	0,003	0,03941	0,3503	0,4188	0,4338	0,4495	0,015	0,252	0,029	0,266	0,012	0,270	0,284
0,236	0,004	0,04374	0,3889	0,3747	0,3908	0,4079	0,017	0,267	0,032	0,283	0,013	0,286	0,302
*0,250	0,004	0,04909	0,4364	0,3345	0,3482	0,3628	0,017	0,281	0,032	0,297	0,013	0,300	0,316
0,265	0,004	0,05515	0,4903	0,2982	0,3099	0,3223	0,018	0,297	0,033	0,314	0,013	0,316	0,333
*0,280	0,004	0,06158	0,5474	0,2676	0,2776	0,2882	0,018	0,312	0,033	0,329	0,013	0,331	0,348
0,300	0,004	0,07069	0,6284	0,2335	0,2418	0,2506	0,019	0,334	0,035	0,352	0,014	0,354	0,372
*0,315	0,004	0,07793	0,6928	0,2121	0,2193	0,2270	0,019	0,349	0,035	0,367	0,014	0,369	0,387
0,335	0,004	0,08814	0,7836	0,1878	0,1939	0,2004	0,020	0,372	0,038	0,391	0,015	0,393	0,412
*0,355	0,004	0,09898	0,8799	0,1674	0,1727	0,1782	0,020	0,392	0,038	0,411	0,015	0,413	0,432
0,375	0,005	0,11045	0,9819	0,1494	0,1548	0,1604	0,021	0,414	0,040	0,434	0,016	0,436	0,456
*0,400	0,005	0,12566	1,1172	0,1316	0,1360	0,1407	0,021	0,439	0,040	0,459	0,016	0,461	0,481
0,425	0,005	0,14186	1,2612	0,1167	0,1205	0,1244	0,022	0,466	0,042	0,488	0,016	0,489	0,511
*0,450	0,005	0,15904	1,4139	0,1042	0,1075	0,1109	0,022	0,491	0,042	0,513	0,016	0,514	0,536
0,475	0,005	0,17721	1,5754	0,09366	0,09646	0,09938	0,024	0,519	0,045	0,541	0,017	0,543	0,565
*0,500	0,005	0,1963	1,746	0,08462	0,08706	0,08959	0,024	0,544	0,045	0,566	0,017	0,568	0,590
0,530	0,006	0,2206	1,961	0,07512	0,07748	0,07995	0,025	0,058	0,047	0,600	0,017	0,600	0,624
*0,560	0,006	0,2463	2,190	0,06736	0,06940	0,07153	0,025	0,606	0,047	0,630	0,017	0,630	0,654
0,600	0,006	0,2827	2,514	0,05876	0,06046	0,06222	0,027	0,649	0,050	0,674	0,018	0,674	0,699
*0,630	0,006	0,3117	2,771	0,05335	0,05484	0,05638	0,027	0,679	0,050	0,704	0,018	0,704	0,729
0,670	0,007	0,3526	3,134	0,04708	0,04848	0,04994	0,028	0,722	0,053	0,749	0,019	0,748	0,775
*0,710	0,007	0,3959	3,520	0,04198	0,04318	0,04442	0,028	0,762	0,053	0,789	0,019	0,788	0,815
0,750	0,008	0,4418	3,927	0,03756	0,03869	0,03987	0,030	0,805	0,056	0,834	0,020	0,832	0,861
*0,800	0,008	0,5027	4,469	0,03305	0,03401	0,03500	0,030	0,855	0,056	0,884	0,020	0,882	0,911
0,850	0,009	0,5675	5,045	0,02925	0,03012	0,03104	0,032	0,909	0,060	0,939	0,020	0,937	0,967
*0,900	0,009	0,6362	5,656	0,02612	0,02687	0,02765	0,032	0,959	0,060	0,989	0,020	0,987	1,017
0,950	0,010	0,7088	6,301	0,02342	0,02412	0,02484	0,034	1,012	0,063	1,044	0,021	1,041	1,073
*1,000	0,010	0,7854	6,982	0,02116	0,02176	0,02240	0,034	1,062	0,063	1,094	0,021	1,091	1,123
1,060	0,011	0,8825	7,845		0,01937		0,034	1,124	0,065	1,157	0,022	1,154	1,187
*1,120	0,011	0,9852	8,758		0,01735		0,034	1,184	0,065	1,217	0,022	1,214	1,247
1,180	0,012	1,094	9,722		0,01563		0,035	1,246	0,067	1,279	0,022	1,276	1,309
*1,250	0,013	1,227	10,91		0,01393		0,035	1,316	0,067	1,349	0,022	1,346	1,379
1,320	0,013	1,368	12,17		0,01249		0,036	1,388	0,069	1,422	0,023	1,419	1,453
*1,400	0,014	1,539	13,69		0,01110		0,036	1,468	0,069	1,502	0,023	1,499	1,533
1,500	0,015	1,767	15,71		0,009673		0,038	1,570	0,071	1,602	0,023	1,602	1,638
*1,600	0,016	2,011	17,87		0,008502		0,038	1,670	0,071	1,706	0,023	1,702	1,738
1,700	0,017	2,270	20,18		0,007531		0,039	1,772	0,073	1,809	0,024	1,805	1,842
*1,800	0,018	2,545	22,62		0,006718		0,039	1,872	0,073	1,909	0,024	1,905	1,942
1,900	0,019	2,835	25,21		0,006029		0,040	1,974	0,075	2,012	0,025	2,008	2,046
*2,000	0,020	3,142	27,93		0,005441		0,040	2,074	0,075	2,112	0,025	2,108	2,146
2,120	0,021	3,530	31,38		0,004843		0,041	2,196	0,077	2,235			
*2,240	0,022	3,941	35,03		0,004338		0,041	2,316	0,077	2,355			
2,360	0,024	4,374	38,89		0,003908		0,042	2,438	0,079	2,478			
*2,500	0,025	4,909	43,64		0,003482		0,042	2,578	0,079	2,618			
2,650	0,027	5,515	49,03		0,003099		0,043	2,730	0,081	2,772			
*2,800	0,028	6,158	54,74		0,002776		0,043	2,880	0,081	2,922			
3,000	0,030	7,069	62,84		0,002418		0,045	3,083	0,084	3,126			
*3,150	0,032	7,793	69,28		0,002193		0,045	3,233	0,084	3,276			
3,350	0,034	8,814	78,36		0,001939		0,046	3,435	0,086	3,479			
*3,550	0,036	9,898	87,99		0,001727		0,046	3,635	0,086	3,679			
3,750	0,038	11,04	98,19		0,001548		0,047	3,838	0,089	3,883			
*4,000	0,040	12,57	111,7		0,001360		0,047	4,088	0,089	4,133			
4,250	0,043	14,19	126,1		0,001205		0,049	4,341	0,092	4,387			
*4,500	0,045	15,90	141,4		0,001075		0,049	4,591	0,092	4,637			
4,750	0,048	17,72	157,5		0,000965		0,050	4,843	0,094	4,891			
*5,000	0,050	19,63	174,6		0,000871		0,050	5,093	0,094	5,141			

* Standard diameters to be given preference.

According to IEC 60317 standards

Rotor Hub:

The properties of suitable materials used to manufacture the rotor hub component can be seen in the table below. The data is extracted from the MatWeb materials library and various product catalogues [50].

Material	Density [kg/m^3]	Cost [£/kg][14]
Aluminium (Generic)	2,700.00 [56]	1.80 [52]
Iron (Cast)	7,150.00 [56]	2.72 [53]
Aluminium 2014 T651 (MC)	2,800.00 [56]	3.60 [54]
Aluminium 2024 T6 (MC)	2,780.00 [56]	3.75 [54]
Aluminium LM25-TF (Cast)	2,680.00 [56]	1.87 [55]
Aluminium 6082 (MC)	2,700.00 [56]	2.40 [54]

[14] Currency conversion completed using the following rates: £1.00 = € 1.136; £1.00 = $1.33; £1.00 = ₹90.19.

Permanent Magnets:

The permanent magnet data below is extracted from the Arnold Magnetic Technologies Neodymium-Iron-Boron (NdFeB) catalogue [60]. Additional data specific to the different magnet grades can be seen in the catalogue. [60]

ARNOLD MAGNETIC TECHNOLOGIES

Neodymium-Iron-Boron Magnet Grades

Summary Product List & Reference Guide

Basic Grades

Properties	Br		HcB		HcJ		(BH)max		Temp. Coef.		Tw
Grade**	Typical mT	Typical gauss	min kA/m	min oersted	min kA/m	min oersted	Typical kJ/m3	Typical MGOe	α(Br) %/°C	α(HcJ) %/°C	max °C
N30	1105	11050	796	10000	955	12000	235	30	-0.12	-0.750	80
N33	1150	11500	836	10500	955	12000	259	33	-0.12	-0.750	80
N35	1210	12100	860	10800	955	12000	283	35	-0.12	-0.750	80
N38	1260	12600	860	10800	955	12000	306	38	-0.12	-0.750	80
N40	1285	12850	923	11600	955	12000	318	40	-0.12	-0.750	80
N42	1315	13150	860	10800	955	12000	334	42	-0.12	-0.750	80
N45	1350	13500	860	10800	955	12000	350	44	-0.12	-0.750	80
N48	1400	14000	836	10500	955	12000	374	47	-0.12	-0.750	80
N50	1425	14250	836	10500	955	12000	390	49	-0.12	-0.750	80
N52	1450	14500	836	10500	876	11000	406	51	-0.12	-0.750	60
N55	1490	14900	716	9000	876	11000	430	54	-0.12	-0.750	60
N33M	1175	11750	836	10500	1114	14000	267	34	-0.12	-0.675	100
N35M	1210	12100	868	10900	1114	14000	283	35	-0.12	-0.675	100
N38M	1260	12600	899	11300	1114	14000	307	39	-0.12	-0.675	100
N40M	1285	12850	923	11600	1114	14000	322	40	-0.12	-0.675	100
N42M	1315	13150	955	12000	1114	14000	338	42	-0.12	-0.675	100
N45M	1350	13500	971	12200	1114	14000	354	44	-0.12	-0.675	100
N48M	1395	13950	995	12500	1114	14000	378	48	-0.12	-0.675	100
N50M	1415	14150	1035	13000	1114	14000	390	49	-0.12	-0.675	100
N52M	1445	14450	995	12500	1035	13000	406	51	-0.12	-0.675	100
N30H	1105	11050	796	10000	1353	17000	235	30	-0.12	-0.605	120
N33H	1175	11750	836	10500	1353	17000	267	34	-0.12	-0.605	120
N35H	1210	12100	868	10900	1353	17000	283	35	-0.12	-0.605	120
N38H	1260	12600	899	11300	1353	17000	307	39	-0.12	-0.605	120
N40H	1285	12850	923	11600	1353	17000	322	40	-0.12	-0.605	120
N42H	1300	13000	955	12000	1353	17000	330	41	-0.12	-0.605	120
N45H	1350	13500	971	12200	1353	17000	354	44	-0.12	-0.605	120
N48H	1390	13900	1011	12700	1353	17000	378	48	-0.12	-0.605	120
N50H	1415	14150	1035	13000	1274	16000	390	49	-0.12	-0.605	120
N30SH	1125	11250	811	10200	1592	20000	243	31	-0.12	-0.535	150
N33SH	1175	11750	844	10600	1592	20000	267	34	-0.12	-0.535	150
N35SH	1210	12100	876	11000	1592	20000	283	35	-0.12	-0.535	150
N38SH	1260	12600	907	11400	1592	20000	307	39	-0.12	-0.535	150
N40SH	1285	12850	939	11800	1592	20000	322	40	-0.12	-0.535	150
N42SH	1310	13100	955	12000	1592	20000	330	41	-0.12	-0.535	150
N45SH	1350	13500	979	12300	1592	20000	354	44	-0.12	-0.535	150
N48SH	1390	13900	995	12500	1512	19000	374	47	-0.12	-0.535	150
N28UH	1075	10750	764	9600	1990	25000	227	29	-0.12	-0.465	180
N30UH	1125	11250	812	10200	1990	25000	243	31	-0.12	-0.465	180
N33UH	1175	11750	852	10700	1990	25000	267	34	-0.12	-0.465	180

© Arnold Magnetic Technologies Corp.
770 Linden Avenue, Rochester, NY 14625
Ph: (+1) 585-385-9010
E-mail: info@arnoldmagnetics.com
www.arnoldmagnetics.com
Rev. 151021a

Housing Components:

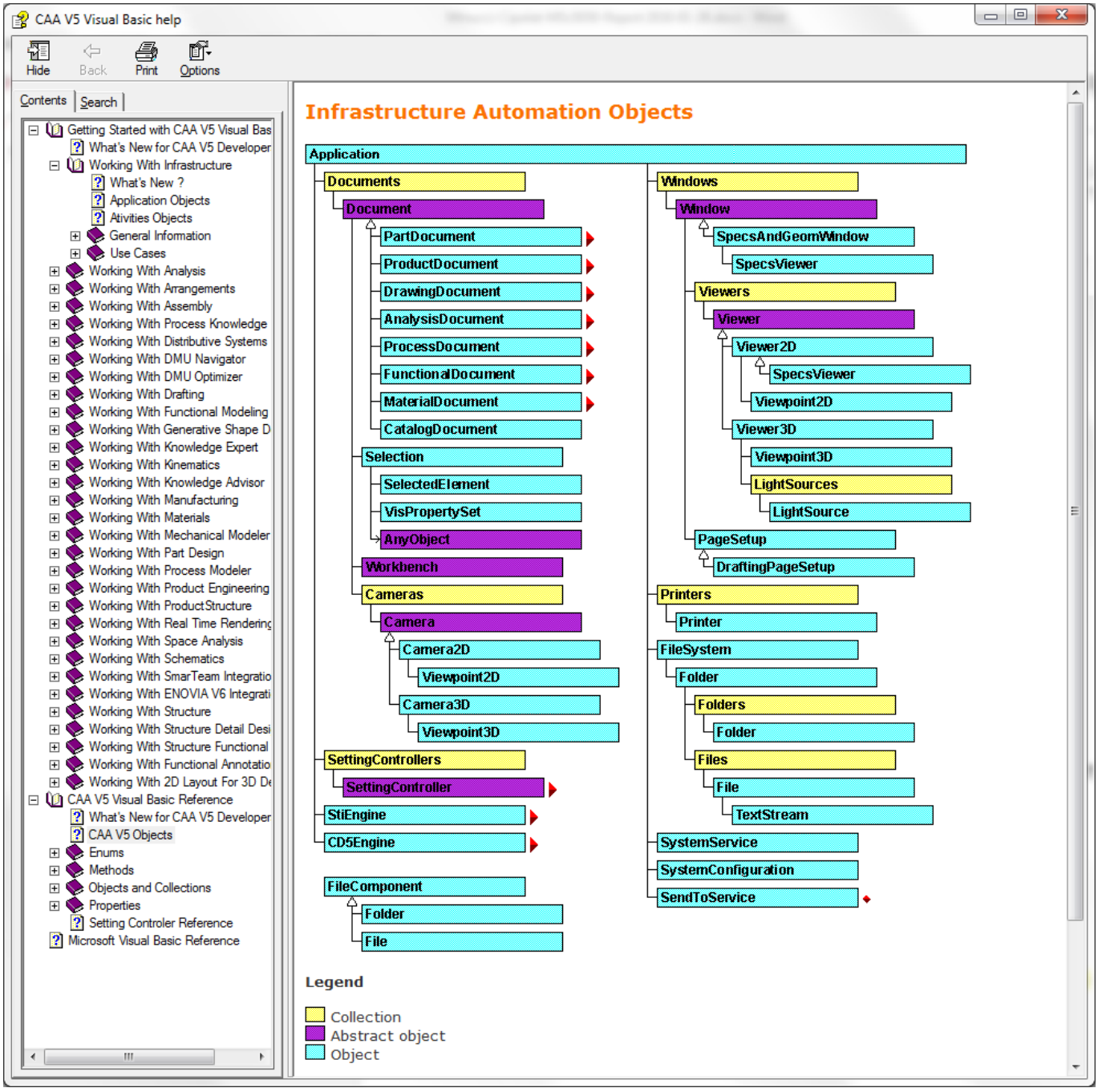
The properties of suitable materials used to manufacture the housing component can be seen in the table below. The data is extracted from the MatWeb materials library and various product catalogues [50].

Material	Density [kg/m^3]	Cost [£/kg][15]
Aluminium (Generic)	2,700.00 [56]	1.80 [52]
Iron (Cast)	7,150.00 [56]	2.72 [53]
Aluminium 2014 T651 (MC)	2,800.00 [56]	3.60 [54]
Aluminium 2024 T6 (MC)	2,780.00 [56]	3.75 [54]
Aluminium LM25-TF (Cast)	2,680.00 [56]	1.87 [55]
Aluminium 6082 (MC)	2,700.00 [56]	2.40 [54]

[15] Currency conversion completed using the following rates: £1.00 = € 1.136; £1.00 = $1.33; £1.00 = ₹90.19.

APPENDIX B: CATIA V5 AUTOMATION OBJECTS

The CATIA V5-6R2016 Automation object library and VB script help documentation, which is included by default in the CATIA V5-6R2016 install, can be seen in the utility titled: *V5-6R2016Automation.chm*. The documentation provides resource required for the development of automation VB scripts. The library includes all the objects and classes that can be accessed through scripting. The figure below is an extract from the utility and illustrates the infrastructure objects. [74]

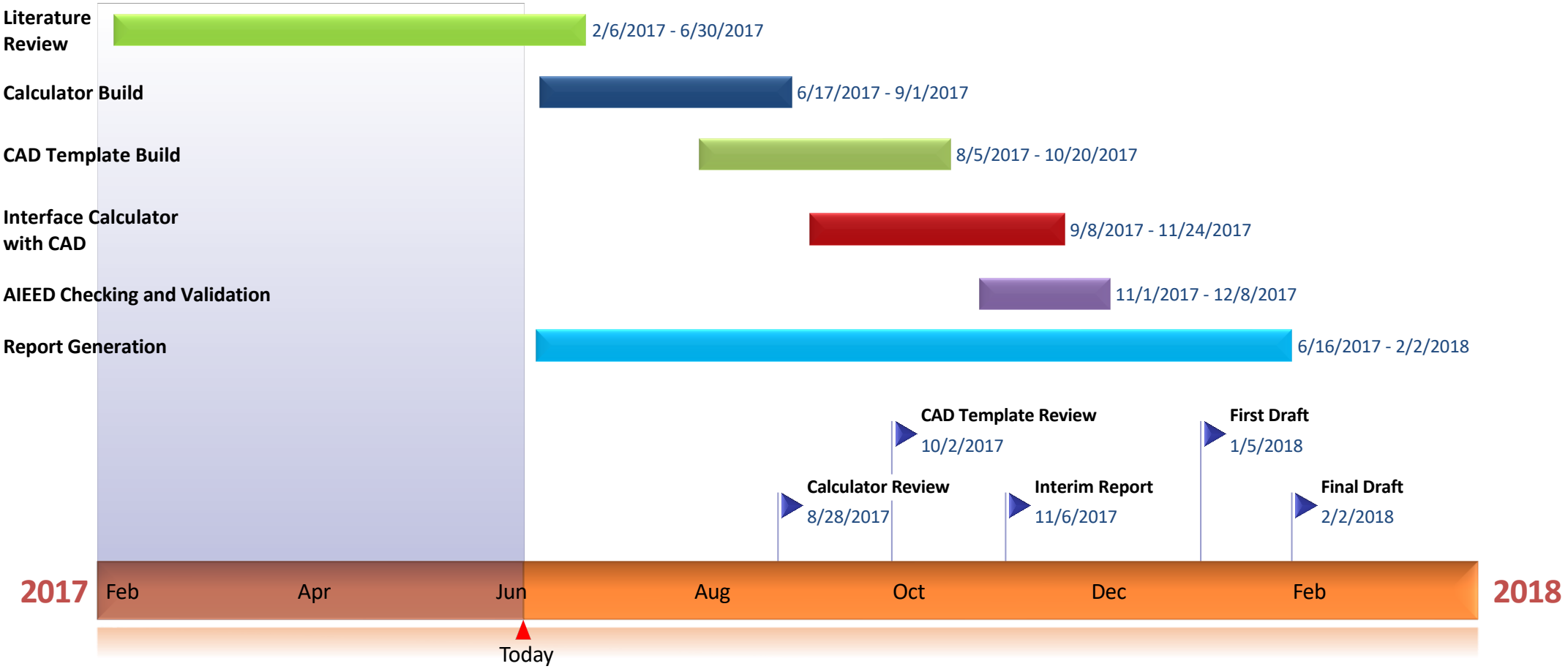


APPENDIX C: PROJECT SCHEDULE

The primary objective of the project is to deliver the foundation for an automated intelligent design tool that will help to improve Integral Powertrain's response time to new electric motor design enquiries. The automated intelligent electric engine design (AIEED) tool project has been broken down into the following milestones:

- Develop an electric motor design calculator able to convert customer requirements data into output geometrical data based on general electric motor design principles and specific Integral Powertrain design rules.
- Create a parametric CAD template for the development of a first-level design model.
- Interface the design calculator with the CAD template to automate the first-level design model generation.
- Estimate the material cost of the electric motor based on the CAD model.

The figure below provides an illustration of the proposed project schedule indicating all key events.



Proposed Project Schedule

APPENDIX D: AIEED TOOL

See *Minucci-Cipolat-MSc5050-AIEED.xlsx*

Automated Intelligent Electric Engine Design (AIEED) Tool pre-requisites:

- Dassault Systemes CATIA V5-6R2016 SP3
- Microsoft Excel 2013

A demonstration video is included for those without access to MS Excel or CATIA V5. Please see *Minucci-Cipolat-MSc5050-AIEED_Walkthrough.mp4*. This contains a walkthrough of the tool to demonstrate its functionality.

Some images illustrating the layout of the tool can be seen below.

	A	B	C	D	E
1	Project Code	TEST	Change Directory	Instructions:	
2	Working Directory	C:\Users\gminucci\Desktop\Test	Reset Directory	1) Complete all input fields (orange)	
3	Build Housing	Build Windings	Build Assembly / Reset Mass / FULL MOTOR BUILD	2) Press **FULL MOTOR BUILD** to complete CAD build process	
4	Build Cover	Build Rotor		3) Go to OUTPUTS to see **Mass** and **Cost** estimates	
5	Build Stator	Build Magnets		4) Go to **Info** for additional instructions and revision information	
6	Customer Requirements - INPUTS				
7	Section	Parameter	Symbol	Units	Value
8	Performance	Maximum Power Output	Pmax	kW	135
9		Maximum Speed	nMax	rpm	19,000
10		Constant Power Speed Range	CPSR	rpm/rpm	2.950
11		Torque Per Unit Rotor Volume	rMPerRotorVolume	Nm/l	153.000
12		Number of Magnet Pole Pairs	NPP	-	6
13		Airgap Length	Lairgap	mm	2.500
14	Materials	Magnet Material Selection	MagMat	-	NdFeB N52
15		Winding Material Selection	WinMat	-	MAGNATEMP CA200 ø0.16
16		Stator Material Selection	StaMat	-	M270-35A
17		Housing Components Material Selection	HouMat	-	Aluminium LM25-TF (Cast)
18		Rotor Material Selection	RotMat	-	Aluminium 2014 T651 (MC)
19	Magnets	Magnet Length	LM	mm	10.000
20		Lamination Stacking Factor	Kst	-	0.990
21		Leakage Factor	Kl	-	0.980
22		Reluctance Factor	Kr	-	1.100
23		Residual Induction	Br20degC	T	1.450
24		Relative Permeability	Mu_r	-	1.040
25	Stator & Windings	Stator tooth slot depth	SD	mm	20.000
26		Tooth Tang Depth	TGD	mm	2.000
27		Stator tooth slot opening	SO	mm	3.500
28		Peak flux density through Stator Yoke	By_pk	T	1.470
29		Peak flux density through Stator Tooth	Bt_pk	T	1.690
30		Number of Winding Turns	nTurns	-	40
31		Number of slots per pole per phase	Nspp	-	0.5
32		Slot Fill, Gross	SFg	-	0.550
33		Cu Winding Resistivity	Rho_Cu_20C	Ω·m	1.680E-08
34	Rotor	Rotor Magnet Outer Diameter	DR	mm	174.000
35		Number of Rotor Spokes	nRotorSpokes	-	3
36		Rotor Hub Web Thickness	WebThk	mm	5.000
37		Rotor Hub Web Draft Angle	WebAng	deg	2.0
38		Resolver Rotor Mount Bolt Thrd Length	ResBoltLen	mm	16.000
39		Resolver Rotor Mount Bolt Thread	ResThrd	-	M8
40		Resolver Rotor Mount C-Bore Length	ResCboreLen	mm	12.300
41		Resolver Rotor Mount C-Bore Diameter	ResCboreDia	mm	15.700
42		Rotor Spline Length	RSLength	mm	27.500
43		Rotor Spline Lead-in Angle	RLAng	deg	30.000
44		Number of Mounting Lugs	nMountingLugs		4

INPUTS | OUTPUTS | MATERIALS | Info

	A	B	C	D	E
1					
2	OUTPUTS				
3	Section	Parameter	Symbol	Units	Value
4	Performance	Maximum Speed	nMax_rads	rad/s	1989.675
5		Max Torque Output	MMax	Nm	200.158
6					
7	Rotor & Magnets	Airgap Flux Density	Bg	T	1.105
8		Permeance Coefficient	Pc	-	4.000
9		Rotor Volume	VR	l	1.308
10		Rotor Length (Stack Length)	LR	mm	55.017
11					
12	Stator	Stator OD	OD	mm	253.587
13		Stator ID	ID	mm	179.000
14		Yoke Depth	WSY	mm	17.294
15		Tooth Width	TWS	mm	20.057
16		Number of stator slots	Ns	-	18.000
17	Mass & Cost	Power Density	Power_density	kW/kg	8.826
18		Stator CAD Mass	StatorMass	kg	8.636
19		Rotor CAD Mass	RotorHubMass	kg	0.749
20		Housing CAD Mass	HousingMass	kg	1.592
21		Magnets CAD Mass	MagnetsMass	kg	2.090
22		Windings CAD Mass	WindingsMass	kg	1.435
23		Total Estimate CAD Mass	CAD_Mass	kg	15.295
24		Total Estimate BOM Cost	CAD_Cost	£	£270.09
25	Material Costs	Stator Core	Scost	£/kg	£0.07
26		Windings	CuCost	£/kg	£5.00
27		Magnets	Mcost	£/kg	£122.04
28		Housing	Hcost	£/kg	£1.87
29		Rotor	Rcost	£/kg	£3.60
30					
31					
32					
33					
34					
35					

INPUTS | OUTPUTS | MATERIALS | Info

	A	B	C	D	E	F	G	H	I	J	K	L	M
1													
2		Materials list											
3		Material	Manufacturer	Density [kg/m^3]	Estimate Cost [£/kg]	Estimate Cost [£/m3]	Resistivity [Ωm]	Lamination Thickness [mm]	Relative permeability	Residual Inductance/Remanence flux density [T]	Coercive Field [A/m]	Source - Properties	Source - Cost
4		Magnets											
5		Generic NdFeB	N/A	7,800.00	120.00	N/A		N/A	0.9800	1.350		https://www.ebay.com/itm/Wholesale-Super-Block-Magnets-	
6		NdFeB N30	Arnold Magnetics	7,500.00	136.84	N/A	1.80E-06	N/A	1.0400	1.105		http://www.arnoldmagnetics.com/wp-content/	https://e-sho
7		NdFeB N33	Arnold Magnetics	7,500.00	201.55	N/A	1.80E-06	N/A	1.0400	1.150		http://www.arnoldmagnetics.com/wp-content/	https://e-sho
8		NdFeB N35	Arnold Magnetics	7,500.00	246.28	N/A	1.80E-06	N/A	1.0400	1.210	-914,375	http://www.arnoldmagnetics.com/wp-content/	https://e-sho
9		NdFeB N38	Arnold Magnetics	7,500.00	203.88	N/A	1.80E-06	N/A	1.0400	1.260	-944,982	http://www.arnoldmagnetics.com/wp-content/	https://e-sho
10		NdFeB N40	Arnold Magnetics	7,500.00	115.78	N/A	1.80E-06	N/A	1.0400	1.285	-967,937	http://www.arnoldmagnetics.com/wp-content/	https://e-sho
11		NdFeB N42	Arnold Magnetics	7,500.00	390.35	N/A	1.80E-06	N/A	1.0400	1.315	-994,718	http://www.arnoldmagnetics.com/wp-content/	https://e-sho
12		NdFeB N45	Arnold Magnetics	7,500.00	293.33	N/A	1.80E-06	N/A	1.0400	1.350	-1,032,976	http://www.arnoldmagnetics.com/wp-content/	https://e-sho
13		NdFeB N48	Arnold Magnetics	7,500.00	112.12	N/A	1.80E-06	N/A	1.0400	1.400	-1,071,235	http://www.arnoldmagnetics.com/wp-content/	https://e-sho
14		NdFeB N50	Arnold Magnetics	7,500.00	166.35	N/A	1.80E-06	N/A	1.0400	1.425	-1,090,364	http://www.arnoldmagnetics.com/wp-content/	https://e-sho
15		NdFeB N52	Arnold Magnetics	7,500.00	122.04	N/A	1.80E-06	N/A	1.0400	1.450		http://www.arnoldmagnetics.com/wp-content/	https://e-sho
16		NdFeB N55	Arnold Magnetics	7,500.00	733.33	N/A	1.80E-06	N/A	1.0400	1.490		http://www.arnoldmagnetics.com/wp-content/uploads/2017/	
17													
38		Windings											
39		Generic Cu	N/A	8,960.00	6.21	N/A	1.68E-08	N/A	N/A	N/A	N/A	https://www.lme.com/Metals/Non-ferrous/Copper#tabIndex=	
40		Emetor Cu	N/A	8,920.00		N/A	1.72E-08	N/A	N/A	N/A	N/A	https://www.emetor.com/edit/materials/copper/	
41		MAGNATEMP CA200 ø0.16	Essex Europe	8,887.81	26.20	N/A	1.68E-08	N/A	N/A	N/A	N/A	http://www.essexeurope.com/uploadedFiles/E	http://www.b
42		MAGNATEMP CA200 ø0.20	Essex Europe	8,890.40	20.12	N/A	1.68E-08	N/A	N/A	N/A	N/A	http://www.essexeurope.com/uploadedFiles/E	https://www.
43		MAGNATEMP CA200 ø0.40	Essex Europe	8,890.40	17.60	N/A	1.68E-08	N/A	N/A	N/A	N/A	http://www.essexeurope.com/uploadedFiles/E	https://www.
44		MAGNATEMP CA200 ø0.50	Essex Europe	8,892.30	13.21	N/A	1.68E-08	N/A	N/A	N/A	N/A	http://www.essexeurope.com/uploadedFiles/E	https://www.
45		MAGNATEMP CA200 ø0.80	Essex Europe	8,890.79	17.38	N/A	1.68E-08	N/A	N/A	N/A	N/A	http://www.essexeurope.com/uploadedFiles/E	https://www.
46		MAGNATEMP CA200 ø0.90	Essex Europe	8,890.67	14.14	N/A	1.68E-08	N/A	N/A	N/A	N/A	http://www.essexeurope.com/uploadedFiles/E	https://www.
47		MAGNATEMP CA200 ø1.00	Essex Europe	8,889.76	16.76	N/A	1.68E-08	N/A	N/A	N/A	N/A	http://www.essexeurope.com/uploadedFiles/E	https://www.
48		MAGNATEMP CA200 ø1.25	Essex Europe	8,890.27	16.76	N/A	1.68E-08	N/A	N/A	N/A	N/A	http://www.essexeurope.com/uploadedFiles/E	https://www.
49		MAGNATEMP CA200 ø1.40	Essex Europe	8,893.19	15.95	N/A	1.68E-08	N/A	N/A	N/A	N/A	http://www.essexeurope.com/uploadedFiles/E	http://www.b
50		MAGNATEMP CA200 ø1.80	Essex Europe	8,889.10	15.95	N/A	1.68E-08	N/A	N/A	N/A	N/A	http://www.essexeurope.com/uploadedFiles/E	http://www.b
51		MAGNATEMP CA200 ø2.00	Essex Europe	8,890.40	15.92	N/A	1.68E-08	N/A	N/A	N/A	N/A	http://www.essexeurope.com/uploadedFiles/E	https://www.
52		MAGNATEMP CA200 ø2.50	Essex Europe	8,890.27	15.95	N/A	1.68E-08	N/A	N/A	N/A	N/A	http://www.essexeurope.com/uploadedFiles/E	http://www.b
53		MAGNATEMP CA200 ø3.15	Essex Europe	8,889.90	15.54	N/A	1.68E-08	N/A	N/A	N/A	N/A	http://www.essexeurope.com/uploadedFiles/E	https://www.

INPUTS | OUTPUTS | **MATERIALS**

APPENDIX E: AIEED TOOL – VBA CODE

See *Minucci-Cipolat-MSc5050-VBScript.pdf*. This includes the full VBA code contained in the AIEED tool. (Digital only)